In Vitro Characterization of Injectable Collagen and Collagen-Genipin Hydrogels for Neural Tissue Engineering

A Thesis Submitted to the College of

Graduate Studies and Research

In Partial Fulfillment of the Requirements

For the Degree of Master of Science

In the Division of Biomedical Engineering

University of Saskatchewan

Saskatoon

By

JINGWEN LI

PERMISSION TO USE

In presenting this thesis in partial fulfilment of the requirements for a Postgraduate degree from the University of Saskatchewan, I agree that the Libraries of this University may make it freely available for inspection. I further agree that permission for copying of this thesis in any manner, in whole or in part, for scholarly purposes may be granted by the professor or professors who supervised my thesis work or, in their absence, by the Head of the Department or the Dean of the College in which my thesis work was done. It is understood that any copying or publication or use of this thesis or parts thereof for financial gain shall not be allowed without my written permission. It is also understood that due recognition shall be given to me and to the University of Saskatchewan in any scholarly use which may be made of any material in my thesis.

Requests for permission to copy or to make other use of material in this thesis in whole or part should be addressed to:

Head of the Division of Biomedical Engineering
57 Campus Drive
University of Saskatchewan
Saskatoon, Saskatchewan, S7N 5A9
Canada

ABSTRACT

Nervous system injury leads to the permanent loss of sensory and motor functions. Injectable hydrogel containing therapeutic agents can be directly injected to the injured cavity as a promising approach for minimally-invasive treatment of nerve injury. However, such injectable hydrogels have not been well developed and documented in the literature. As inspired, this project aims to develop injectable collagen-based gels for nerve injury repair and to characterize *in vitro* for supporting neurite outgrowth of dorsal root ganglia (DRG) explants and dissociated neurons.

To develop collagen-based gels, collagen at varying concentrations (e.g. 1.5, 2 and 2.5 mg/mL) were used to form gels under physiological conditions and genipin (0.25-5 mM) were applied as the chemical crosslinker. Characterization studies showed that collagen-based hydrogels could form porous and fibrillary gels within a time period of 40 s at 37 °C and genipin could significantly improve the mechanical property of gels and the resistance to degradation.

To evaluate the cytotoxicity of the injectable hydrogels and compare the cell behaviour in two-dimensional (2D) and three-dimensional (3D) environments, rat primary Schwann cells (PRSCs) were seeded onto and encapsulated within the gels, and the cell viability was examined at Day 3 by the Live/Dead assay. The results showed that collagen gels provide superior support for PRSCs survival in both 2D and 3D cultures, for example, with a cell viability of 96 % and 95 %, respectively, for the collagen gel with a concentration of 1.5 mg/mL. Collagen chemically crosslinked by genipin at 0.25 and 0.5 mM exhibited a permissive but less favorable environment to PRSCs comparing with pure collagen. Genipin over 1 mM inhibited the PRSCs survival significantly in both 2D and 3D cultures.

DRG explant and dissociated neuron cultures were examined as *in vitro* cell models to evaluate the therapeutic efficacy of collagen and collagen-genipin gels for nerve injury repair and the cellular response was also characterized and compared to each other. Preliminary 2D cultures were shown to greatly support neurite extension and 2.5 mg/mL collagen gel supported the most neurite extension and branching development. It was shown that genipin had a significant effect on the neurite density but not neurite length of DRG explants, whereas the dissociated neurons

were more sensitive to genipin. Enrichment of culture medium with nerve growth factor (NGF) could significantly enhance the neurite length and density.

PRSCs as the supportive cells were co-cultured with DRG explants/dissociated neurons in 3D hydrogels. Confocal microscopy showed that the neurites of DRG explants and dissociated neurons could extend freely within the physical collagen gels, and dissociated neurons exhibited pseudo-unipolar phenotype in 3D environment indicating true axonal extension. Moreover, genipin had a significantly inhibitory effect on dissociated neurons whereas the explants were more tolerant to genipin possibly due to the preserved cellular components and interactions. It was also shown that hydrogels infiltrated with PRSCs could enhance the neurite elongation and branches dramatically. Our research has determined the therapeutic potency of injectable collagen-based gels containing the PRSCs for nerve injury repair and gained new insights into the use of the injectable gel as a delivery substrate in neural tissue engineering.

ACKNOWLEDGMENTS

I would like to express my sincere gratitude to my supervisors, Dr. Daniel Chen and Dr. David Schreyer, for their exceptional guidance and tremendous support during my graduate study at the University of Saskatchewan. I also want to thank my advisory committee members: Dr. Assem Hedayat and Dr. Ning Zhu for the kind examination and advice on my research work.

I would also like to acknowledge the valuable assistance from Eiko Kawamura at WCVM Imaging centre, Dr. Supratim Ghosh's Lab and LASU at University of Saskatchewan.

Financial support from the Saskatchewan Health Research Foundation (SHRF) and the scholarship from University of Saskatchewan are gratefully acknowledged.

I also appreciate the support from my colleagues in Tissue Engineering Research Group and Cameco MS Neuroscience Research Center at Saskatoon City Hospital, including Dr. Zohreh Izadifar, Mr. Md. Aslam Sarker, Mr. Fu You, Mr. Liqun Ning, Mrs. Mindan Wang and Dr. Ning Zhu. I specially thank Ms. Peng Zhai, Dr. Ajay Rajaram and Ms. Stephanie England for their assistance with research involving animal surgery and technical support for my experiments.

A special thank you to Mr. Ang Li for the encouragement and accompany through all the difficulties in life. I would also like to acknowledge my friends: Ms. Xue Han, Ms. Xue Wang, Ms. Qi Zhao, Dr. Chunzi Zhang and Mr. Zhen Wang for their encouragement and support during my study in Canada.

Finally, I wish to thank my parents Mr. Fu Li and Mrs. Yunyan Cui for their constant love and encouragement. Without them, I couldn't finish my graduate study.

TABLE OF CONTENTS

LIST OF TABLES

Page

LIST OF FIGURES

Page

LIST OF ABBREVIATIONS

DRG	dorsal root ganglia
2D	two dimensional
3D	three dimensional
PRSC	primary Schwann cell
NGF	nerve growth factor
CNS	central nervous system
PNS	peripheral nervous system
MAG	myelin-associated glycoprotein
OMgp	oligodendrocyte myelin glycoprotein
CSPG	chondroitin sulphate proteoglycans
NT-3	neurotrophin-3
GDNF	glial cell line-derived neurotrophic factor
BDNF	brain-derived neurotrophic factor
NT-4/5	neurotrophin-4/5
FDA	Food and Drug Administration
ECM	extracellular matrix
PLA	poly(lactic acid)
PGA	poly(glycolic acid)
PEG	poly(ethylene glycol)
PVA	poly (vinyl alcohol)
PC12	pheochromocytoma cells
DMEM	Dulbecco’s Modified Eagle’s medium
PBS	phosphate buffered saline
SEM	scanning electron microscopy
ANOVA	analysis of variance
FBS	fetal bovine serum

PLL	poly-$_L$-lysine
G’	storage modulus
G’’	loss modulus
FTIR	Fourier transform infrared spectroscopy

CHAPTER 1

INTRODUCTION

1.1 Nervous System Injury

1.1.1 Physiology of the Nervous System

The nervous system can be fundamentally divided into the central nervous system (CNS) and the peripheral nervous system (PNS). Neurons and neuroglial cells are the main cellular components of both the CNS and PNS. A neuron is composed of a cell body, axon and dendrites (Figure 1.1 (a)). The axon is a long process emitting from the cell body and transmits action potentials away from the soma, whereas dendrites are short processes carrying electrical messages towards the cell body. Besides the neurons, the glial cells play important roles in supporting the neurons' growth, producing neurotrophic factors, myelinating the axon, etc. Glial cells in the CNS consist of microglia, astrocytes, oligodendrocytes and ependymal cells. Those in the PNS include Schwann cells, satellite cells and enteric glia cells. Axons can be myelinated by oligodendrocytes in the CNS, whereas the myelinating cells are Schwann cells in the PNS. Moreover, an individual axon is myelinated by a series of single Schwann cells in the PNS, whereas one oligodendrocyte can myelinate several CNS axons (Figure 1.1 (b)).

The CNS is composed of the brain and spinal cord. In spinal cord, a butterfly-shaped gray matter and white matter (Figure 1.2) arrangement is observed. The neural cell bodies, dendrites and glial cells locate in gray matter, whereas the white matter contains mostly oligodendrocytes and bundles of myelinated axons, which appear white in color. The gray matter of the spinal cord has pairs of projections into the surrounding white matter, including ventral horn and dorsal horn. Sensory signals enter into the dorsal horns of the gray matter via the dorsal roots. The dorsal root contains bundles of sensory axons, whereas the somas of sensory neurons are located in the dorsal root ganglia (DRG). The spinal cord is defined as part of the CNS, but the DRG is considered parts of the PNS. The PNS includes all of the cranial and spinal nerves arising from the brainstem and spinal cord. Nerves consisting of numerous axons convey sense signals inward to the CNS and motor messages outward to the rest of the body [1].

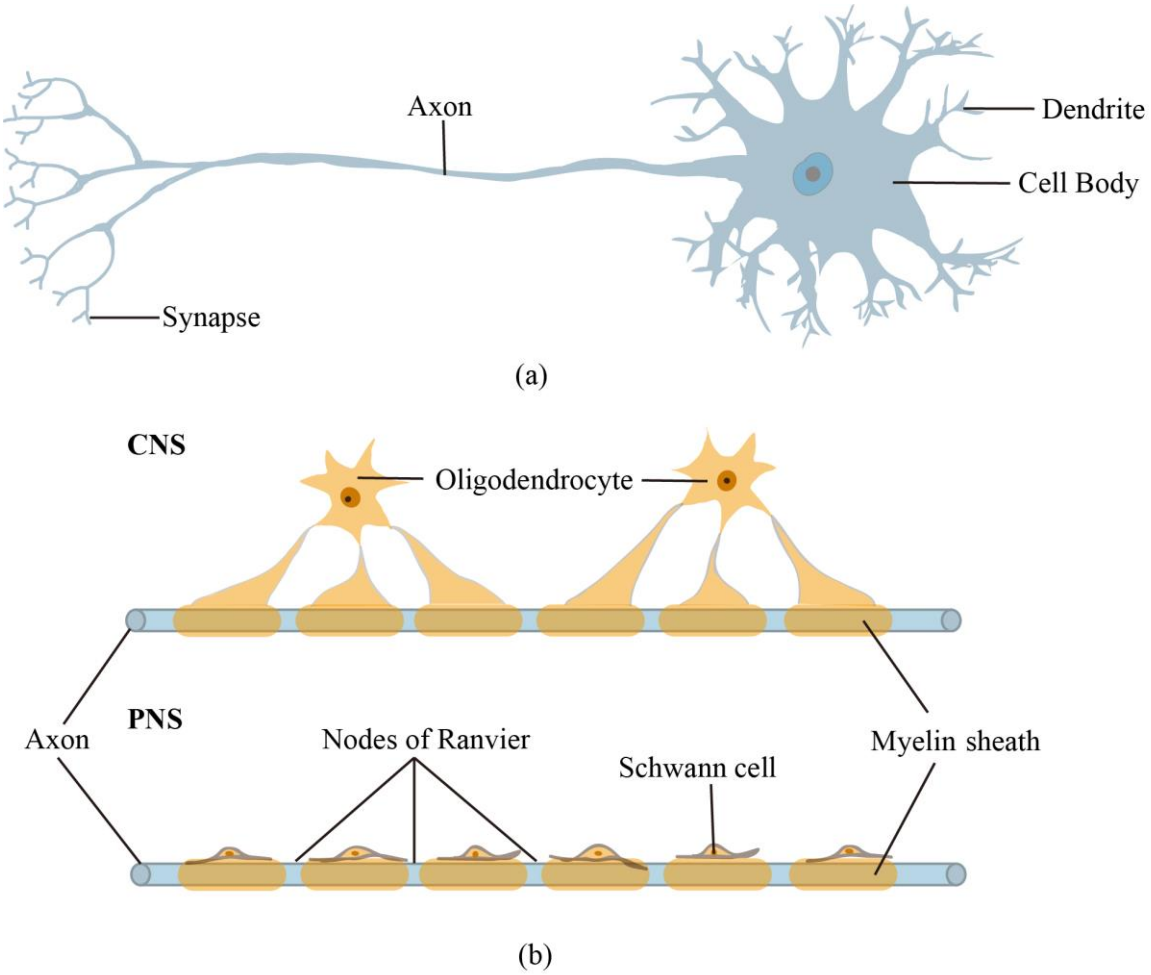

Figure 1.1 (a) Structure of a typical neuron; (b) Myelin sheath of the CNS and PNS axon.

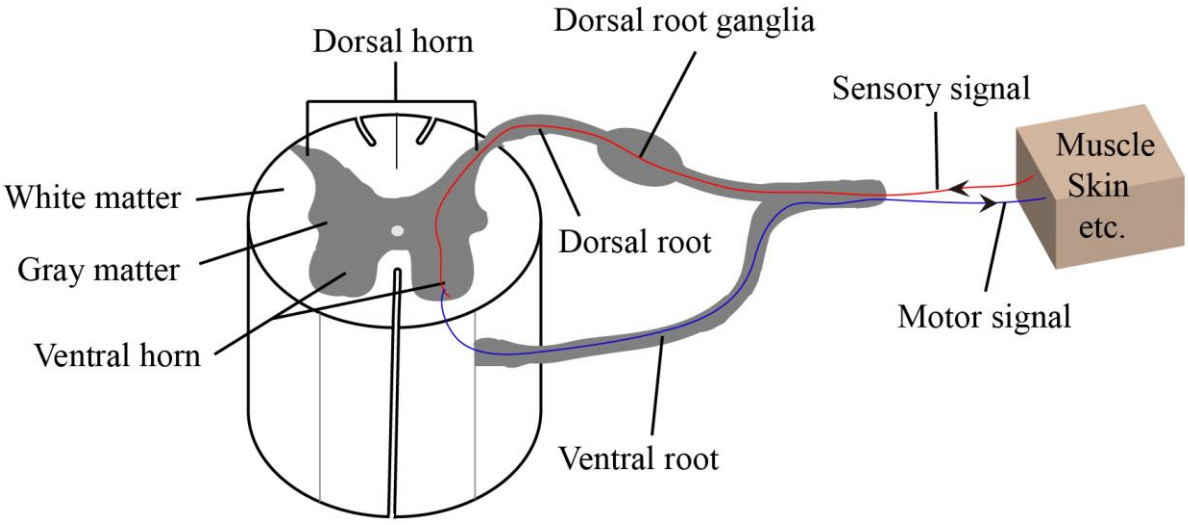

Figure 1.2 Cross-section of spinal cord and the overview of the signal conduction.

1.1.2 CNS Injury and Regeneration

Injury to the spinal cord and brain can lead to the catastrophic and permanent loss of sensory and motor functions. These injuries can result from a trauma (falls, gunshot wounds and vehicle accidents), stroke or genetic disorder. A key difference between the CNS and PNS is the inability of axonal regeneration in the CNS. Interestingly, the injured DRG can undergo axonal sprouting and regeneration in the PNS, but axonal regeneration stops entering the spinal cord at the dorsal root entry zone [2-4]. Besides the intrinsic inability of axonal regeneration in the CNS, the challenges of the CNS regeneration include the inhibitory glial environment, the glial scar surrounding the lesion site and the lack of neurotrophic factors [5] (Figure 1.3).

After a CNS injury, the myelin sheaths become damaged and the axons are exposed to the inhibitory environment. Many inhibitory molecules responsible for the failure of CNS regeneration have been identified, such as Nogo, myelin-associated glycoprotein (MAG), oligodendrocyte myelin glycoprotein (OMgp), etc. [6-13]. Researchers have found that neutralization of the inhibitory environment can promote axonal sprouting. For example, blockade of Nogo-A, MAG and OMgp have shown to promote the growth cone formation and axonal regeneration [14-20].

In addition to the damaged myelin, the glia scar is another barrier to the axonal regeneration. After the CNS injury, the astrocytes can isolate the lesion site and alleviate the inflammation to avoid further damage. However, the reactive astrocytes around the injured area can proliferate and form the glial scar [21, 22]. Studies have shown that the glial scar not only is a physical barrier but also releases chemical inhibitors, such as chondroitin sulphate proteoglycans (CSPGs) [23-26]. Researches have shown that axons stop growing once reaching the glial scar site [27, 28]. Modification of the CSPGs allows axons to regenerate around the lesion site [29-32].

Advances in recent years have identified many inhibitory molecules and characterized the potential inhibitory mechanisms after the CNS injury. However, clinical treatment is still very limited. In addition to the administration of the anti-inflammatory drug (methylprednisolone) and physical rehabilitation, other clinical therapies are still in experimental stages [33, 34]. Current clinical treatments target on the inflammation control and maintenance of the existing muscle function, whereas completely functional recovery after the CNS injury is rarely achieved. Therefore, to improve long-distance axonal regeneration and hence functional recovery, further attempts should focus on not only addressing the inhibitory environment but also stimulating the intrinsic growth of the neurons to achieve functional regeneration.

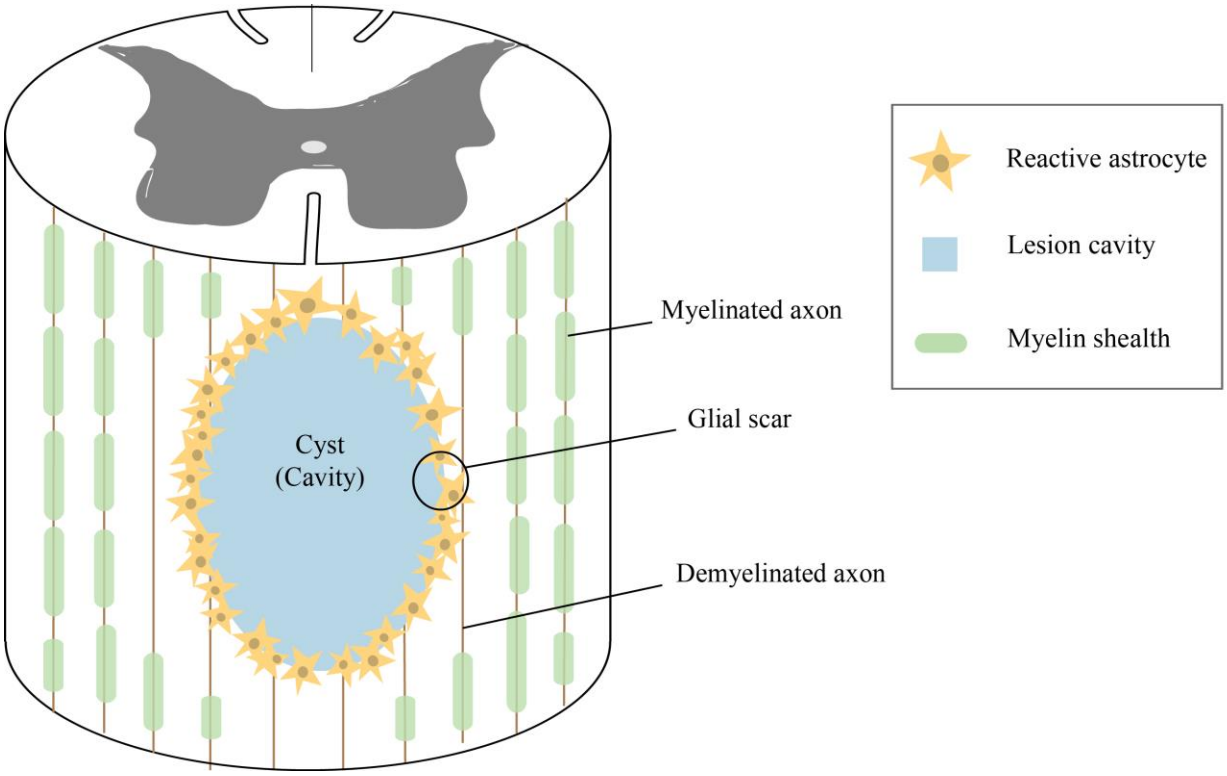

Figure 1.3 Illustration of the CNS injury (spinal cord). After the CNS injury, many myelin sheaths are damaged and the reactive astrocytes start to proliferate to form the glial scar, which is inhibitory to the nerve regeneration. Cysts filled with fluid usually exist at the injured site.

1.1.3 PNS Injury and Regeneration

PNS injury can result from traumatic or non-traumatic incidents which may lead to great loss of sensory and motor functions. After a peripheral nerve is transected, a series of response from the proximal and distal ends are induced (Figure 1.4 (a-b)). Within hours of injury, the proximal ends of the severed axons are sealed and swollen due to the enrichment of organelles. The distal stump undergoes a calcium-mediated process called the Wallerian degeneration. During Wallerian degeneration, the damaged axons disconnect from the cell body, and severed axons and myelin break down into fragments. Schwann cells and macrophages then play a key role in removing axonal and myelin debris from the distal injury site. This cleaning process may require one week to several months [35-37].

Unlike the CNS injury, nerves can regenerate by themselves in the PNS if the injury gap is small. Following the debris clearance, axons begin to sprout and regenerate at the nodes of Ranvier of the proximal end and re-innervate towards the distal end (Figure 1.4 (c)). During axonal regeneration, Schwann cells also promote the formation of a basal lamina and release growth

factors and cytokines to guide the axonal outgrowth [38, 39]. Functional recovery may be partially achieved after several months to years, depending on the levels of injury. However, if the nerve gap is big, autologous nerve grafts are required to connect the two ends of the damaged nerves. Even though autografts provide superior biocompatibility, there are disadvantages including the trauma to the donor site. Complete functional recovery is rare, especially when the defects are extensive [40]. Further research should be focused on the development of alternative repair-promoting devices to the grafts, and combinations of cellular and molecular therapies to aid the nerve regeneration.

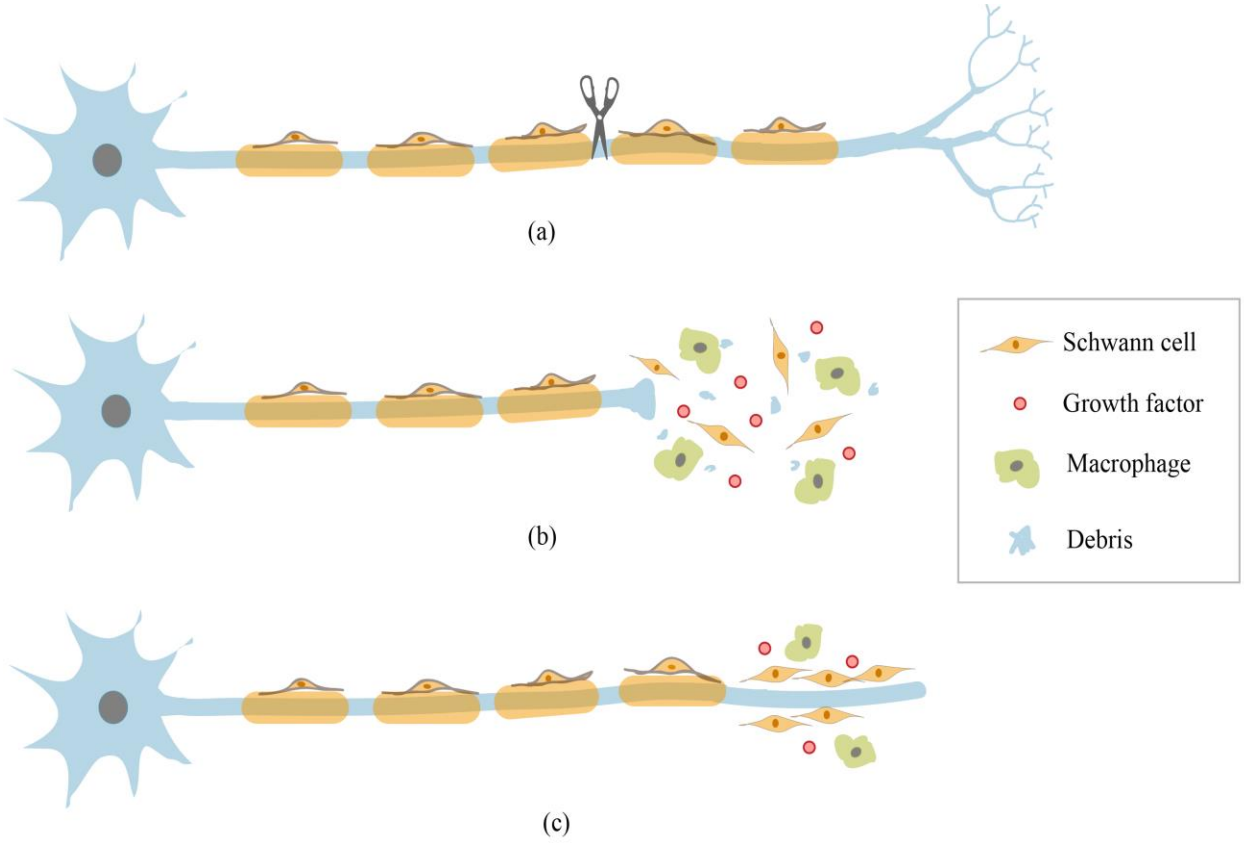

Figure 1.4 Illustration of the PNS injury and regeneration. After the peripheral nerve is injured (a), the proximal end becomes swollen and the distal axons are disconnected from the cell body. (b). Following debris clearance by the macrophages, Schwann cells can promote axonal regeneration (c).

1.1.4 DRG as *In Vitro* Models for Nerve Injury Repair

DRG are swellings beside the spinal cord in which the cell bodies of primary sensory neurons reside (Figure 1.2). Sensory neurons of adult rats exist *in vivo* as mostly pseudo-unipolar morphology and convey sensory signals from the periphery to the CNS. The pseudo-unipolarization (transforming from bipolar form) occurs during prenatal development (Figure 1.5) [41, 42]. Each sensory neuron has one single axon with afferent branches projecting to the spinal cord and the PNS [39]. Even though DRG neurons have axons in both the CNS and PNS, only their peripheral end can regenerate *in vivo* due to the different glial environment in the CNS and PNS [2-4]. The reaction of DRG after the PNS and CNS injury has been widely investigated. It has been demonstrated that injury to the PNS and CNS can result in neuronal cell death in DRG [43-45]. The fundamental challenge for the CNS or PNS injury repair is the lack of successfully axonal elongation. Since DRG is closely related to the CNS and PNS injury, it can be exploited as the excellent *in vitro* cell models to evaluate the therapeutic potency of biomaterials, molecular and cellular therapies for nerve injury repair. And the neurite/axonal outgrowth of DRG sensory neurons can be used to evaluate nerve regeneration potential and provide important insights into new therapies *in vitro*.

Recent advances have shown that the central axons of DRG can access beyond the dorsal root entry zone and enter into the spinal cord with the support of neurotrophic factors such as neurotrophin-3 (NT-3), nerve growth factor (NGF) and glial cell line-derived neurotrophic factor (GDNF) after dorsal root injury [46, 47]. Research of suitable substrates delivering those neurotrophins and supportive cells to the injured site has drawn great attention for long-distance nerve injury repair. In our research, DRG explants and dissociated neurons are employed as *in vitro* models to study the effect of injectable hydrogels carrying Schwann cells on axonal outgrowth.

Adult rat DRG can be directly dissected as explants or dissociated into the individual sensory neurons as shown in Figure 1.6 [48]. Each model has its own advantages and disadvantages. DRG explants are clusters of sensory neurons and glial cells. The unique advantages of the DRG explant model are simulation of the original state *in vivo*, and preservation of the original cell components in DRG and their cell-cell interactions, which are lost in the DRG dissociated neuron model. Comparing with the DRG explant model, dissociated DRG neuron offers a great opportunity to unveil how therapies affect the axonal regeneration of individual sensory neuron while minimizing

other influences [49]. Mature DRG sensory neurons exist as mostly pseudo-unipolar form *in vivo*, whereas *in vitro* culture of sensory neurons shows bipolar and multipolar morphology [50]. It has been demonstrated that the DRG explant and dissociated neuron cultures respond to many guidance neurotrophins including NT-3, NGF, GDNF and brain-derived neurotrophic factor (BDNF) [51-53]. Co-cultures with Schwann cells also enhance axonal regeneration, which is coordinated with the cell transplantation results in animal models [54]. The DRG culture offers great opportunities to model axonal regeneration *in vitro*. And the easy control and manipulation of the extrinsic factors in the DRG culture environment make it a powerful tool to study nerve injury repair *in vitro*.

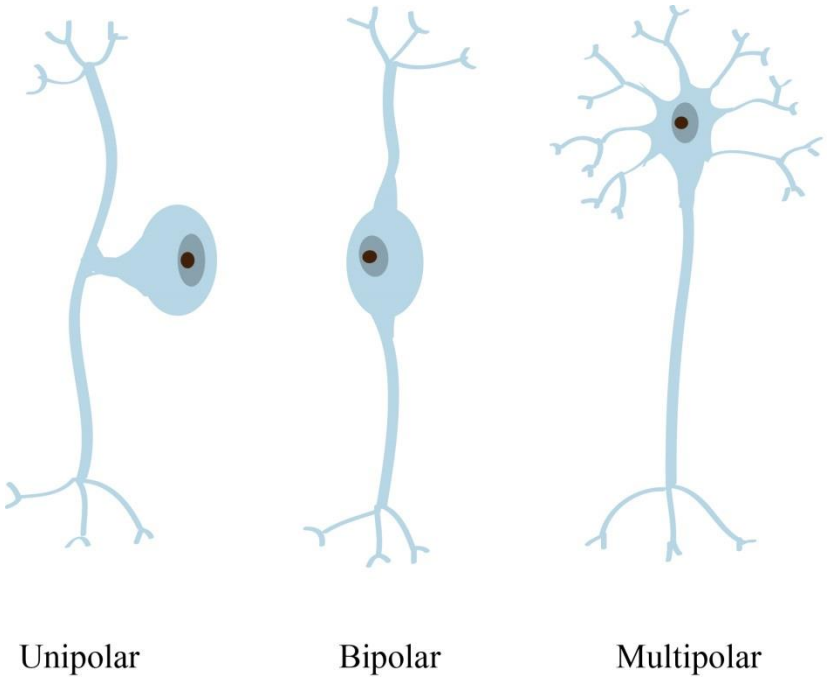

Figure 1.5 Basic neuron types: unipolar, bipolar and multipolar morphology.

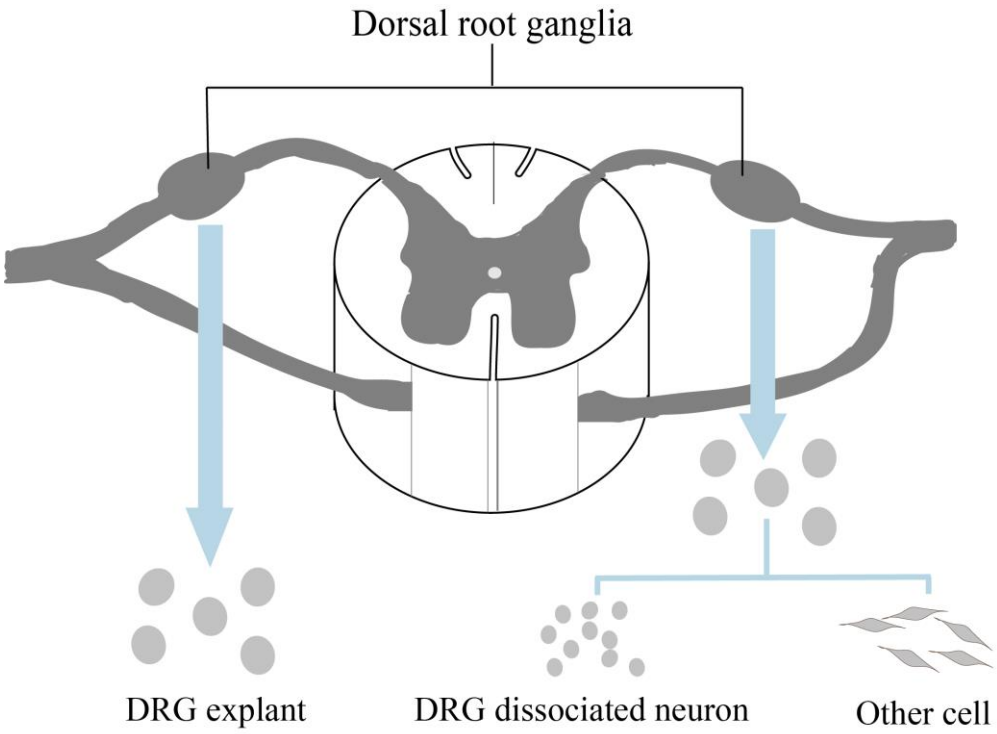

Figure 1.6 Schematic views of the DRG explants and dissociated sensory neurons.

1.2 Tissue Engineering Strategies for Nerve Injury Repair

To date, many promising advances in tissue engineering have been achieved in promoting and guiding the axonal regeneration for nerve injury repair, such as the conduit or scaffold system, delivery of supportive cells and bioactive molecules, or combinational therapies. Major tasks of neural tissue engineering aim at developing or manufacturing devices to improve the connectivity of the injured site, neutralize the inhibitory environment after injury, enhance the intrinsic ability of axonal regeneration, and promote physical guidance and re-myelination of regenerating axons [55]. Progresses in neural tissue engineering are briefly reviewed in the following aspects: guidance, cellular and molecular therapies.

1.2.1 Guidance Therapy

For PNS injury, an autologous nerve graft is the standard clinical treatment when the nerve gap is big. However, this treatment induces problems of sensation loss and morbidity at the donor site, potential neuropathic pain and relatively low success rate of fully functional recovery [35]. In the past few years, enormous efforts have been made in studying alternatives to autologous nerve grafts and manufacturing the nerve guidance devices and fillings for nerve injury repair.

The guidance device can either be a conduit [56] or a patterned scaffold which simulates the

nerve autograft to connect the lesion gap and guide axonal regeneration. Researchers have successfully fabricated the nerve guidance conduits with naturally derived materials including hyaluronic acid [57], collagen [58], alginate[59], fibrin [60] or synthetic polymers [61]. Novel manufacturing techniques, including rapid prototyping, also lead to more controllable architecture and microstructure of patterned scaffolds. Several biodegradable nerve conduits have been approved by the US Food and Drug Administration (FDA) for the peripheral nerve repair. Most of the approved conduits (NeuraGen®, Neuroflex®, NeuroMend®, and NeuroMatrix®) are comprised of type-I collagen. It has been reported that the collagen-based conduits demonstrated supportive, semipermeable and protective environment for nerve regeneration *in vitro* and *in vivo* [62-64]. However, the defect length applied for the collagen conduits is limited up to 3 cm [65, 66] and the functional recovery is not equivalent to nerve autografts [67]. To achieve equivalent or excessive therapeutic effect as the nerve autografts, combinational strategy should be considered. Researchers have directly infiltrated Schwann cells, stem cells, or nerve growth factors into the hollow conduits to assist nerve repair and studies have shown significant enhancement of axonal regeneration along the conduits walls at 2 weeks [68, 69]. To deliver the therapeutic agents in an efficient and prolonged manner, injectable hydrogels can be adopted to encapsulate the cells and neurotrophic factors as the therapeutic additives.

Comparing with the PNS injury, complex regenerative obstacles exist around the CNS injury site and impede the functional recovery significantly. Unfortunately, successfully functional recovery of CNS has not been achieved through current treatments. To date, advances in tissue engineering provide remarkably promising strategies for the CNS injury repair. A wide variety of tissue-engineered devices applied for the CNS injury have been investigated. These devices include the hydrogels, nanofibrous scaffolds, single and multi-channel guidance conduits [55, 70]. Injectable hydrogels have unique advantages over other types of devices. Direct injection of hydrogel solution enriched with ant-inflammatory drugs, supportive cells and neurotrophic factors into the lesion site could fill the void and localize *in situ* to establish a permissive environment for nerve injury repair. Most importantly, injectable hydrogels provide minimally invasive procedures when compared to other surgical implants especially for the most common focal types of injury.

1.2.2 Cellular Therapy

Various types of cells have been extensively investigated to stimulate axonal sprouting and improve nerve regeneration. Those cells include glial cells (Schwann cells, astrocytes), stem or

progenitor cells, and olfactory ensheathing cells [34, 40, 63, 71]. Comparing with other cells, Schwann cells have unique advantages of secretion of multiple growth factors and potentially autologous sources. In our project, rat primary Schwann cells (PRSCs) were seeded onto or encapsulated within the injectable hydrogels to evaluate the potency of cell-delivery substrates on neurite outgrowth of DRG *in vitro*. Here, we review some progresses with the emphasis on PRSCs for nerve injury repair.

PRSCs are glial cells found in the PNS and hold significant promise for both the CNS and PNS repair. In life, they not only insulate and protect the PNS axons with myelin sheaths, but also lead to a more permissive environment by expressing and secreting nerve growth factors (NT-3, BDNF and GDNF) [72, 73] and extracellular matrix (ECM) components (collagen, laminin and fibronectin) [74, 75], which are essential for the neuronal survival and axonal extension. Transplantation of PRSCs to the lesion site *in vivo* has been shown to aid the nerve regeneration applied for both the PNS and CNS injury [76-79]. However, the application of autologous PRSCs is limited due to the time-consuming isolation and expansion process.

Following the PNS injury, PRSCs play important roles in bridging the lesion gap, re-myelinating regenerated axons, and providing guidance and neurotrophic support [38]. When a large injury gap exists, combinational strategy of PRSCs and tissue-engineered devices has been adopted to achieve enhanced nerve recovery. Compared to the conduit only, hollow collagen conduit infiltrated with PRSCs has shown to support more regenerated axons and enhanced functional recovery *in vivo* compared to conduit only [80]. Collagen sheets with PRSCs attached were rolled to efficiently increase the number of adherent cells and implanted to the rat sciatic nerve. Conduit containing the PRSCs has shown to improve the functional recovery than conduit only and the efficacy is dependent on the numbers of PRSCs [81]. Hydrogel containing the PRSCs can be applied as the conduit filling and has demonstrated enhanced nerve recovery [82-87]. In general, PRSCs-loaded conduits are beneficial for large gap injury with the length up to 6 cm [88], and enhanced nerve regeneration has been demonstrated compared to conduit only, but still not as good as the autografts.

As described earlier, injured CNS axons cannot regenerate by their own due to multiple factors. Although PRSCs are absent in the native CNS environment, extensive experiments have shown that transplantation of PRSCs can enhance axonal regeneration by clearing the debris [89], reducing cystic cavity [90, 91], re-myelinating axons and producing neurotrophins [77, 92]. Direct

injection of PRSCs to the injured site has shown positive effects on promoting the outgrowth of DRG axons and reducing the posttraumatic cavitation after spinal cord injury [71, 76]. Polymer conduit filled with PRSCs and Matrigel™ mixture has demonstrated improved axonal outgrowth and elongation compared to conduit and conduit-Matrigel™ only [78]. However, the regenerated axons fail to leave the transplantation site and the migration of PRSCs in white matter is restricted probably due to the intrinsically inhibitory environment [40]. Therefore, additional strategies are required to enhance the efficacy of nerve regeneration for the CNS injury including incorporation of neurotrophic factors and the aid of tissue-engineered devices.

1.2.3 Molecular Therapy

The neurotrophin family includes NGF, BDNF, NT-3 and neurotrophin-4/5 (NT-4/5). Additional proteins with neurotrophic properties include GDNF and CNTF. Extensive research has demonstrated that the neurotrophic factors can promote neuronal survival, axonal outgrowth and branching development [93-95]. Among the neurotrophin family, NGF has been one of the most extensively investigated neurotrophic factors. In our project, NGF was supplemented into the culture medium to evaluate the efficacy of neurotrophins on neurite outgrowth of DRG neurons. The following section will review the studies of NGF in neural tissue engineering.

NGF is crucial during the development of the nervous system and plays important roles in nerve regeneration after the PNS or CNS injury. Firstly, studies have shown that NGF could promote the survival and outgrowth of sensory neurons [96]. The mini-pump delivery of NGF, NT-3 and GDNF (but not BDNF) leads to the outgrowth of damaged axons and functional regeneration after dorsal root injury [46]. NGF can also be delivered by gene-modified fibroblast grafts, which has been demonstrated to induce robust neurite outgrowth of sensory neurons into the injured spinal cord [97]. However, extensive sprouting of the non-injured sensory axons caused by NGF is probably associated with chronic pain [98, 99].

To deliver the neurotrophin to the injured site in an efficient and controllable manner, tissue-engineered devices are widely used to encapsulate and release neurotrophic molecules. NGF could be integrated into a wide range of devices, such as conduits, microspheres, hydrogels, scaffolds, etc., and delivered via diffusion or released with the degradation of the devices [55]. Alginate, chitosan, poly (lactic acid) (PLA), poly (glycolic acid) (PGA), etc. have been frequently used to fabricate microspheres which hold great promise for the controlled release of biomolecules. The nerve conduits loaded with NGF-filled microspheres lead to dense fiber outgrowth of rat sciatic nerve gap compared

to the negative control groups [100]. Hydrogel is another superior substrate for the prolonged delivery of the neurotrophic factors. It has been demonstrated that hydrogels of low stiffness such as collagen, laminin or fibrin induce enhanced nerve regeneration than stiffer gels [101]. Moreover, NGF with gradient concentrations within the hydrogels has shown to guide the axonal outgrowth to the correct targets [102, 103].

1.3 Injectable Hydrogel for Nerve Injury Repair

Compared with the preformed scaffolds, injectable anisotropic hydrogels for nerve injury repair have recently drawn much attention due to the minimally invasive injection procedure, simulation of *in vivo* environment, improved graft integration, the capacity of filling the cavity of the injured site, etc [104, 105]. Prior to the injection, bioactive molecules and supportive cells can be incorporated by mixing with the hydrogel solution. Once injected to the lesion site, the injectable system will conform to the cavity shape and gel *in situ* under physiological conditions (Figure 1.7). Following gelation, these matrices could not only provide guidance and support for the regenerated axons but also prolong the delivery of therapeutic agents for nerve injury repair. Injectable hydrogel could be directly injected into the cyst after the CNS injury or accommodated within the nerve conduit for the PNS injury considering the requirements of mechanical support (Figure 1.8).

1.3.1 Materials

A wide variety of naturally-derived materials and synthetic polymers have been extensively investigated for nerve injury repair. To optimize and select the best candidate, a few design parameters need to be considered, including: biocompatibility, swelling behaviour, degradation rate, gelation property (gelation temperature, gelation time and gel strength), porosity, support for neural survival and neurite outgrowth, etc.

Natural materials featuring the superior biocompatibility can be divided into protein-based (collagen, fibrin, hyaluronic acid and Matrigel^{TM}) and polysaccharide-based (agarose, chitosan, methyl cellulose and alginate). To varying degrees, they can simulate the native ECM environment and provide a permissive environment for nerve regeneration. However, rapid degradation *in vivo* may limit their applications in many cases. In contrast, synthetic materials, such as poly(ethylene glycol) (PEG), poly(vinyl alcohol) (PVA), poly(glycolic acid) (PGA) and poly(lactic acid) (PLA), can provide a finely tunable degradation rate, greater mechanical strength, tailorable functional groups, etc. However, incompatibility with cell adhesion and neurite outgrowth has motivated the

modification of these synthetic polymers. By the covalent crosslinking of the reactive functional groups and biomolecules or combining with other natural materials, they may show great potential in neural tissue engineering [104, 106]. Here, we review some widely investigated natural materials.

Type I collagen is the major component of ECM throughout the body and has been extensively investigated for nerve injury repair. Also, several collagen-based products including nerve conduits, matrices, etc. have achieved approvals from the FDA [107, 108]. Gelation of collagen can be induced at physiological conditions. Research has demonstrated the favorable environment of collagen gels for neural survival and neurite outgrowth for both the injured CNS and PNS [109-111]. Due to the non-load bearing nature of spinal cord and brain, the collagen solution can be directly injected to the lesion site and fill the cavity *in situ*. Collagen gels can also be used as the fillings of the nerve conduits which hold great promise and exhibit positive outcomes for PNS injury [112]. Moreover, the amino acid sequences on collagen contain biologically adhesive sites for the supportive cells.

Given the rapid degradation of collagen gels *in vivo*, chemical crosslinkers (glutaraldehyde, diphenylphosphoryl azide, genipin, etc.) may be required to optimize the degradation rate and mechanical property. However, potential cytotoxicity may be induced by the crosslinking agent's residues. Compared to other crosslinking agents, genipin extracted from the gardenia fruit has attracted interest due to its low toxicity. It has been determined that genipin is about 10,000 times less cytotoxic than glutaraldehyde to 3T3 fibroblasts [113]. The detailed crosslinking mechanisms will be discussed in the next section.

Fibrin is another promising candidate of the injectable materials and the commercial fibrin sealant (Tisseel/Tissucol®) has been widely used for clinical hemostasis. Fibrin is the major component of the blood clots, which are biological gels that form through enzymatic crosslinking. Fibrin shows great efficacy of promoting neurite outgrowth and neural survival. Von et al. have determined that injection of fibrin gel into the cavity after rat spinal cord injury can integrate with the host tissue well and promote robust axonal outgrowth [114]. Incorporation of NT-3 into the fibrin gels have been demonstrated to promote robust neuronal outgrowth into the lesion site in the short term after rat spinal cord injury [115-117]. Fibrin hydrogel can also be modified with bioactive peptide domains [118, 119] to deliver and release the supportive cells and neurotrophins in a controllable manner. Similar to the collagen gel, fibrin hydrogel is less resistant to degradation

and has relatively weak mechanical property [120].

Other natural materials including chitosan, alginate and agarose are derived from non-animal source and have been widely used in tissue engineering due to the biodegradability, biocompatibility, ease of operation and enhanced mechanical property. Due to the non-animal and non-ECM origins, unmodified materials may require harsh gelation conditions and usually exhibit less intrinsic support for neurite outgrowth and neuronal survival. For example, alginate solution can easily form gels in the presence of divalent cations, however, an inhibitory effect on olfactory ensheathing glia, Schwann cells and DRG neurons has been demonstrated [121]. Modifications of these materials lead to enhanced cell adhesive and mild gelation process. For example, water soluble chitosan can be copolymerized with poly-L-lysine [122] and ionic crosslinking can be induced by β-glycerol phosphate [123]. Alginate has been covalently coupled with RGD peptide to improve the cell binding properties and alginate-RGD gels containing the supportive cells have shown significant enhancement of neuronal survival and neurite outgrowth [124, 125].

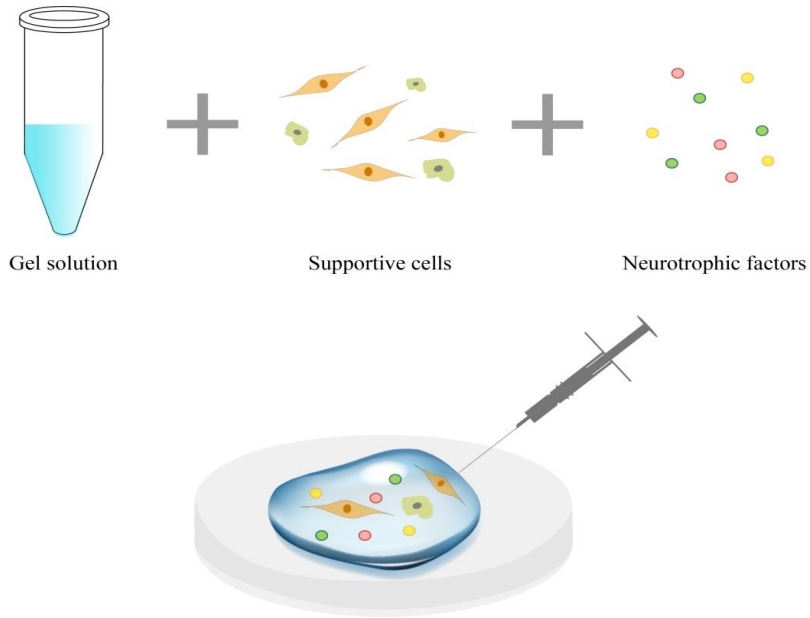

Figure 1.7 Illustration of the injectable hydrogels carrying supportive cells and neurotrophic factors.

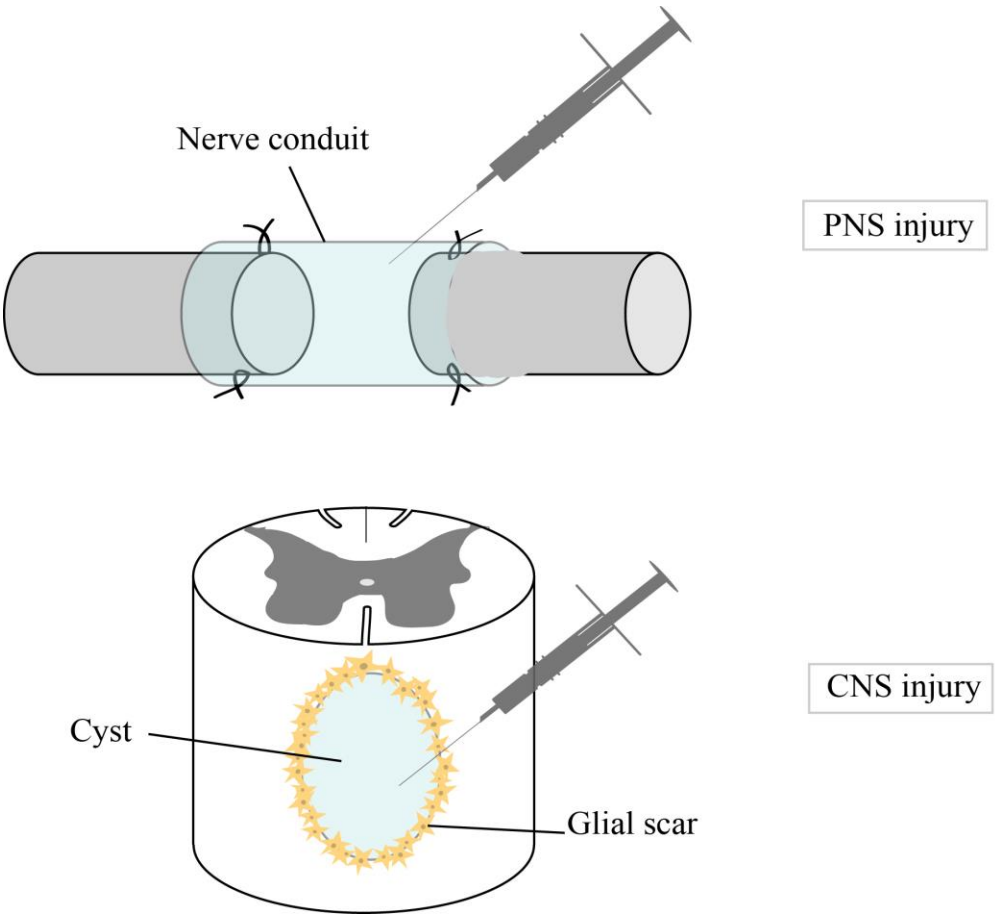

Figure 1.8 Strategies of injectable hydrogels for the PNS and CNS injury. Injectable hydrogels can be used as the fillings of the nerve conduits for the PNS injury, especially for large lesion gaps. For the CNS injury, gel solution can be directly injected to the cyst to gel *in situ* and promote axonal regeneration.

1.3.2 Physical vs. Chemical Crosslinking

Injectable hydrogels in tissue engineering can be classified into physical and chemical gels based on their gelation mechanisms [126]. Physical gels can undergo the liquid to gel transition triggered by physical stimuli such as temperature, pH, ionic concentration, self-assembly, etc. The advantages of physical gels include mild gelation process, no potentially cytotoxic crosslinkers involved, and the permissive substrates for cellular and molecular delivery. However, the mechanical strength of physical gels is typically weak and the physical gel can degrade easily *in vivo*. Chemical crosslinking generally results from the covalent bonding induced by chemical crosslinkers. Chemical gels can provide improved mechanical strength and resistance to degradation [105]. Since the residual crosslinkers cannot be effectively washed away prior to the

injection and gelation *in situ*, the crosslinkers should be non-cytotoxic. Table 1.1 has listed the gelation mechanism of commmonly injectable materials. In this research, we aim to explore the therapeutic potency of physically and chemically crosslinked collagen gels in nerve injury repair. Here, we take collagen and collagen-genipin gels for examples to evaluate the usefulness of the physical and chemical crosslinking mechanisms.

The collagen utilized in our project is 4 mg/mL type I rat tail collagen in a 0.1% acetic acid solution (Advanced BioMatrix, CA, USA). The collagen solution was neutralized on ice and allowed to gel at physiological temperature. The basic units of type I collagen are two α1(I) and one α2(I) chains which are highly enriched in the amino acid residues including glycine, proline and hydroxylysine. Under physiological conditions, these chains will spontaneously wrap around one another to form a unique triple helix structures. Numerous triple helices could twist together to induce the fibrous network which supports and promotes neurite extension (Figure 1.9) [127].

Alternatively, collagen can be covalently crosslinked to enhance the resistance to degradation and mechanical strength. The reaction may occur with the amino groups of lysine residues, the carboxyl groups or the hydroxyl groups [128]. Genipin extracted from fruits can be applied to crosslink the amino groups of the collagen and produce a deep blue colorant which can be used for food dyes. A scheme of the crosslinking mechanism between the amino groups and genipin is shown in the Figure 1.10 [129]. It has been demonstrated that the covalent bonding can enhance the stability of the collagen gels significantly [130]. Moreover, the genipin concentration could notably affect the degradability, swelling ratio, crosslinking level, and mechanical strength of collagen gels [131-134].

Table 1.1 Gelation Mechanisms of the Injectable Hydrogels for Nerve Injury Repair

	Material	**Gelation Mechanism**
Natural Material	Collagen	Thermal/Chemical crosslinking
	Fibrin	Enzymatic crosslinking
	Matrigel™	Thermal crosslinking
	Hyaluronic acid	Thermal/Chemical/Free radical crosslinking
	Chitosan	Ionic/Chemical crosslinking
	Alginate	Ionic crosslinking
Synthetic Material	PEG	Chemical/Radiation/Free radical crosslinking
	PVA	Thermal/Chemical/Free radical crosslinking

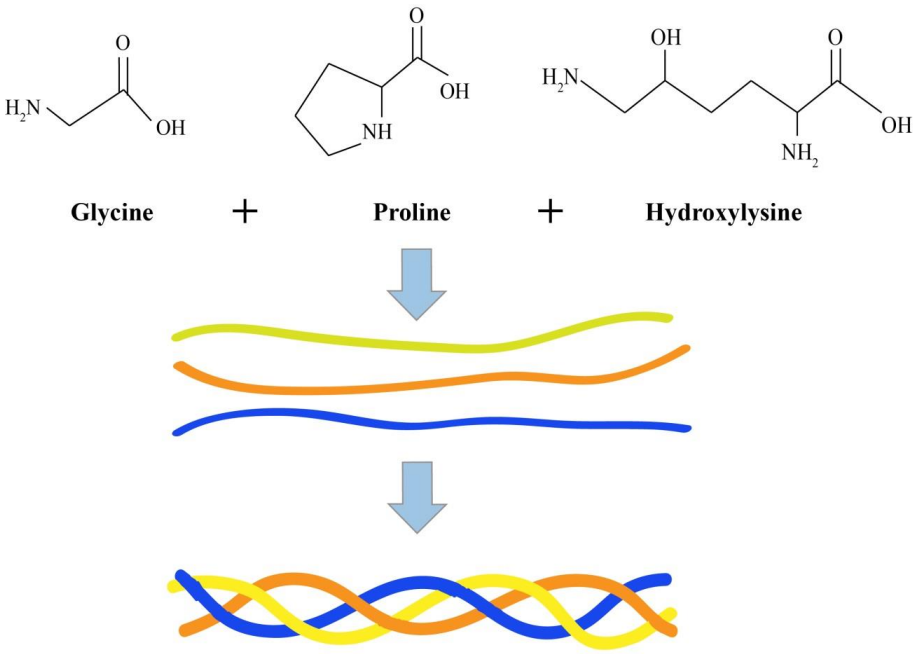

Figure 1.9 Structure of the physical collagen gels. Collagen gel is composed of the network of numerous triple-helix chains which contain glycine, proline and hydroxylysine.

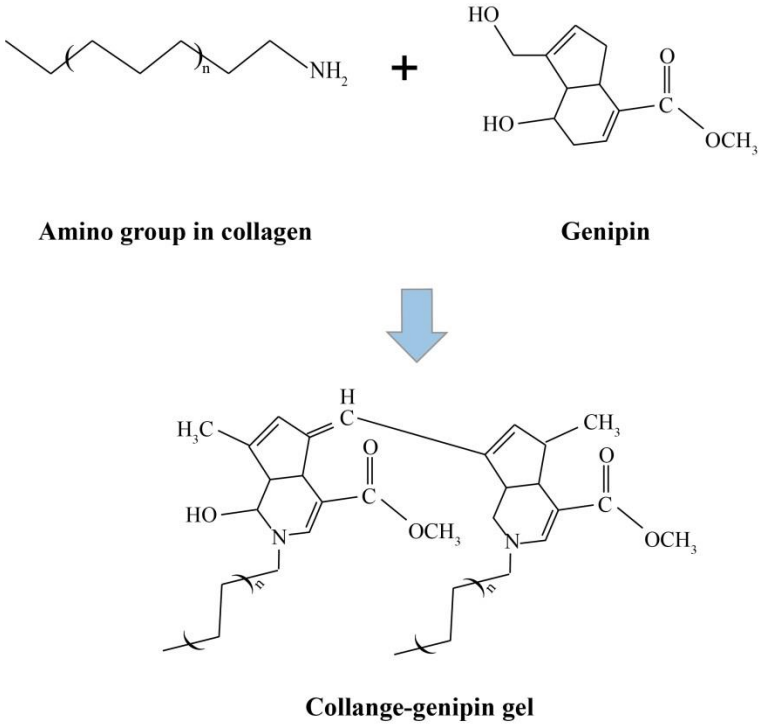

Figure 1.10 Scheme of the crosslinking mechanism of the collagen-genipin gel. The amino groups can be covalently crosslinked by genipin [106].

1.4 *In Vitro* Studies of Collagen and Collagen-genipin Gels for Nerve Injury Repair

Studies have shown that physically crosslinked collagen gels can support a wide range of cells, including fibroblasts, neural stem/progenitor cells, Schwann cells, olfactory ensheathing cells, DRG sensory neurons, etc. [135-140]. Celinda et al. have reported that the neurites of DRG explants can extend downwards and penetrate within the 3D collagen gels from the 2D-3D interaction surface and the length decreased with the increasing depth into the collagen gel [141]. Studies by Bozkurt et al. have shown that the Schwann cells packed within the DRG explants can migrate into the oriented 3D collagen sponge and provide guidance for the DRG axons within the scaffold [140]. Willits et al. have determined that the neurites of dissociated DRG neurons can grow within the collagen gels and that there is a correlation between the gel stiffness and the neurite extension [142].

Combinational strategy of molecular and cellular therapy in physical collagen gels has also been widely investigated to provide the controlled delivery of beneficial factors and promote neurite outgrowth. Katelyn et al. has characterized the supportive role of 3D collagen gels in neurite outgrowth of the dissociated DRG neurons. However, incorporation of 10 and 100 μg/mL laminin within the gel can reduce the neurite outgrowth without impacting the stiffness of the gels [143]. Suk et al. cultured neuron-like pheochromocytoma cells (PC12) on collagen gels with or without NGF. The results have shown that NGF could be released steadily from the gels to support the survival and neuronal differentiation of the PC12 cells [144]. In another study from Gingras et al., it has been determined that the addition of 10 ng/mL NGF can promote the neurite outgrowth of DRG sensory neurons cultured on the collagen gel [145].

Most of the biocompatibility studies of the chemical collagen-genipin gels were evaluated using the biomaterials in which the unreacted genipin residues have already been rinsed away. For example, Sundararaghavan et al. prepared the collagen gels, allowed the gels to crosslink in culture medium containing 1 or 10 mM genipin, and then replaced with genipin-free medium. The neurites of DRG explants can be directed and improved by the gradient stiffness of the gels [131]. It has also shown that the collagen gels crosslinked by 5 mM and 10 mM genipin lead to reduced cell survival of L929 fibroblasts compared to the collagen gel only [130]. However, the injectable hydrogels cannot be washed prior to the implantation due to the *in situ* application. Studies have demonstrated that mesenchymal stem cells and astrocytes can survive and proliferate within the collagen-genipin gels without the wash [131, 146]. Very limited studies

have been performed to evaluate the neurite outgrowth of DRG cultured on or within the injectable collagen-genipin gels.

1.5 Objectives

Injectable hydrogels have drawn great attention for their potential applications to neural tissue engineering. The overall goal of this research is to develop injectable collagen and collagen-genipin hydrogels and evaluate their therapeutic efficacy combining with cellular and molecular therapies for *in vitro* nerve injury repair. The specific objectives of this research are listed as follows.

(1) To synthesize collagen-based gels that are crosslinked either physically or chemically and to characterize the gels in terms of gelation properties, swelling and degradation behaviours and microstructures. The effect of collagen and genipin concentration on the gel properties will be evaluated and the appropriate formulations will be also determined according to the gelation behaviours and feasibility for subsequent studies.

(2) To evaluate the cytotoxicity of the injectable hydrogels to PRSCs in both 2D and 3D environments. The influence of collagen and genipin concentration on PRSCs viability will be studied and the appropriate formulation will be determined. Cell morphology and viability of PRSCs seeded onto and encapsulated within the hydrogels will also be compared.

(3) To examine the neurite outgrowth of DRG explants and dissociated neurons seeded on the surface of collagen and collagen-genipin gels in culture medium enriched with or without NGF. The effect of collagen/genipin concentration and NGF as molecular therapy for neurite outgrowth will be determined. Neurite length and morphology of DRG explants and neurons in a 2D injectable hydrogel system will be compared to assess the role of *in vitro* cell models for nerve injury repair.

(4) To assess the efficacy of the injectable hydrogel system infiltrated with the PRSCs in the neurite outgrowth of DRG explants and dissociated sensory neurons in the 3D environment. The influence of collagen/genipin concentration will be determined and the combinational strategy of PRSCs and injectable hydrogels for neurite outgrowth *in vitro* will be evaluated. Moreover, the response of different cell models to the injectable hydrogel system will be compared to study the cell-cell interactions and axonal structures of sensory neurons. The distinct DRG behaviour in 2D and 3D hydrogel system will be studied to lay the groundwork for future *in vivo* studies.

CHAPTER 2
MATERIALS AND METHODS

2.1 Hydrogel Preparation

The desired concentration of collagen gel solution was prepared on ice by mixing rat-tail type I collagen solution (4 mg/mL) (Advanced BioMatrix, USA), 10 × Dulbecco's Modified Eagle's medium (DMEM) (Sigma-Aldrich, Canada) and 1 × DMEM, and neutralized by 1 N NaOH (Sigma-Aldrich, Canada) to a pH of 7.0. Gelation of collagen gel was induced by transferring the mixture into a 37 °C incubator. To prepare collagen-genipin hydrogel, a stock solution of 20 mM genipin (Wako Pure Chemical, Japan) in 1 × phosphate buffered saline (PBS) (Sigma-Aldrich, Canada) was prepared freshly before mixing. Prior to gelation, genipin solution was mixed on ice with collagen solution, 10 × DMEM, 1 × DMEM and 1 N NaOH to a pH of 7.0. The mixture was then allowed to gel at 37 °C. The samples prepared for characterization studies are shown in Table 2.1.

2.2 Characterization of Collagen and Collagen-Genipin Hydrogels

Collagen and collagen-genipin hydrogels were characterized in terms of their rheology, swelling property, degradability and morphology *in vitro*.

2.2.1 Rheological Test

Rheological measurements were performed using an AR-G2 rheometer (TA instruments, DE, USA) with a cone and plate geometry (40 mm, 2°). Samples shown in Table 2.1 were initially prepared on the plate of the rheometer set at 15 °C.

A time sweep test was carried out to determine the gelation time and gel strength at 37 °C. Samples were warmed from 15 to 37 °C in 5 seconds, and the storage modulus (G') and loss modulus (G'') were obtained by time sweeps over a period of 0 to 300 s with a frequency of 1 Hz at a constant of 5 % strain amplitude. G' and G'' curves were plotted and the gelation time was defined as the crossover point of the G' and G''. During the time sweep test, G' indicated how gel strength varied over time.

A temperature sweep test was performed to determine the gelation temperature. Samples were warmed from 15 to 37 °C at the rate of 1 °C/min, and G' and G'' were measured with a frequency of 1 Hz at a constant of 5 % strain amplitude. G' and G'' curves were plotted and the gelation temperature was also defined as the crossover point of the G' and G''.

Table 2.1 Experimental Groups for Characterization Study

Formulation	Abbreviation	Number of Samples
1.5 mg/mL collagen	Col 1.5	3
2 mg/mL collagen	Col 2	3
2.5 mg/mL collagen	Col 2.5	3
2 mg/mL collagen + 0.25 mM genipin	Col 2-Gp 0.25	3
2 mg/mL collagen + 0.5 mM genipin	Col 2-Gp 0.5	3
2 mg/mL collagen + 1 mM genipin	Col 2-Gp 1	3
2 mg/mL collagen + 5 mM genipin	Col 2-Gp 5	3

2.2.2 Swelling Behaviour Test

Hydrogels shown in Table 2.1 were prepared as previously. After gelation occurred, the swelling behaviour was evaluated by immersing the gels in PBS for 24 hours at 37 °C. After 24 hours, excess PBS was removed with filter paper and the weight of each sample was measured. The swelling ratio of the hydrogels was calculated as:

$$\text{Swelling ratio} = [(W_S - W_0)/W_0] \times 100\ \% \quad (2.1)$$

where W_S is the wet weight of the swollen hydrogel and W_0 is the initial dry weight of the hydrogel after lyophilization by FreeZone freeze dry systems (Labconco, USA).

2.2.3 Degradation Test

Degradability of collagen and collagen-genipin hydrogels in PBS was determined by incubating the samples in PBS at 37 °C. Hydrogels shown in Table 2.1 were prepared as described previously and allowed to gel at 37 °C for 5 min. The initial dry weight of the hydrogel was obtained immediately after gelation and freeze-drying. At day 1, 7, 15 and 30, the hydrogel was removed from PBS, lyophilized and weighed. Degradability of the hydrogels was assessed by the percentage of weight remaining, which was calculated by the following equation:

$$W_R = [(W_0 - Wt)/W_0] \times 100\ \% \quad (2.2)$$

where W_R is the percentage of weight remaining, W_0 is the initial dry weight of the sample and Wt

is the dry weight of the sample after degradation.

2.2.4 Gel Morphology

Scanning electron microscopy (SEM) was employed to study the structure and morphology of the hydrogels. Gels shown in Table 2.1 were prepared as previously, frozen in liquid nitrogen and then lyophilized overnight. Freeze dried samples were fixed with conductive tape on a metal stub, sputter coated with a gold rod under vacuum, and then examined under a Phenom Pure desktop SEM (PhenomWorld, Eindhoven, Dutch) at a 15 kV accelerating voltage. The pore size and fiber diameter were estimated by ImageJ 1.48^{TM} software (National Institutes of Health, MD, USA).

2.2.5 Statistical Analysis

Data were reported as mean ± standard error of the mean. Level of significance was calculated using one-way analysis of variance (ANOVA), and Tukey's post-hoc test was applied for multi-comparisons among the experimental groups. Statistical analyses were performed using GraphPad Prism 6.0^{TM} software (GraphPad Software, San Diego, USA).

2.3 Characterization of Biocompatibility

2.3.1 Schwann Cell Culture

PRSCs were isolated from the sciatic nerves of adult male Sprague-Dawley rats euthanized with 2 % isoflurane. All materials were purchased sterile or filter sterilized with 0.22 μm filter prior to cell culture. Sciatic nerves wrapped in the muscle tissue from the upper dorsal thigh were cut and transferred to cold DMEM. After removing all connective tissue under dissecting microscope, nerve fragments were incubated with 10 mg/mL collagenase (Sigma-Aldrich, Canada) at 37 °C in a 5 % CO_2 incubator for 60 min. Homogeneous cell suspension was achieved by repeated trituration using a fire-polished Pasteur pipette. PRSCs were centrifuged and cultured in DMEM with 10% fetal bovine serum (FBS) (ThermoFisher Scientific, Canada) in a plastic tissue culture dish at 37 °C in a 5 % CO_2 incubator. Cells were passed at 85-100 % confluence and re-suspended in DMEM with 10 % FBS. PRSCs from two to five passages were used for the Live/Dead assay to determine the biocompatibility of collagen and collagen-genipin hydrogels.

2.3.2 Gel Preparation and Cell Seeding

To assess the biocompatibility, PRSCs were seeded either onto, or encapsulated within, the hydrogels as shown in Table 2.2. For PRSCs plated on the surface of the gels, hydrogels were prepared on the sterile 12-mm round glass coverslips in a 24-well plate and allowed to gel

completely at 37 °C. Coverslips were pre-coated with 1 mg/mL poly-$_L$-lysine (PLL) (Sigma-Aldrich, Canada) to prevent gels from detachment. PRSCs re-suspended in fresh DMEM with 10 % FBS were seeded over the hydrogels and tissue culture plate at a density of 40,000 cells/mL, and then incubated in culture medium at 37 °C in a 5 % CO_2 incubator. For PRSCs encapsulated in the gels, cells re-suspended in medium were gently pre-mixed with gel solution on ice at a density of 40,000 cells/mL and then gelation was induced by warming up to 37 °C. The mixtures were incubated in DMEM with 10 % FBS at 37 °C in a 5 % CO_2 incubator. Medium was replaced at 24 h and 48 h. PRSCs were seeded on the PLL-coated coverslips as a positive control.

Table 2.2 Experimental Groups for Live/Dead Assay

Formulation	**Number of Samples**	
	PRSC seeded onto the hydrogels	**PRSC encapsulated in the hydrogels**
1.5 mg/mL collagen	3	3
2 mg/mL collagen	3	3
2.5 mg/mL collagen	3	3
2 mg/mL collagen + 0.25 mM genipin	3	3
2 mg/mL collagen + 0.5 mM genipin	3	3
2 mg/mL collagen + 1 mM genipin	3	3
2 mg/mL collagen + 5 mM genipin	3	3

2.3.3 Live/Dead Assay

Cell viability and morphology were evaluated on day 3 by Live/Dead assay as following procedures. Samples were incubated with 1 μM calcein AM and 2 μM propidium iodide (Sigma-Aldrich, Canada) in DMEM with 10 % FBS for 1 h at 37 °C in a 5 % CO_2 incubator. Cells seeded onto the gels were imaged under Carl Zeiss Axiovert 100 fluorescent microscope (Carl Zeiss, Jena, Germany), while cells encapsulated in the gels were observed under Leica SP5 confocal microscope (Leica Microsystems, Wetzlar, Germany). Live cells were indicated by green fluorescence while dead cells were shown in red. Cell viability (%) was calculated as:

$$\text{Cell viability} = [(N_L/ (N_D+N_L)] \times 100\ \% \quad (2.3)$$

where N_L is the number of live cells and N_D is the number of dead cells.

2.3.4 Data Analysis

Live and dead cells in the images were analyzed and counted by ImageJ 1.48^{TM} software. Confocal images for single sample were merged by the z-project plugin of ImageJ prior to the counting. Ten random fields of the image for each sample were chosen for calculation. Data were reported as mean ± standard error. Statistical significance was assessed by one-way ANOVA followed by Tukey's test or Dunnett's test performed using GraphPad Prism 6.0^{TM} software.

2.4 Characterization of *In Vitro* Neurite Outgrowth Assay

2.4.1 DRG Explant and Dissociated Neuron Culture

DRG explants and dissociated neurons were obtained from adult male Sprague-Dawley rats euthanized with 2 % isoflurane. The vertebral columns were removed and kept in ice-cold L15 medium (Sigma-Aldrich, Canada). By cutting vertebral columns and pulling spinal cord, the ganglia were transferred to a 10 cm tissue culture dish containing 5 mL L15 medium on ice. Nerve roots and all surrounding connective tissue were carefully removed. The DRGs were dissected into the DRG explants under a dissecting microscope.

Dissociated DRG sensory neurons were prepared from dissected DRG explants by incubating in 10 mg/mL collagenase in L15 medium for 90 minutes, and then in 2 mg/mL trypsin for 30 minutes at 37°C. The sensory neurons were triturated to homogeneity using a fire-polished Pasteur pipette with decreasing bore sizes, and then washed in ice-cold L15 medium with 10 % horse serum (HS). DRG sensory neurons were centrifuged and re-suspended in DMEM with 10 % HS for cell seeding.

2.4.2 Gel Preparation and Cell Seeding

For explants and neurons seeded onto the hydrogels as shown in Table 2.3, hydrogels were prepared on the PLL-coated sterile coverslips in the 24-well plate on ice and allowed to gel completely at 37 °C. Three DRG explants per sample, or neurons at a final density of 10,000 cells/mL in fresh DMEM with 10% HS, were seeded onto the hydrogels and incubated at 37 °C in a 5 % CO_2 incubator for 10 days. The culture medium was supplemented with or without 50 ng/mL NGF (Sigma-Aldrich, Canada) to assess how NGF affected the neurite outgrowth. The medium was replaced after 24 h and every 48 h thereafter. DRG explants or neurons were seeded on laminin-coated coverslips as positive control.

For explants and neurons encapsulated within the hydrogels as shown in Table 2.4, three DRG explants per sample or neurons at a final density of 10,000 cells/mL were re-suspended in DMEM

with 10 % HS and mixed with gel solutions on ice. With or without the addition of PRSCs at a density of 40,000 cells/mL, gel mixtures were incubated in DMEM with 10 % HS at 37 °C in a 5 % CO_2 incubator and allowed to gel completely. The medium was replaced after 24 h and every 48 h thereafter. DRG explants or neurons were seeded on laminin-coated coverslips as positive control.

2.4.3 Immunocytochemistry

After 10 days culture, collagen and collagen-genipin gels with explants or dissociated neurons were fixed with 4 % paraformaldehyde at room temperature for 20 minutes and rinsed three times with PBS. Samples were then blocked with blocking solution (10 % HS, 0.05 % Tween 20 and 1 % bovine serum albumin in PBS) for 1 hour at room temperature and treated with the primary antibody (rabbit anti-beta III tubulin, Abcam Inc., Canada) diluted 1:500 overnight at 4 °C. After washing three times for 30 minutes with 0.05 % Tween 20 in PBS, the secondary antibody (goat anti-rabbit IgG Alex Fluor 488, Abcam Inc., Canada) was added and incubated for 1 hour at room temperature. Samples were then washed three times for 30 mins with 0.05 % Tween 20 in PBS and mounted on coverslips with Fluoromount-G (SouthernBiotech, USA). Cells-plated gels were imaged by conventional fluorescent microscopy, while cell-encapsulated gels were examined using a confocal microscope.

2.4.4 Data Analysis

Images were analyzed and measured with ImageJ 1.48^{TM} software. Neurite outgrowth of explants was quantified as the average neurite length and the density of neurites emitting from the explant. The neurite density was defined as the number of pixels covered by neurites divided by the total number of pixels covered by neurites and explant, which diminished the variation resulting from the differences of explant size. Neurite outgrowth of dissociated neurons was evaluated in terms of the average neurite length and the percentage of neurite-bearing neurons. Data were reported as mean ± standard error. Level of significance was calculated by one-way or two-way ANOVA with GraphPad Prism 6.0^{TM}. Tukey's and Dunnett's post-hoc tests were applied for multiple comparisons among the experimental groups or comparisons with the control group.

Table 2.3 Neurite Outgrowth Assay for DRG-plated Hydrogels

Formulation	DRG explants		DRG neurons	
	Conditions	No.	Conditions	No.
Laminin-coated coverslips	+/- NGF medium	3	+/- NGF medium	3
1.5 mg/mL collagen	+/- NGF medium	3	+/- NGF medium	3
2 mg/mL collagen	+/- NGF medium	3	+/- NGF medium	3
2.5 mg/mL collagen	+/- NGF medium	3	+/- NGF medium	3
2 mg/mL collagen + 0.25 mM genipin	+/- NGF medium	3	+/- NGF medium	3
2 mg/mL collagen + 0.5 mM genipin	+/- NGF medium	3	+/- NGF medium	3

Table 2.4 Neurite Outgrowth Assay for DRG-encapsulated Hydrogels

Formulation	DRG explants		DRG neurons	
	Conditions	No.	Conditions	No.
Laminin-coated coverslips	+/- PRSC	3	+/- PRSC	3
1.5 mg/mL collagen	+/- PRSC	3	+/- PRSC	3
2 mg/mL collagen	+/- PRSC	3	+/- PRSC	3
2.5 mg/mL collagen	+/- PRSC	3	+/- PRSC	3
2 mg/mL collagen + 0.25 mM genipin	+/- PRSC	3	+/- PRSC	3
2 mg/mL collagen + 0.5 mM genipin	+/- PRSC	3	+/- PRSC	3

CHAPTER 3

Experimental Results

3.1 Hydrogel Preparation

Collagen and collagen-genipin solutions were formulated on ice and incubated at 37 °C until gel formation. DMEM was added as the pH indicator to determine the neutralization point as the color changed from yellow to red. Figure 3.1 shows the effect of different formulations and time on the appearance of the hydrogels. With the increase of collagen concentration, collagen solutions (1.5, 2 and 2.5 mg/mL) transformed into intact and firm gels, which appeared from transparent to translucent color immediately after gelation occurred. 2 mg/mL collagen crosslinked by different concentrations of genipin (0.25, 0.5, 1 and 5 mM) displayed transparent color at 37 °C right after gelation as shown in Figure 3.1 (a). After incubation at 37 °C for 24 hours, the presence of genipin induced blue colorant. Gel color deepened with increasing the genipin concentration as shown in Figure 3.1 (b).

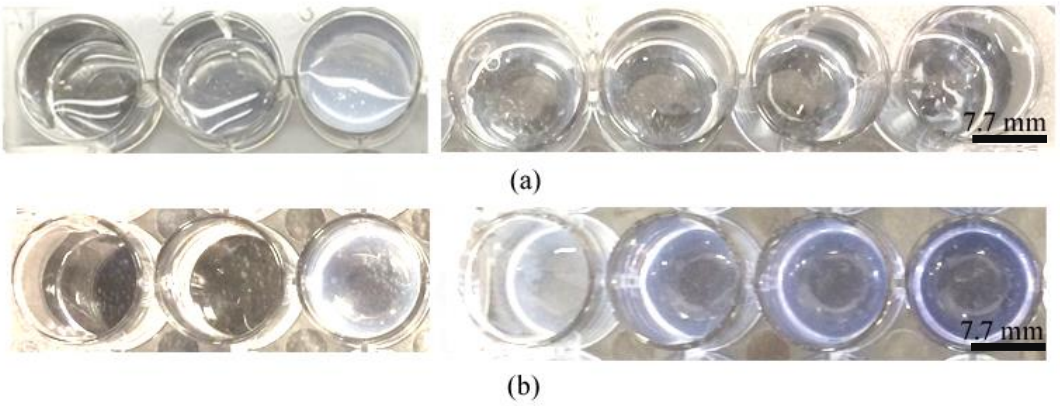

Figure 3.1 Appearance of collagen and collagen-genipin hydrogels obtained: (a) immediately after gelation, and (b) after incubation at 37 °C for 24 hours. From left to right: 1.5, 2 and 2.5 mg/mL collagen gels and 2 mg/mL collagen containing 0.25, 0.5, 1 and 5 mM genipin, respectively.

3.2 Characterization of Collagen and Collagen-Genipin Hydrogels

The gelation properties, swelling behaviour, degradability and gel morphology were evaluated to compare and characterize the physically and chemically crosslinked hydrogels.

3.2.1 Gelation Properties

To determine the gelation time, gelation temperature and gel strength, the storage modulus (G') and loss modulus (G'') data were obtained in a rheological test. G' and G'' curves were plotted to investigate the viscoelastic properties of collagen and collagen-genipin hydrogels.

Figure 3.2 shows an example of rheological data of 2 mg/mL collagen (Col 2) hydrogel. Figure 3.2 (a) (b) display the G' and G'' curves of the time sweep test ranging from 0 to 300 s at 37 °C. G' and G'' showed a tendency to increase and crossed at a point indicating gel formation. After gelation occurred, G' became larger than G'' and reached a plateau. Gel strength (G') of the plateau was recorded at 300 s. Figure 3.2 (c) (d) show the G' and G'' curves of the temperature sweep test ranging from 15 to 37 °C and the crossover point represents the gelation temperature.

Gelation time as determined by the method described above is shown in Figure 3.3 (a). The gelation time of physically crosslinked collagen gels (1.5, 2 and 2.5 mg/mL) was 35.8 ± 0.8, 32.5 ± 1.1 and 27.3 ± 0.8 s, respectively. One-way ANOVA showed collagen concentration affected the gelation time significantly. Tukey's test showed significant differences except between Col 1.5 and Col 2. For collagen-genipin gels, one-way ANOVA demonstrated no significant effect of genipin concentration on gelation time when compared to 2 mg/mL collagen.

Figure 3.3 (b) shows the determination of gelation temperature. The gelation temperature of 1.5, 2 and 2.5 mg/mL collagen gels was 32.5 ± 0.4, 31.0 ± 0.5 and 29.5 ± 0.5 °C, respectively. Gelation temperature decreased with increasing collagen concentration. One-way ANOVA indicated a significant effect of collagen concentration on gelation temperature. Tukey's post-hoc test determined that there was a significant difference of gelation temperature between 1.5 and 2.5 mg/mL collagen gels. The gelation temperature of 2 mg/mL collagen crosslinked by the highest concentration of genipin (5 mM) was 30.8 ± 0.7 °C. Statistically, there was no significant effect of genipin concentration on gelation temperature when compared to 2 mg/mL collagen.

Gel strength represented by G' was obtained in the time sweep test at 300 s. As shown in Figure 3.3 (c), the gel strength of 1.5, 2 and 2.5 mg/mL collagen gels was 39.7 ± 1.3, 43.9 ± 2.1 and 54.3 ± 4.1 Pa, respectively. Gel strength increased with increasing collagen concentration. One-way ANOVA demonstrated the significant effect of collagen concentration on gel strength.

For collagen-genipin gels, the gel strength of Col 2-Gp 5 was 58.9 ± 1.7 Pa with an increase of 34 % when compared to Col 2. Genipin concentration has a significant effect on the gel strength at 300 s as determined by one-way ANOVA.

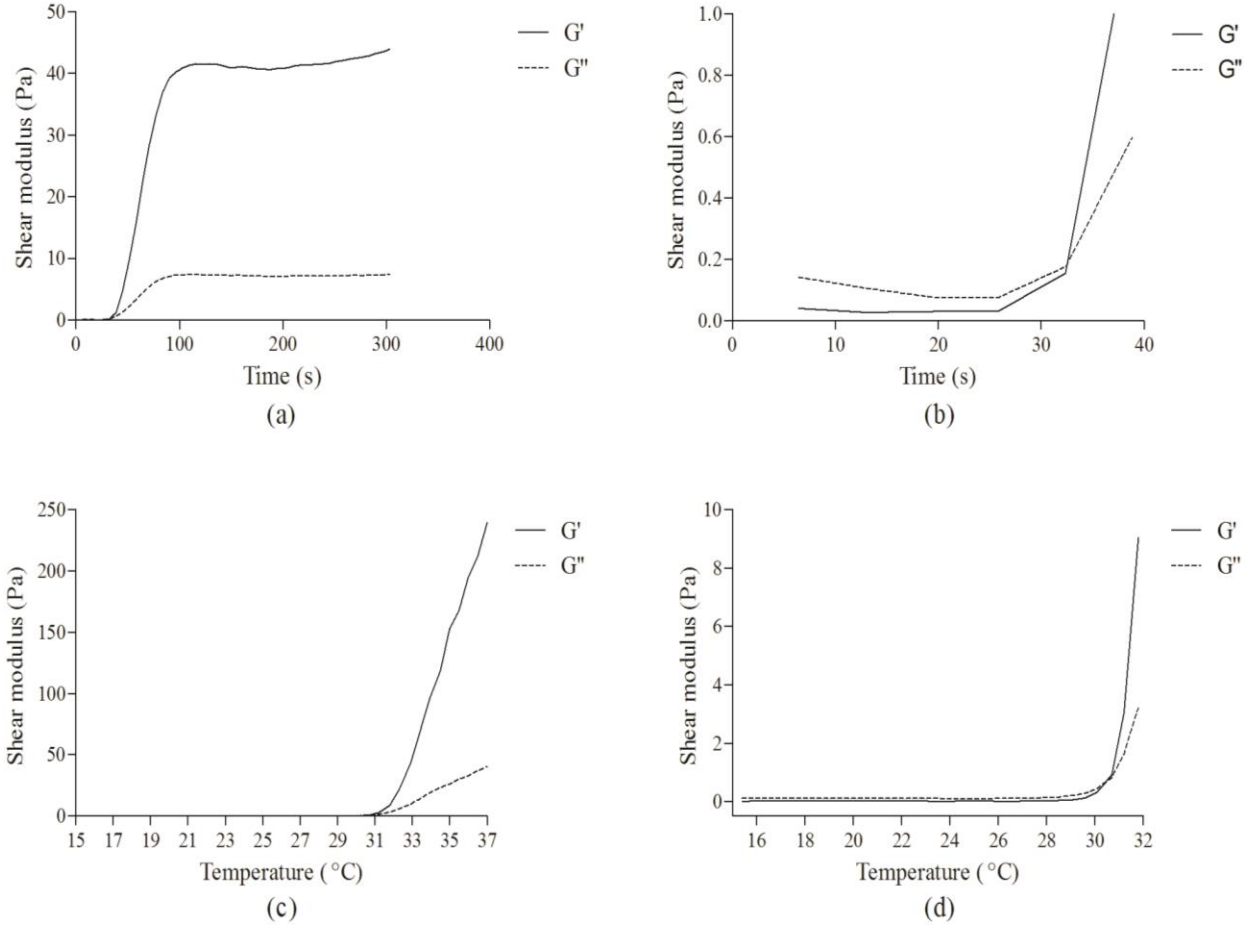

Figure 3.2 Examples of rheological data of 2 mg/mL collagen hydrogel: (a) Time sweep test ranging from 0-300 s at 37 °C, a constant 5 % strain and a frequency of 1 Hz; (b) Close-up view of the crossover point of G' and G'' in the time sweep test; (c) Temperature sweep test ranging from 15-37 °C at a 5 % strain and a frequency of 1 Hz; (d) Close-up view of the crossover point of G' and G'' in the temperature sweep test.

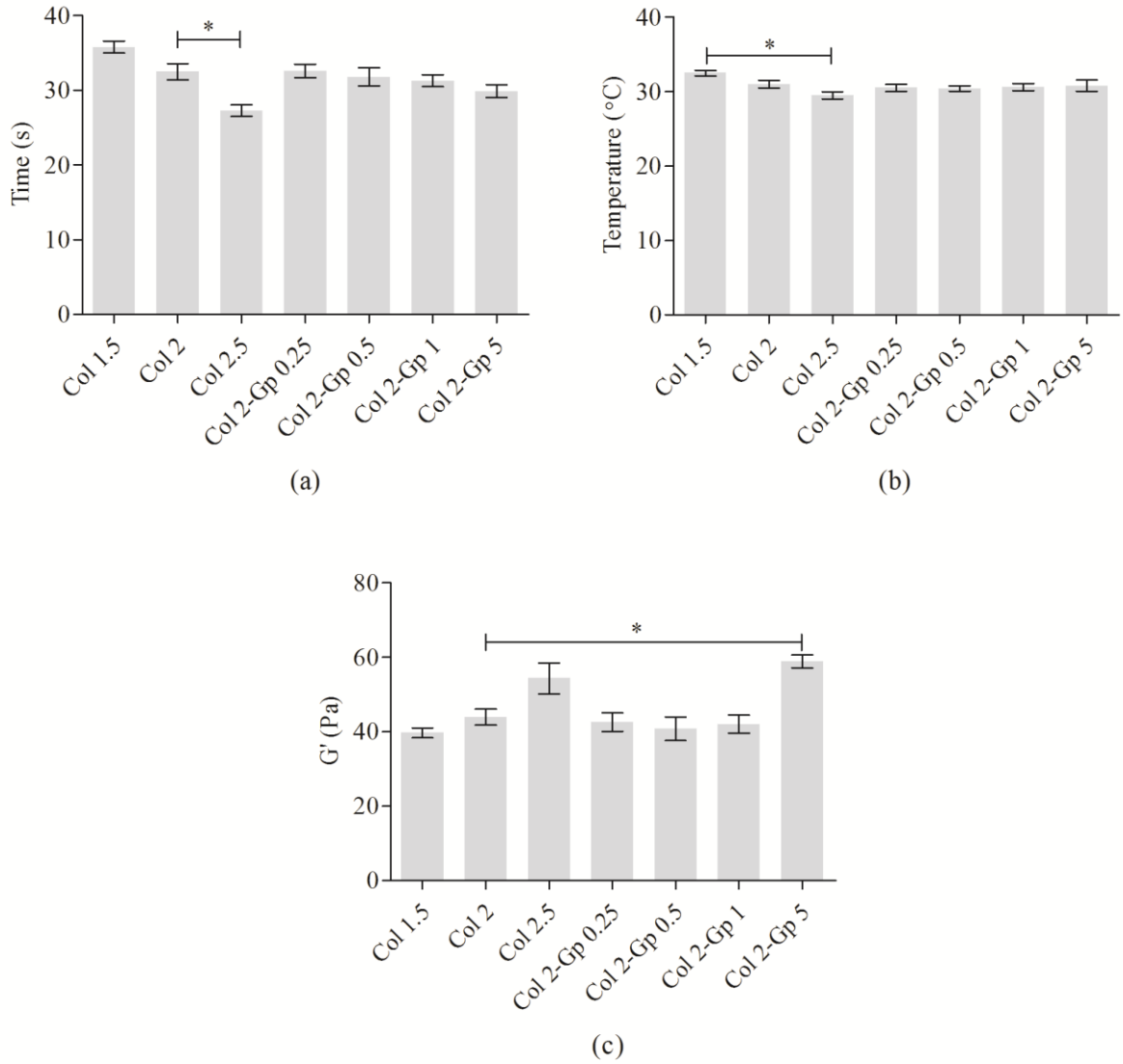

Figure 3.3 Results of the rheological test of collagen and collagen-genipin hydrogels: (a) Gelation time at 37 °C; (b) Gelation temperature; (c) Gel strength (G') at 300 s. Error bars stand for standard error. n=3, *p<0.05, **p<0.01, ***p<0.0001.

3.2.2 Swelling Ratio

To investigate the swelling behaviour of physically and chemically crosslinked gels in PBS, the swelling ratio was calculated and shown in Figure 3.4. The swelling ratio of collagen gels (1.5, 2 and 2.5 mg/mL) was 1116 ± 33, 818 ± 48 and 698 ± 26 %, respectively. Swelling ratio decreased with the increase of collagen concentration. One-way ANOVA demonstrated the significant effect of collagen concentration on the swelling behaviour. Compared to Col 2, the addition of genipin (0.25, 0.5, 1 and 5 mM) led to a decrease of the swelling ratio: 664 ± 49, 724 ± 44, 529 ± 45 and 464 ± 22 %, respectively. A statistically significant effect of genipin concentration on the swelling ratio was determined. In the presence of 1 and 5 mM genipin, swelling ratios were significantly reduced from the value of 2 mg/mL collagen gel.

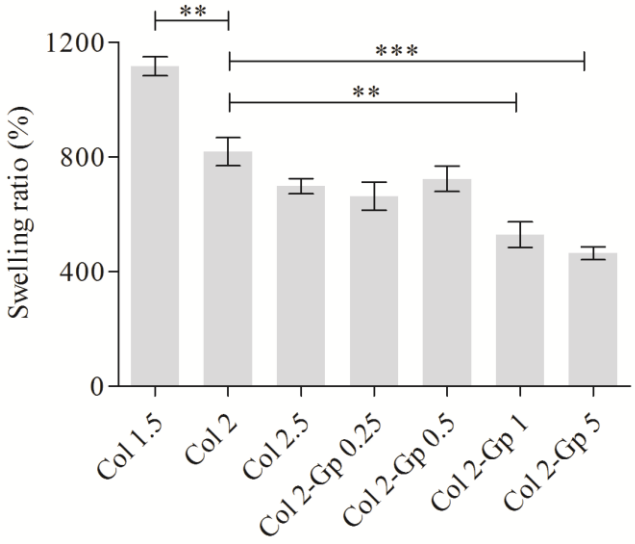

Figure 3.4 Swelling ratio of collagen and collagen-genipin hydrogels immersed in PBS for 24 h at 37 °C. Error bars stand for standard error. n=3, *p<0.05, **p<0.01, ***p<0.0001.

3.2.3 Degradation Study

Collagen is regarded to be one of the most promising natural biomaterials, however its rapid degradation *in vivo* limits its application. Therefore, how to optimize the degradation property should be considered. In this study, degradation experiments were performed to evaluate the effects of the physical and chemical crosslinking mechanisms induced by temperature and genipin, respectively, on degradation behaviour. Degradability was assessed by the weight remaining ratio (%) obtained on day 1, 7, 15 and 30 after incubation in PBS. The results are presented in Figure 3.5.

After immersion in PBS for 1 day, the weight remaining ratios of collagen gels (1.5, 2 and 2.5 mg/mL) was 91 ± 2.4, 92 ± 1.3 and 95 ± 2.7 %, and the value for 2 mg/mL collagen crosslinked by the highest concentration of genipin (5 mM) was 96 ± 1.6 %. One-way ANOVA revealed no significant differences among all experimental groups.

On day 7, the weight remaining ratios of collagen gels (1.5, 2 and 2.5 mg/mL) decreased to 80 ± 2.3, 88 ± 2.2 and 92 ± 1.3 %, respectively. Weight remaining ratio of collagen gels increased with increasing collagen concentration. One-way ANOVA confirmed the significant effect of collagen concentration on degradation behaviour of the physically crosslinked gels. There was no significant difference between 2 mg/mL collagen and 2 mg/mL collagen crosslinked by genipin (0.25-5 mM).

On day 15, the percentage of weight remaining for collagen gels (1.5, 2 and 2.5 mg/mL) was 71 ± 4.4, 74 ± 2.6 and 85 ± 0.9 %, respectively. Resistance to degradation was enhanced with increasing the collagen concentration. The weight remaining of collagen-genipin gels ranged from 81 ± 1.1 (0.25 mM) to 88 ± 2.2 % (5 mM). Compared to Col 2, significant difference between Col 2 and Col 2-Gp 5 was indicated by Tukey's test. One-way ANOVA determined the significant effect of collagen concentration on degradation behaviour. On the contrary, there was no significant effect of genipin concentration on degradability.

The weight remaining of 2 mg/mL collagen was reduced from 92 ± 1.3 % on day 1 to 55.3 ± 1.0 % on day 30, whereas the weight remaining ratio of 2 mg/mL collagen crosslinked by highest concentration of genipin changed from 96 ± 1.6 % on day 1 to 77 ± 1.9 % on day 30. Two-way ANOVA demonstrated significant effects of collagen concentration and degradation time on degradation behaviour of collagen gels. Compared to 2 mg/mL collagen gel only, the weight remaining ratio increased significantly with the presence of genipin, whereas no significant effect of genipin concentration was indicated statistically.

The results indicated that the weight remaining ratio increased significantly as increasing collagen concentration. Compared to the 2 mg/mL collagen only, crosslinking induced by genipin can improve the resistance to degradation of collagen gels in PBS starting from day 15 to day 30. However, genipin concentration had no significant effect on degradation behaviour in PBS at a period of 30 days.

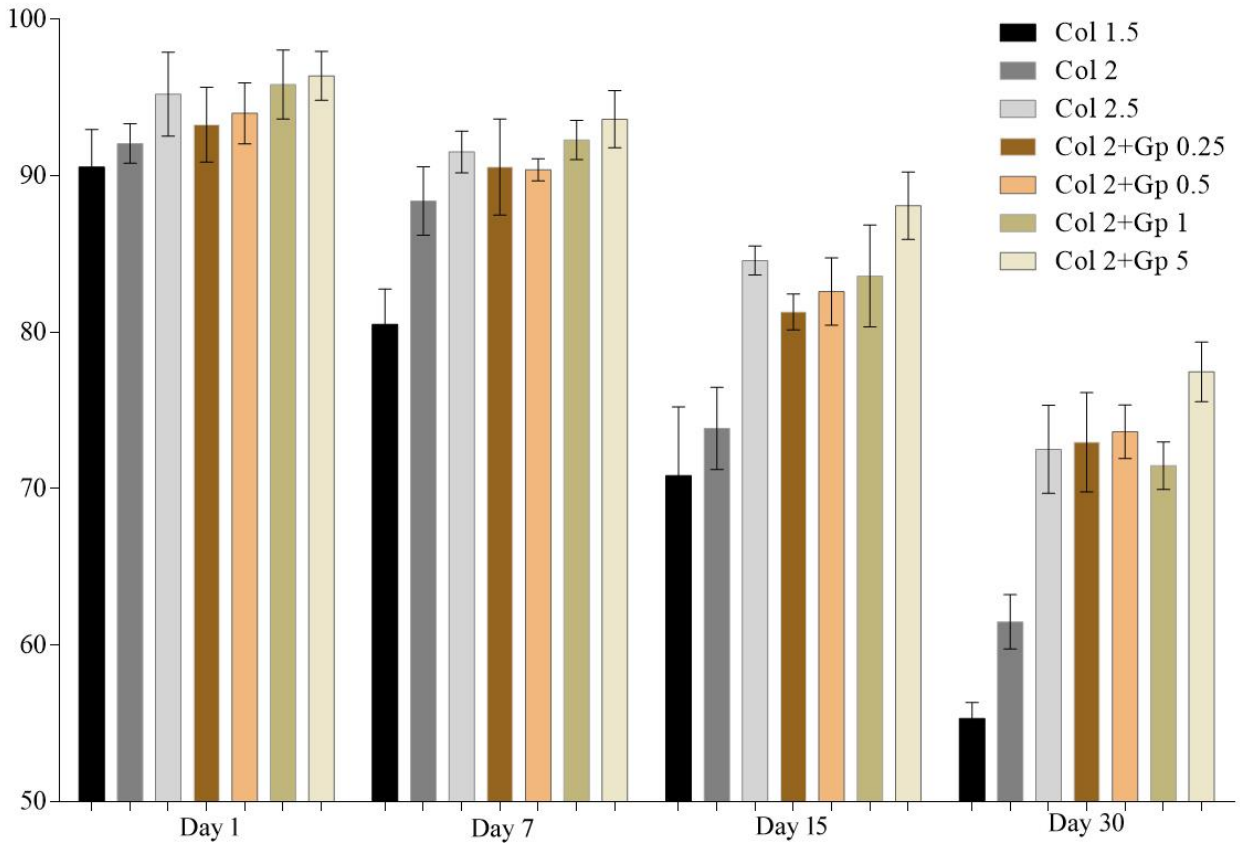

Figure 3.5 Weight remaining ratio of collagen and collagen-genipin hydrogels incubated in PBS for 1, 7, 15 and 30 days. Error bars stand for standard error. n=3.

3.2.4 Gel Morphology

To evaluate the morphology and inner-structure of collagen and collagen-genipin hydrogels, cross-sections of the lyophilized gels were exposed and observed under SEM microscope (Figure 3.6).

SEM images (Figure 3.6 (a-c)) of physically crosslinked collagen gels exhibit fibrous and porous structures with the average pore size of 3.3 μm and fiber diameter of 230 nm, approximately. There was no obvious effect of collagen concentration on the pore size or fiber diameter. However, with the increase of collagen concentration, the portion of porous network decreased slightly.

Figure 3.6 (d-g) displays the SEM images of chemically crosslinked collagen-genipin gels. Comparing with the SEM image of 2 mg/mL collagen gel only (Figure 3.6 (b)), hydrogels containing high concentration of genipin exhibited a very dense fibrillary network. In the presence of 0.25 mM genipin, the average pore size decreased to 1.5 μm and the fiber diameter was reduced to 160 nm, approximately. With the increase of genipin concentration, the pore structure

diminished slightly and the fiber diameter remained at a similar level. Collagen hydrogel crosslinked by 5 mM genipin aggregated and collapsed to very dense fibrillary clusters and few pore structures were observed. With the addition of genipin, the shrinkage of the porous structure shown in the SEM images correlated with the results of the swelling behaviour.

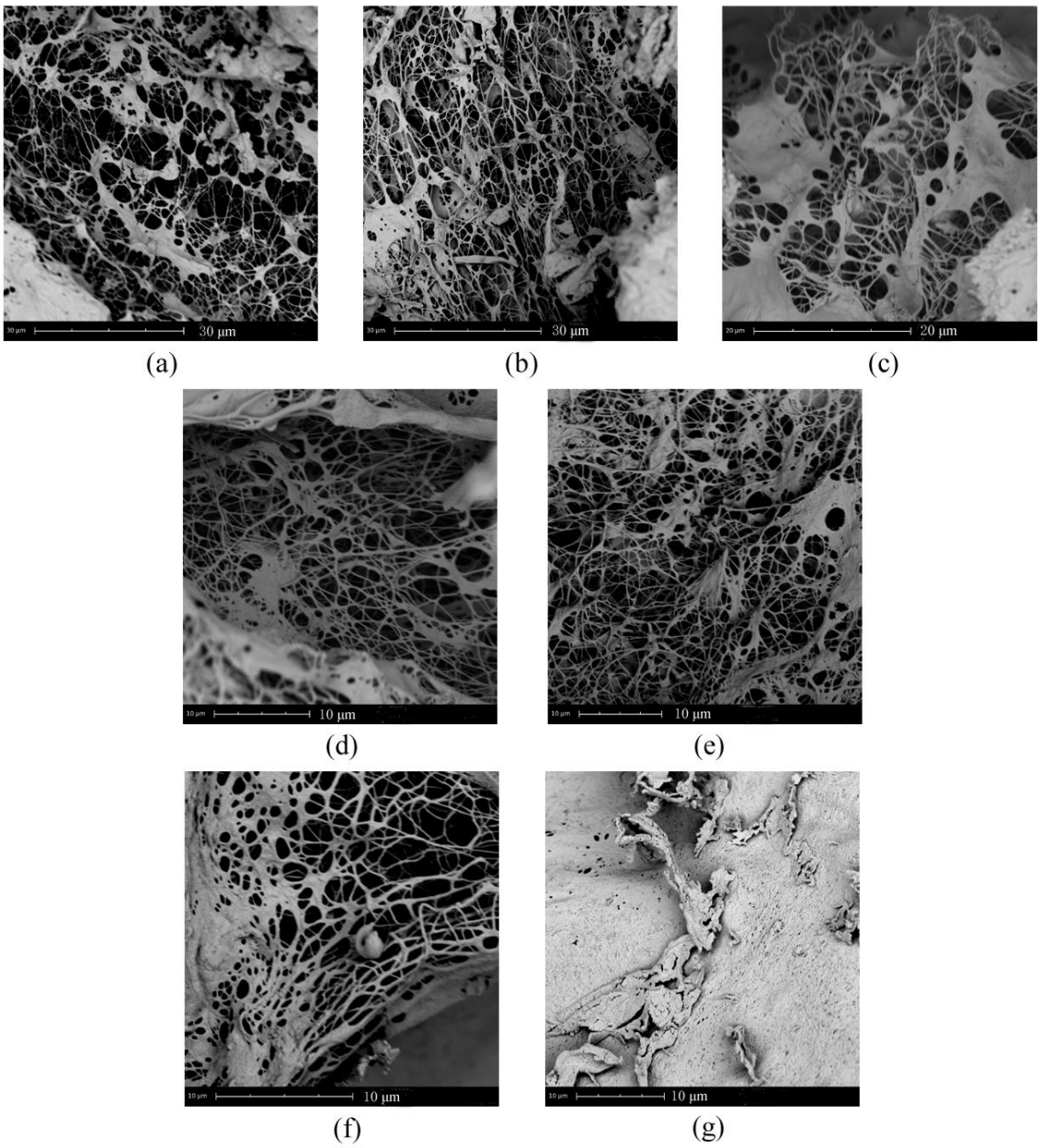

Figure 3.6 SEM images of the cross-section area of collagen and collagen-genipin hydrogels: (a-c) 1.5, 2 and 2.5 mg/mL collagen gels; (d-g) 2 mg/mL collagen gels crosslinked by 0.25, 0.5, 1 or 5 mM genipin, respectively.

3.3 Biocompatibility

The long-term strategy for this project is to produce a gel with a permissive environment for infiltrated supportive cells to bridge the injured site and promote axonal regeneration. PRSCs are one of the most promising candidates for cell transplantation in the application of nerve injury repair. To evaluate the biocompatibility of PRSCs on 2D or 3D environment *in vitro*, PRSCs were seeded onto the surface or encapsulated within the collagen and collagen-genipin gels, and then cultured for 3 days. Biocompatibility was evaluated by two parameters: cell viability and cell morphology.

3.3.1 Schwann Cell Culture

PRSCs cultured on tissue culture plate served as positive control. After 3 days culture, PRSCs displayed typical spindle-like morphology and the majority of the cells were alive indicated by green fluorescent in the Live/Dead assay as shown in Figure 3.7 (a) and Figure 3.9 (a).

3.3.2 Biocompatibility of Cell-plated Hydrogels

PRSCs were seeded onto the preformed collagen and collagen-genipin gels and cultured for 3 days. Cell viability and morphology were evaluated by Live/Dead assay and observed by fluorescence microscopy.

As shown in Figure 3.7 (b-d), PRSCs cultured on physically crosslinked collagen gels exhibited spindle-like morphology. Figure 3.8 shows that the cell viability of the positive control and the collagen gels of 1.5, 2 and 2.5 mg/mL was 98 ± 0.7, 96 ± 0.8, 84 ± 1.4 and 85 ± 2.0 %, respectively. One-way ANOVA determined that there was a significant difference of cell viability between the positive control and collagen gels. Comparing to the tissue culture plate, collagen concentration had a significant effect on PRSCs viability as indicated. Cell viability decreased with increasing collagen concentration.

For chemically crosslinked gels, the majority of surviving PRSCs seeded onto the Col 2-Gp 0.25 and Col 2-Gp 0.5 gels displayed spherical (Figure 3.7 (e) and (f)). However, very few viable PRSCs were observed on 2 mg/mL collagen gels crosslinked by higher concentrations of genipin (1 or 5 mM) and all surviving cells exhibited a spherical shape, which indicated high cytotoxicity and non-favorable environment for PRSCs (Figure 3.7 (g) and (h)). Cell viability of PRSCs seeded on 2 mg/mL collagen gels crosslinked by 0.25 and 0.5 mM genipin was 68 ± 1.2 and 62 ± 1.4 %, with a decrease of 19 % and 26 % when compared to 2 mg/mL collagen gel.

To summarize, PRSCs seeded onto 1.5 mg/mL collagen gels had the highest cell viability

among all experimental groups and exhibited typical spindle-like morphology. Compared to the chemically crosslinked collagen-genipin gels, physically crosslinked collagen gels provided more favorable environment possibly resulting from the adhesive property of collagen. The Live/Dead assay indicated that high concentrations of genipin (1 or 5 mM) inhibited the cell viability of PRSCs significantly.

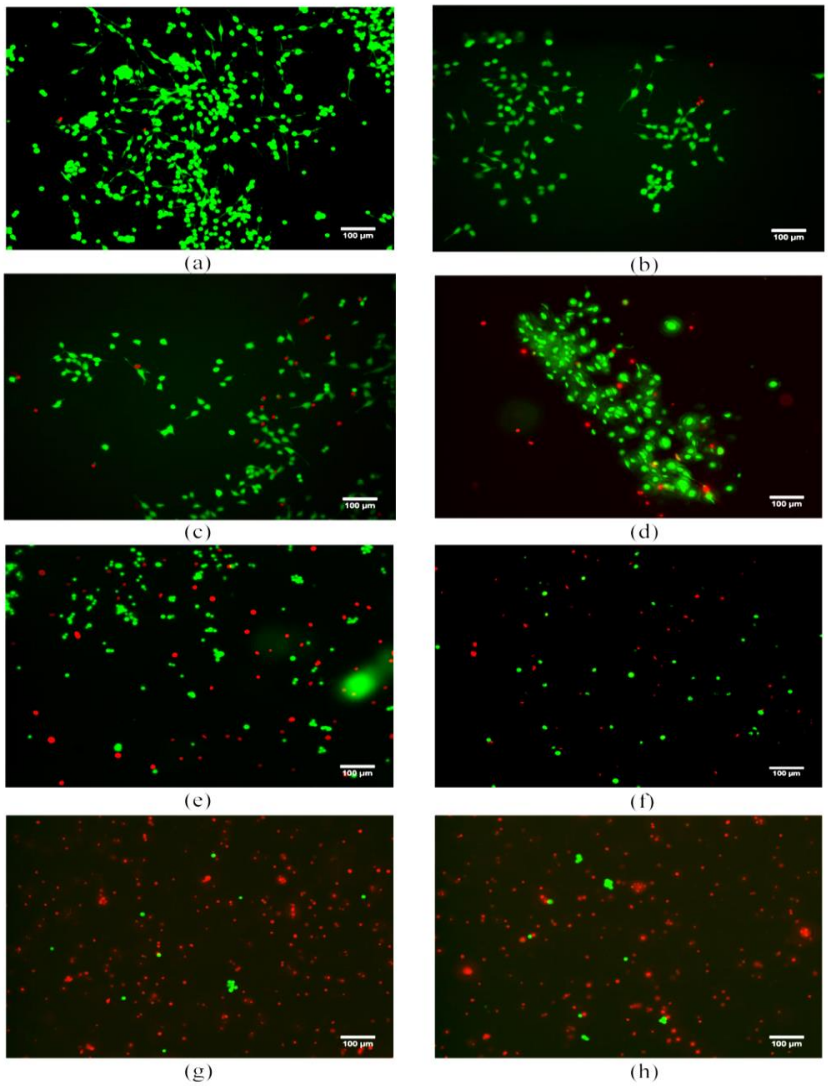

Figure 3.7 Live/Dead staining of rat PRSCs cultured on the surface of collagen and collagen-genipin hydrogels for 3 days: (a) tissue culture plate; (b-d) 1.5, 2 and 2.5 mg/mL collagen gels; (e-h) 2 mg/mL collagen gels crosslinked by 0.25, 0.5, 1 and 5 mM genipin, respectively. Green and red fluorescence indicate live and dead PRSCs, respectively. Scale bar=100 μm.

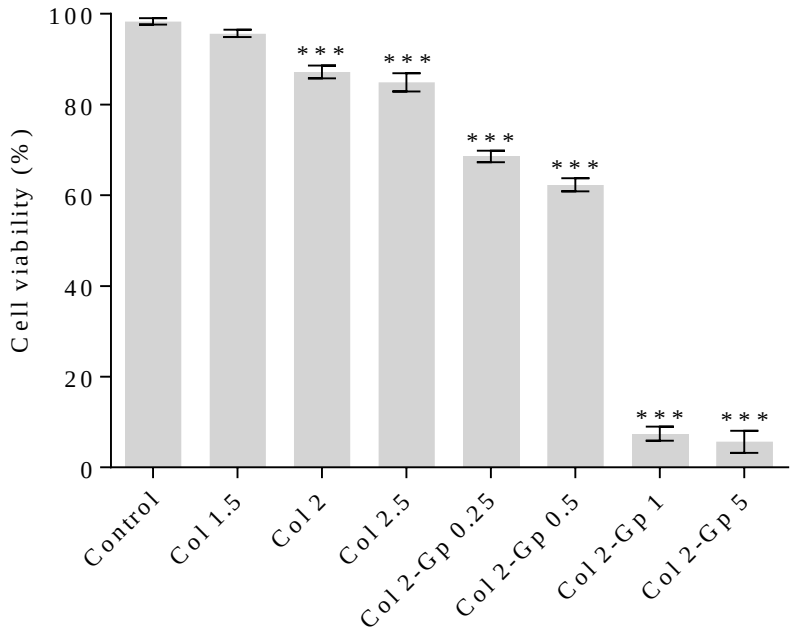

Figure 3.8 Cell viability of rat PRSCs cultured on different surfaces for 3 days. * indicates a statistically significant difference when compared to the control group (tissue culture plate). n=3, *p<0.05, **p<0.01, ***p<0.0001. Error bars stand for standard error.

3.3.3 Biocompatibility of Cell-encapsulated Hydrogels

PRSCs were mixed with the gel solution thoroughly on ice and transferred to a 37 °C incubator immediately, preventing cells from sinking to the glass bottom, and were then cultured for 3 days. Cell viability and morphology were evaluated by Live/Dead assay and observed under a confocal microscope. Figure 3.9 shows the max-intensity stacks of confocal images. PRSCs cultured on tissue culture plate served as positive control as shown in Figure 3.9 (a).

After cultured for 3 days, PRSCs encapsulated into 1.5, 2 and 2.5 mg/mL collagen gels displayed typical spindle shape as shown in Figure 3.9 (a-c). Cell viability within the collagen gels (1.5, 2 and 2.5 mg/mL) was 95 ± 1.4, 89 ± 1.0 and 81 ± 1.7 %, respectively. Cell viability decreased with increasing collagen concentration. Comparing to the tissue culture plate, one-way ANOVA determined that there was a significant effect of collagen concentration on cell viability. There was a strong correlation of cell viability of PRSCs either seeded onto or encapsulated within the physically crosslinked collagen gels.

For collagen-genipin gels, cell viability of PRSCs encapsulated within 2 mg/mL collagen gel crosslinked by 0.25 mM genipin was 71 ± 2.1 %, with a decrease of 27 % and 20 % comparing to

the viability of tissue culture plate and 2 mg/mL collagen gels, respectively. The majority of surviving cells exhibited spherical as shown in Figure 3.9 (d). Very few PRSCs survived within 2 mg/mL collagen gels crosslinked by 0.5 mM genipin and all cells were dead in 2 mg/mL collagen gels crosslinked by higher concentration of genipin. One-way ANOVA indicated a significant effect of genipin concentration on cell viability. Significant differences of cell viability for collagen-genipin gels were also determined when compared to the positive control group or 2 mg/mL collagen gel only.

These results demonstrated that PRSCs were less tolerant to 3D environment with the presence of genipin. Physically crosslinked collagen gels showed higher cell viability than collagen-genipin gels either in 2D or 3D experiments. Due to the cytotoxicity of high concentration genipin confirmed by 2D and 3D Live/Dead assays, 0.25 and 0.5 mM genipin were applied for the following studies.

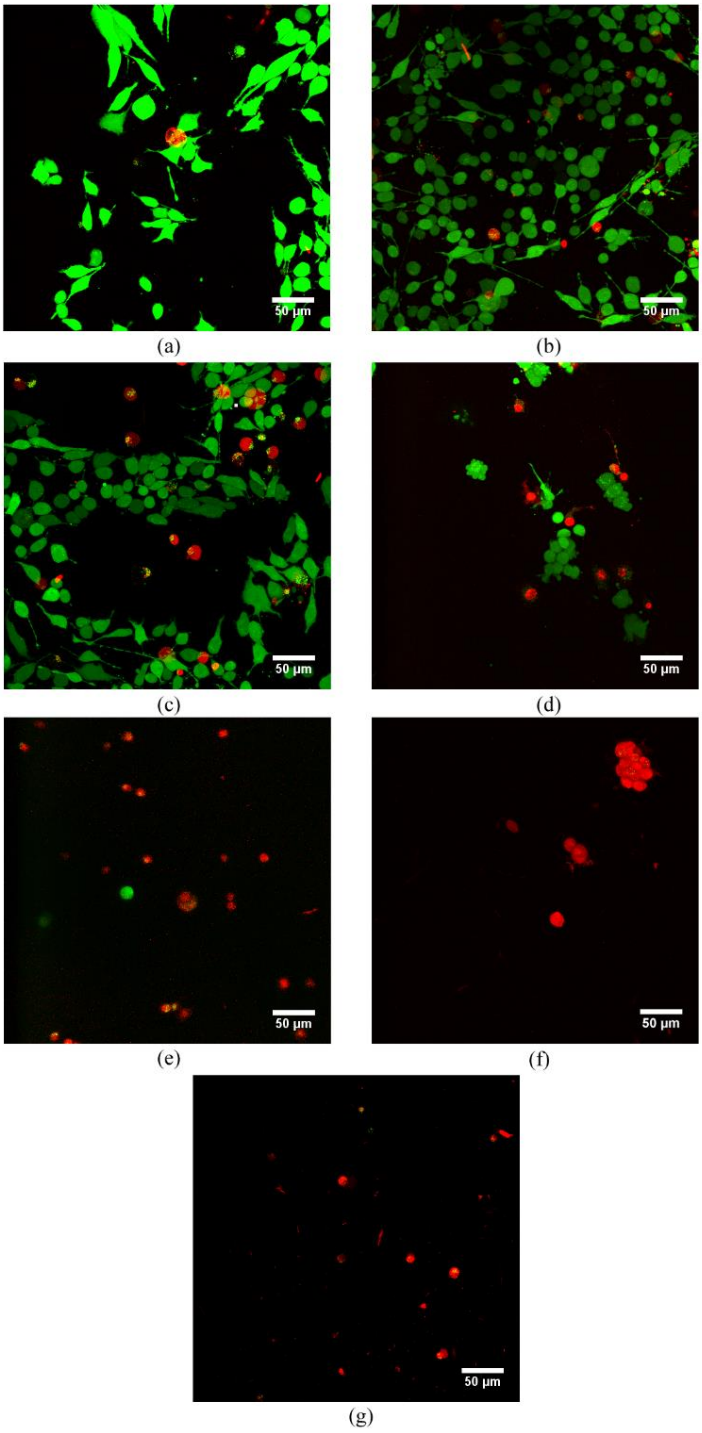

Figure 3.9 Live/Dead staining of rat PRSCs encapsulated within collagen and collagen-genipin hydrogels cultured for 3 days: (a-c) 1.5, 2 and 2.5 mg/mL collagen gels; (d-g) 2mg/mL collagen gels crosslinked by 0.25, 0.5, 1 and 5 mM genipin, respectively. Green and red fluorescence indicate live and dead PRSCs, respectively. Scale bar=50 µm.

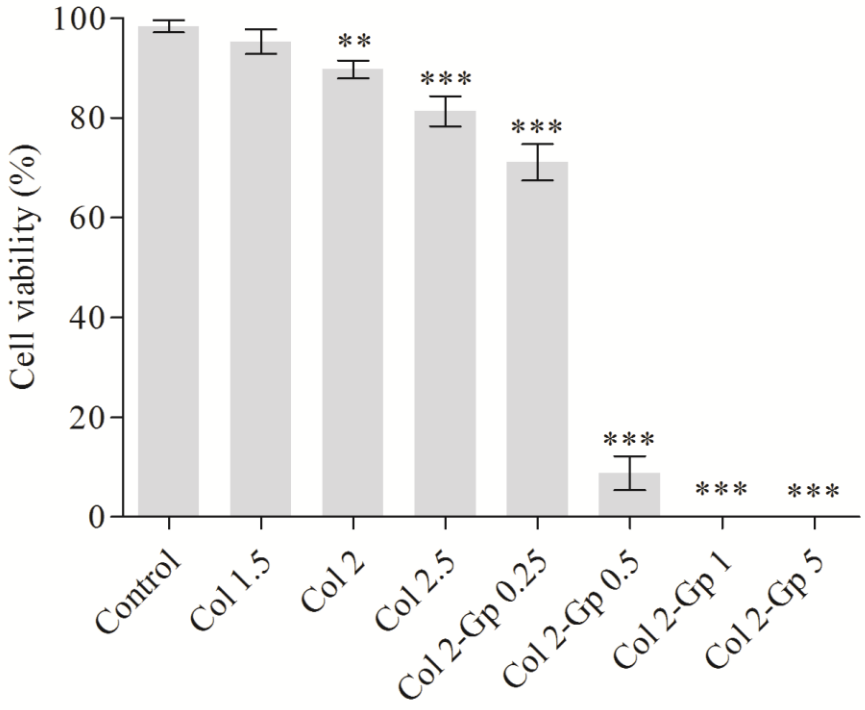

Figure 3.10 Cell viability of rat PRSCs cultured within collagen and collagen-genipin gels for 3 days. * indicates a statistical difference when compared to the control group (tissue culture plate). n=3, *p<0.05, **p<0.01, ***p<0.0001. Error bars stand for standard error.

3.4 DRG Explants and Dissociated Neurons Culture

DRG explant and dissociated DRG sensory neuron are excellent *in vitro* models to explore the mechanisms of axonal regeneration and evaluate the potentially therapeutic effect of the hydrogels. DRG explant is a cluster of sensory neurons and other supporting cells. The unique advantage of the DRG explant model is that it can simulate the original state *in vivo* and preserve the original cell components in DRGs and the cell-cell interactions, which are lost in the dissociated DRG neuron model. Mature DRG sensory neuron exists in a pseudo-unipolar form *in vivo*. Mostly bipolar and rarely multipolar morphology are also present in developing DRG sensory neurons *in vivo*. In a favorable culture environment, DRG neurons can grow neurites. Long processes can differentiate into axons, whereas other short neurites can differentiate into dendrites. Comparing with the DRG explant model, dissociated DRG neuron model offers a better opportunity to visualize how the gels affect the regeneration of individual neurite of sensory neuron while still minimizing other influences. However, dissociation entails greater disruption of normal cell-cell interactions.

3.4.1 DRG Explant Culture

DRG explants were dissected from the DRGs and the average dimeter of each explant ranged from 600 to 900 μm. DRG explants were evaluated immunohistochemically. Figure 3.11 shows the images obtained immediately after dissection to evaluate the originally cellular structure of DRG explants. Green staining (Figure 3.11 (a) (d)) indicated neuronal soma and neurites, while red staining (Figure 3.11 (b) (e)) indicated PRSCs. As shown in Figure 3.11, DRG explants were composed of sensory neurons and PRSCs. Some resident macrophages were also likely present, but not visualized in these preparations. Since PRSCs play important roles as myelination of axons, trophic support for neurons, etc., they were found widely distributed within and around the explant. Figure 3.11 (c) (e) show the merged staining images indicating the preserved relationship between sensory neurons and PRSCs.

DRG explants were cultured in DMEM/10 % HS for 10 days on laminin-coated coverslips as the control group. Since explants could easily detach from the laminin-coated coverslips during the culture and staining process, careful handling and multiple explants were needed. Figure 3.12 (a) shows the image of a DRG explant cultured on laminin-coated coverslips after 10 days culture. It was shown that a few neurites elongating from the explant.

3.4.2 DRG Dissociated Neuron Culture

DRG neurons were dissociated from the DRG explants and re-suspended in fresh medium. Neurons were observed under a fluorescence microscope and displayed spherical and smooth morphology prior to cell culture. DRG neurons were then seeded on laminin-coated coverslips as a control. Following culture in DMEM/10 % HS for 10 days, neurite outgrowth was stained immunohistochemically using β-III tubulin antibody. As shown in Figure 3.12 (b), neurite regeneration and abundant neurite structures were observed. The majority of neurons with neurites exhibited multipolar morphology.

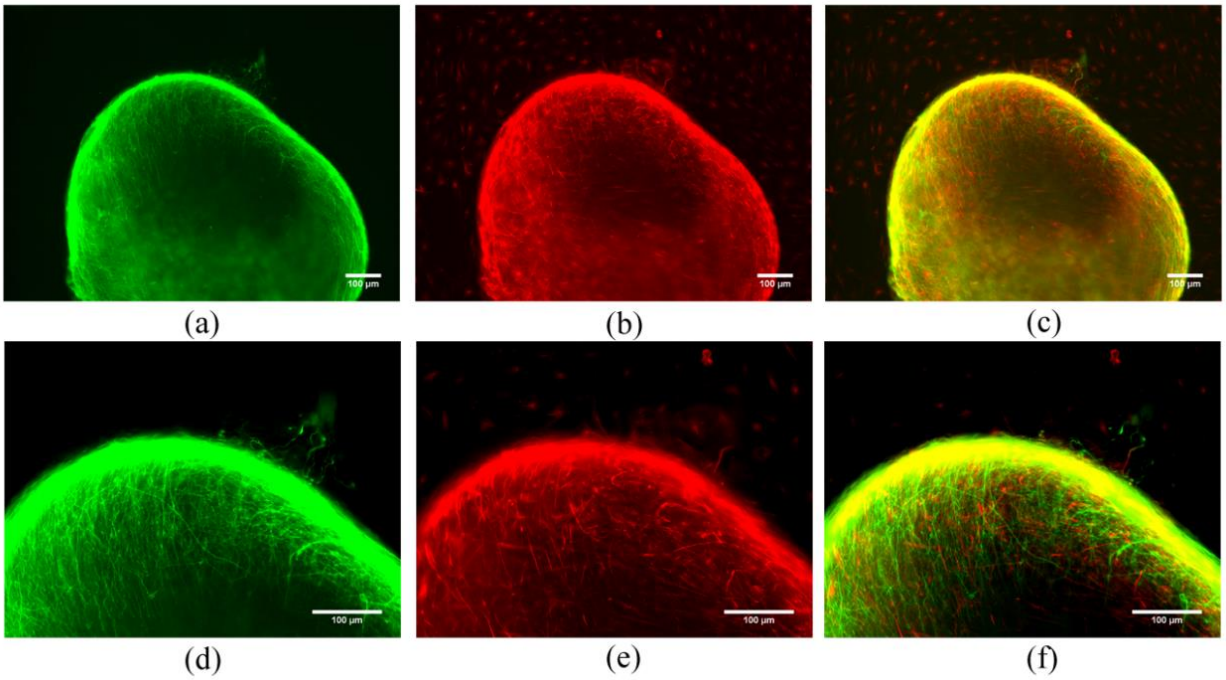

Figure 3.11 Immunofluorescent staining of DRG explant obtained immediately after dissection: (a-c) 10 x magnifications of explant stained by β-III tubulin, S-100 and merged image, respectively; (d-f) 20 x magnifications of explant stained by β-III tubulin for neurons (green), and S-100 for PRSCs (red), and merged images. Scale bar=100 µm.

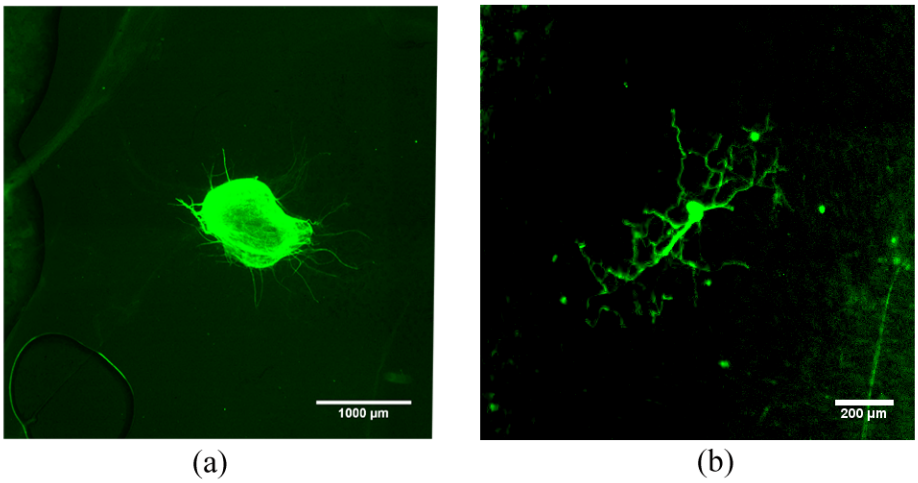

Figure 3.12 Immunofluorescent staining of a DRG explant (a) and a dissociated neuron (b) cultured on laminin-coated coverslips for 10 days. Scale bars are indicated in the images.

3.5 Neurite Outgrowth Assay for DRG-plated Hydrogels

Explants and dissociated neurons were seeded onto the hydrogels to evaluate: the effect of collagen and collagen-genipin gels on neurite outgrowth; the differences of the neurite outgrowth in two different models *in vitro*; and the response of DRG to NGF.

3.5.1 Neurite Outgrowth of DRG Explants Seeded onto the Hydrogels

DRG explants were seeded onto the hydrogels and cultured for 10 days to assess whether collagen and collagen-genipin gels could provide favorable environment for neurite regeneration following injury. 50 ng/mL NGF was also added to the culture medium in some cultures to evaluate the response of DRG explants to NGF.

After 10 days culture, DRG explants were stained immunohistochemically using β-III tubulin antibody and the regenerated neurites were visualized as shown in Figure 3.13. Neurite outgrowth was quantified as the average neurite length (μm) and neurite density (%). DRG explants were cultured on laminin-coated coverslips with (+) or without (-) NGF-conditioned medium as the control groups.

Figure 3.13 shows the immunofluorescent images of DRG explants seeded onto the gels with or without NGF in the culture medium. Control group (+) and experimental groups (+) cultured in DMEM/10 % HS/NGF displayed substantially denser and longer neurites scattering from the explants when compared to those cultured in medium without NGF (-). For the collagen gels, DRG explants seeded onto 2.5 mg/mL collagen gel exhibited the most neurite extension and neurite branches under both conditions as shown in Figure 3.13 (g) and (h). For the collagen-genipin gels, the neurite extension and the length of sprouting neurites from the explants seeded onto Col 2-Gp 0.25 and Col 2-Gp 0.5 were significantly reduced when cultured in NGF free medium (Figure 3.13 (i) and (k)). With the addition of NGF to the medium, the neurite outgrowth of the explants seeded onto the collagen-genipin gels was enhanced greatly (Figure 3.13 (j) and (l)).

To further elucidate how the gels and NGF affected the neurite outgrowth, the results of quantification analysis were shown in Figure 3.14. The average neurite length of the control group cultured in medium without or with NGF was 580 ± 53 and 863 ± 45 μm, and the neurite density was 14 ± 2.5 and 75 ± 3.3 %, respectively.

For explants cultured in NGF-free medium (-), 2.5 mg/mL collagen gel had the highest average neurite length of 935 ± 39 μm and neurite density of 77 ± 2.9 %, which was increased by 61 % and 63 % comparing with the control group (-). For collagen gels only (-), one-way ANOVA

determined that the effect of collagen concentration on the average neurite length and neurite density was significant. The average neurite length for Col 2.5 was higher than Col 1.5 and Col 2, while Tukey's test showed no significant difference of the average neurite length between Col 1.5 and Col 2. Statistically, the neurite density increased greatly with increasing collagen concentration. For collagen-genipin gels (-), there was no significant difference of the average neurite length among Col 2, Col 2-Gp 0.25 and Col 2-Gp 0.5. The neurite density decreased significantly with the presence of genipin, whereas there was no significant difference between Col 2-Gp 0.25 and Col 2-Gp 0.5 as determined by Tukey's post-hoc test.

For explants cultured in NGF-conditioned medium (+), 2.5 mg/mL collagen gel had the highest average neurite length of 1326 ± 83 μm and neurite density of 85 ± 3.6 %, which was increased by 54 % and 9 % comparing with the control group (+), respectively. For collagen gels only, the average neurite length and neurite density increased with the increase of collagen concentration. One-way ANOVA determined that there was a significant effect of collagen concentration on the average neurite length and neurite density. For collagen-genipin gels, one-way ANOVA determined that there was a significant effect of genipin concentration on the average neurite length among Col 2, Col 2-Gp 0.25 and Col 2-Gp 0.5. The neurite density decreased noticeably with the increase of genipin concentration, while no significant difference between Col 2 and Col 2-Gp 0.25 was seen using Tukey's test.

Quantitative results confirmed that NGF-conditioned medium enhanced both the average neurite length and neurite density significantly. 2.5 mg/mL collagen gel provided the most favorable environment for the neurite outgrowth of DRG explants among all the groups in both conditions. Two-way ANOVA determined that NGF and collagen concentration had significant effects on the neurite outgrowth among collagen gels. Also, the neurite outgrowth of explants seeded on collagen-genipin gels were significantly affected by the presence of NGF and genipin concentration.

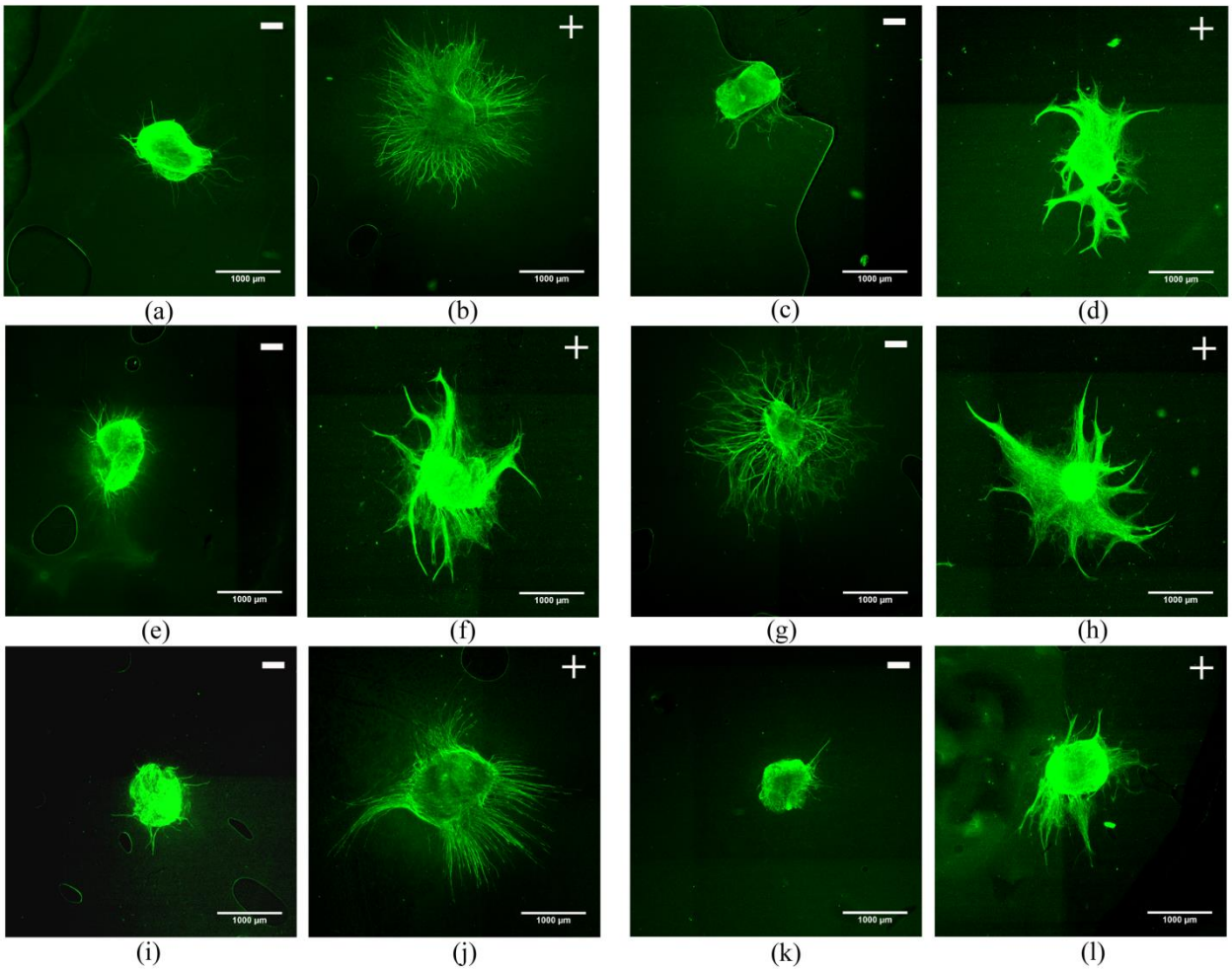

Figure 3.13 Immunofluorescent staining of DRG explants cultured on the collagen and collagen-genipin gels for 10 days in DMEM/10 % HS medium enriched with (+) or without (-) NGF. From top to bottom: (a-b) Control groups: DRG explants on laminin-coated coverslips; (c-d) Explants on 1.5 mg/mL collagen hydrogels; (e-f) Explants on 2 mg/mL collagen hydrogels; (g-h) Explants on 2.5 mg/mL collagen hydrogels; (i-j) Explants on 2 mg/mL collagen hydrogels crosslinked by 0.25 mM genipin; (k-l) Explants on 2 mg/mL collagen hydrogels crosslinked by 0.5 mM genipin. Scale bar=1000 μm

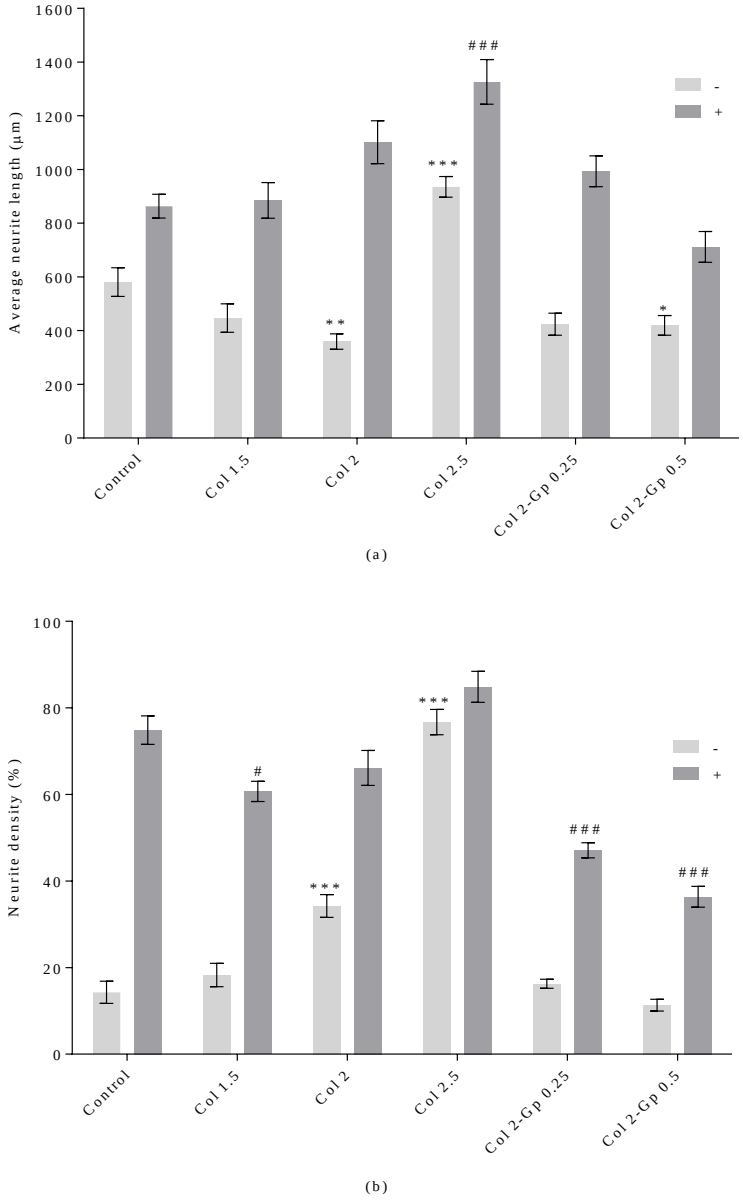

Figure 3.14 Quantitative analysis of neurite outgrowth of DRG explants cultured on the surface of collagen and collagen-genipin gels in DMEM/10 % HS medium conditioned with (+) or without (-) NGF for 10 days: (a) Average neurite length per explant (µm, n=3); (b) Neurite density (%, n=3), is defined as the number of pixels covered by neurites divided the total number of pixels covered by neurites and explant. *p<0.05, **p<0.01, ***p<0.0001 when compared to the control group cultured in culture medium without NGF. #p<0.05, ##p<0.01, ###p<0.0001 when compared to the control group cultured in NGF-conditioned medium. Error bars stand for standard error.

3.5.2 Neurite Outgrowth of DRG Neurons Seeded onto the Hydrogels

To assess the effect of NGF-conditioned medium and different substrates on the neurite regeneration of sensory neurons, DRG dissociated neurons were seeded onto the collagen and collagen-genipin gels and cultured in medium with (+) or without (-) NGF. Figure 3.15 shows the morphology of the sensory neurons and the results of quantitative analysis were displayed in Figure 3.16.

DRG neurons cultured on laminin-coated coverslips exhibited abundant neurite outgrowth as shown in Figure 3.15 (a). Comparing with the control group (-), neurons seeded onto 2 and 2.5 mg/mL collagen gels (-) exhibited longest growth among all experimental groups (-). Connections between neurons were observed on 2.5 mg/mL collagen gel (Figure 3.15 (g)). For collagen-genipin gels (-), the length of regenerated neurites was reduced significantly and few neurons with very short neurites were observed for Col 2-Gp 0.5 mM genipin (-) as shown in Figure 3.15 (k).

With the addition of NGF in the culture medium (+), longer growth and more neurite-bearing neurons were observed among all groups. As shown in Figure 3.15 (d), (f) and (h), the number of branching process decreased with increasing collagen concentration. DRG neurons seeded onto 1.5 mg/mL collagen gel (+) exhibited more short neurites comparing with other experimental groups (+). The average neurite length of collagen-genipin gels (+) decreased considerably when compared to the collagen gel only (+) as shown in Figure 3.15 (j) and (l).

As shown in Figure 3.16, the average neurite length of neurons cultured in medium (-/+ NGF) was 407 ± 23 and 762 ± 45 μm, and the percentage of neurite-bearing neurons was 36 ± 1.4 and 43 ± 0.5 %, respectively.

For neurons cultured in NGF-free medium, statistical differences of the average neurite length (μm) and the percentage of neurite-bearing neurons (%) between the control group (-) and experimental groups (-) were found. For collagen gels, the average neurite length of neurons cultured on 1.5 mg/mL collagen gel (-) decreased significantly when compared to the control group (-), whereas there was no significant differences of the neurite length among the control (-), Col 2 (-) and Col 2.5 (-). The percentage of neurite-bearing neurons seeded on collagen gels was reduced by 40 % when compared to the control group (-), and collagen concentration had no significant effect on the result. For collagen-genipin gels, one-way ANOVA determined the significant effect of genipin concentration on the neurite outgrowth when compared to 2 mg/mL collagen. The average neurite length and percentage of neurite-bearing neurons was reduced significantly with

increasing genpin concentration.

For neurons cultured in NGF-containing medium, NGF enhanced both the average neurite length and the ratio of neurite-bearing neurons significantly. There was a significant difference of the neurite outgrowth between the control group (+) and experimental groups (+). One-way ANOVA determined collagen concentration had a significant effect on the average neurite length, and average neurite length increased with increasing collagen concentration. Thus, both NGF and collagen concentration had significant effects on the average neurite length and the percentage of neurite-bearing neurons for collagen gels. In the presence of genipin, the average neurite length reduced significantly with increasing genipin concentration. There was no significant difference of the percentage of neurite-bearing neurons among all the experimental groups. Two-way ANOVA showed that there were significant effects of NGF and genipin concentration on the neurite outgrowth among Col 2, Col 2-Gp 0.25 and Col 2-Gp 0.5 (-/+).

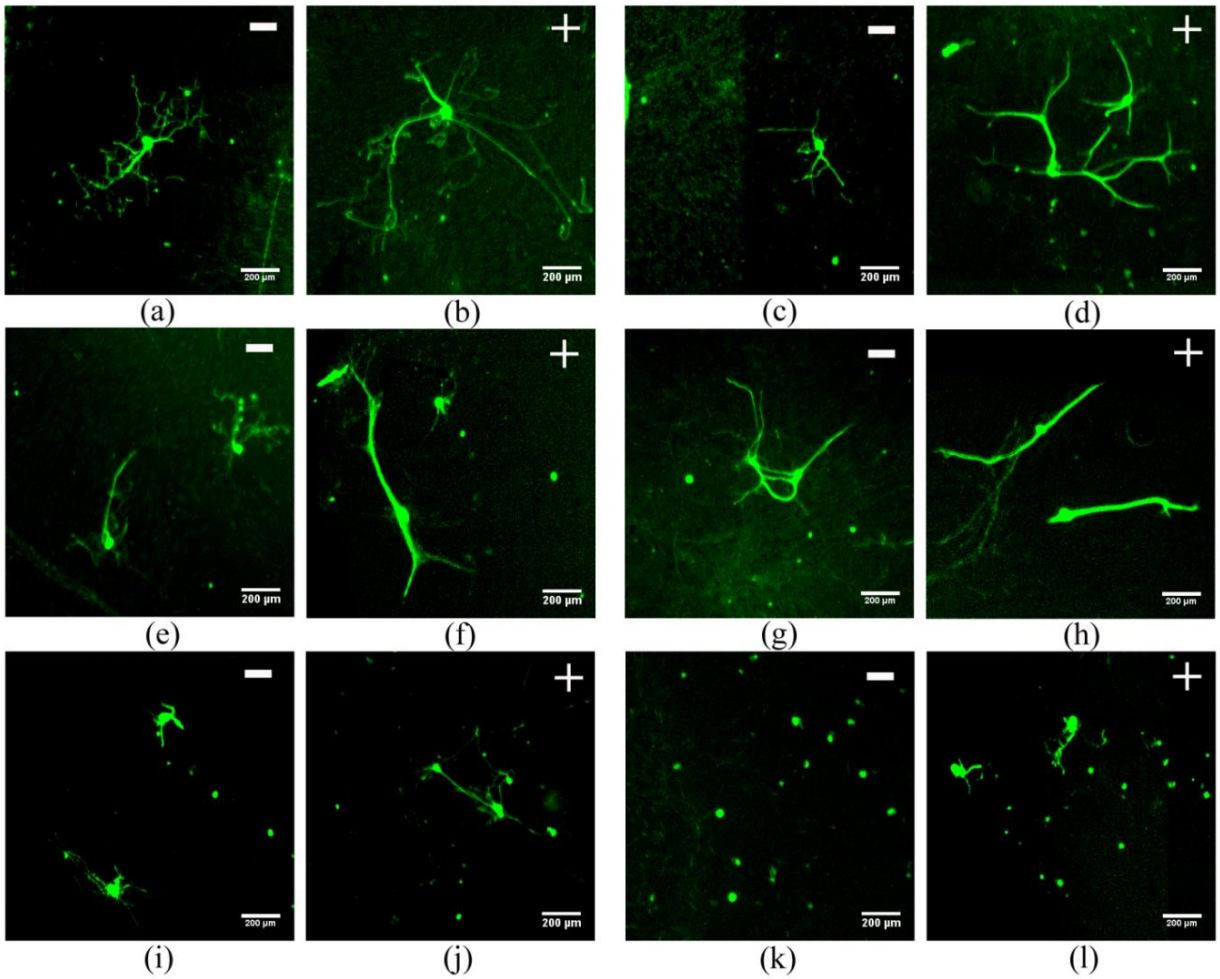

Figure 3.15 Immunofluorescent staining of dissociated DRG neurons cultured on the collagen and collagen-genipin gels for 10 days in DMEM/10 % HS medium enriched with (+) or without (-) NGF: (a-b) DRG neurons cultured on laminin-coated coverslips; (c-d) DRG neurons cultured on 1.5 mg/mL collagen hydrogels; (e-f) DRG neurons cultured on 2 mg/mL collagen hydrogels; (g-h) DRG neurons cultured on 2.5 mg/mL collagen hydrogels; (i-j) DRG neurons cultured on 2 mg/mL collagen hydrogels crosslinked by 0.25 mM genipin; (k-l) DRG neurons cultured on 2 mg/mL collagen hydrogels crosslinked by 0.5 mM genipin. Scale bar=200 μm.

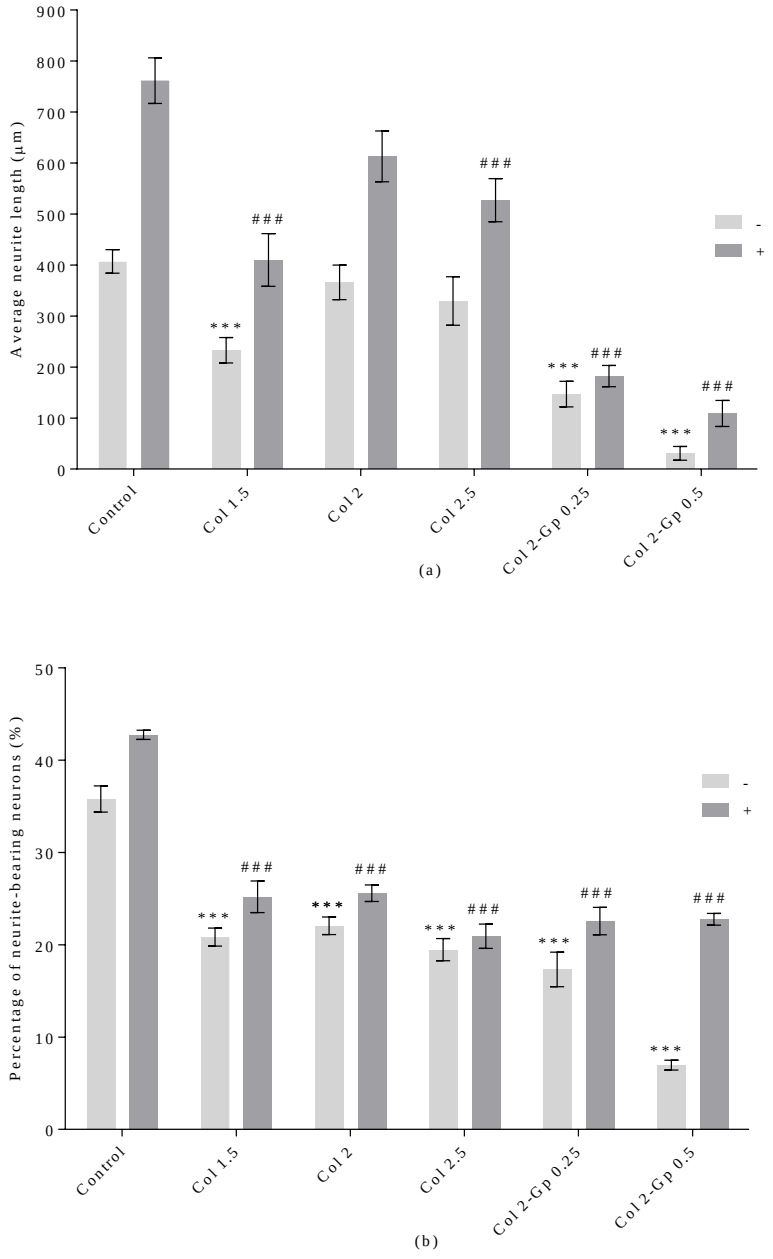

Figure 3.16 Quantitative analysis of neurite outgrowth of dissociated DRG neurons cultured onto the collagen and collagen-genipin gels for 10 days in DMEM/10 % HS medium conditioned with (+) or without (-) NGF: (a) Average neurite length per neuron (µm, n=10); (b) Percentage of neurite-bearing neurons (%, n=3). *p<0.05, **p<0.01, ***p<0.0001 when compared to the control group cultured in medium without NGF. #p<0.05, ##p<0.01, ###p<0.0001 when compared to the control group cultured in NGF-conditioned medium. Error bars stand for standard error.

3.6 Neurite Outgrowth Assay for DRG-encapsulated Hydrogels

3D hydrogels more closely mimicked the environment *in vivo*, therefore incorporation of explants or neurons into the gels was performed to evaluate: the effect of collagen and collagen-genipin gels on neurite outgrowth; the neurite outgrowth of two different models in vitro; and the effect of gels enriched with PRSCs on neurite outgrowth.

3.6.1 Neurite Outgrowth of DRG Explants Encapsulated in the Hydrogels

To evaluate whether incorporation of PRSCs within the injectable hydrogels would enhance neurite outgrowth, explants were encapsulated within the collagen and collagen-genipin gels enriched with or without PRSCs and cultured for 10 days in DMEM/10 % HS. After 10 days culture, DRG explants were stained immunohistochemically and observed under confocal microscopy. DRG explants were cultured on laminin-coated coverslips with or without PRSCs as the control groups (Figure 3.17 (a-b)).

Figure 3.17 shows immunofluorescent images of DRG explants encapsulated within the gels with (+) or without (-) supplementary PRSCs. In all conditions, neurites grew and extended from the explants within the hydrogels. For explants cultured in collagen gels without PRSCs (-), neurite outgrowth was enhanced with increasing collagen concentration (Figure 3.17 (c), (e) and (g)). Neurite length and neurite density increased dramatically when PRSCs were also incorporated within (+). Comparing with the 2 mg/mL collagen gel, fewer and shorter neurites were observed in the presence of 0.25 or 0.5 mM genipin in both conditions as shown in Figure 3.17 (i-l).

Figure 3.18 (b) and (d) display the representative 3D reconstruction images from stacked confocal images of neurite regeneration in 2 mg/mL collagen gel. It was shown that DRG neurites could penetrate and grow within the gels and that neurite outgrowth was enhanced significantly with the addition of PRSCs.

Quantitative analysis of neurite outgrowth was defined as the average neurite length (μm) and the neurite density (%). The average neurite length in 3D gels was measured by the tracing tools in ImageJ. Neurite density was calculated by the max stack images of the confocal images. Quantitative assessment of neurite outgrowth within the injectable hydrogels was shown in Figure 3.19.

For hydrogels containing no supplementary PRSCs (-), the average neurite length within a 2 mg/mL collagen gel was 324 ± 32 μm, with a decrease of 38 % comparing with the control group (-). One-way ANOVA showed no significant effect of collagen concentration on the average

neurite length. The neurite density of 2 mg/mL collagen gel was 15 ± 1.9 %. No statistically significant difference in neurite density was observed among the control group (-), Col 1.5, Col 2 and Col 2.5. For collagen-genipin gels, the average neurite length of Col 2-Gp 0.25 and Col 2-Gp 0.5 decreased by 55 % and 42 % when compared to the control group (-). The presence of genipin had no significant effect on the average neurite length comparing with 2 mg/mL collagen gel. With the addition of genipin, the neurite density of collagen-genipin gels decreased significantly when compared to 2 mg/mL collagen gel only.

For hydrogels enriched with supplementary PRSCs, the average neurite length and neurite density for Col 2 were 509 ± 25 μm and 36 ± 1.9 %. Comparing to the control group (+), both the average neurite length and neurite density for Col 2.5, Col 2-Gp 0.25 and Col 2-Gp 0.5 were significantly reduced, whereas there was no significant difference among the control, Col 1.5 and Col 2. When compared to the 2 mg/mL collagen gel only, 0.25 and 0.5 mM genipin had a significantly negative effect on: the average neurite length with a decrease of 48 % and 28 %; and the neurite density with a decrease of 27 % and 21 %. Quantitative analysis determined that the neurite regeneration within the hydrogels supplemented with PRSCs was enhanced significantly.

For collagen gels, two-way ANOVA determined PRSCs had a significant effect on the average neurite length and neurite density, whereas collagen concentration only had a significant effect on the neurite density. For collagen-genipin gels, PRSCs and genipin concentration had significant effects on both the average neurite length and neurite density.

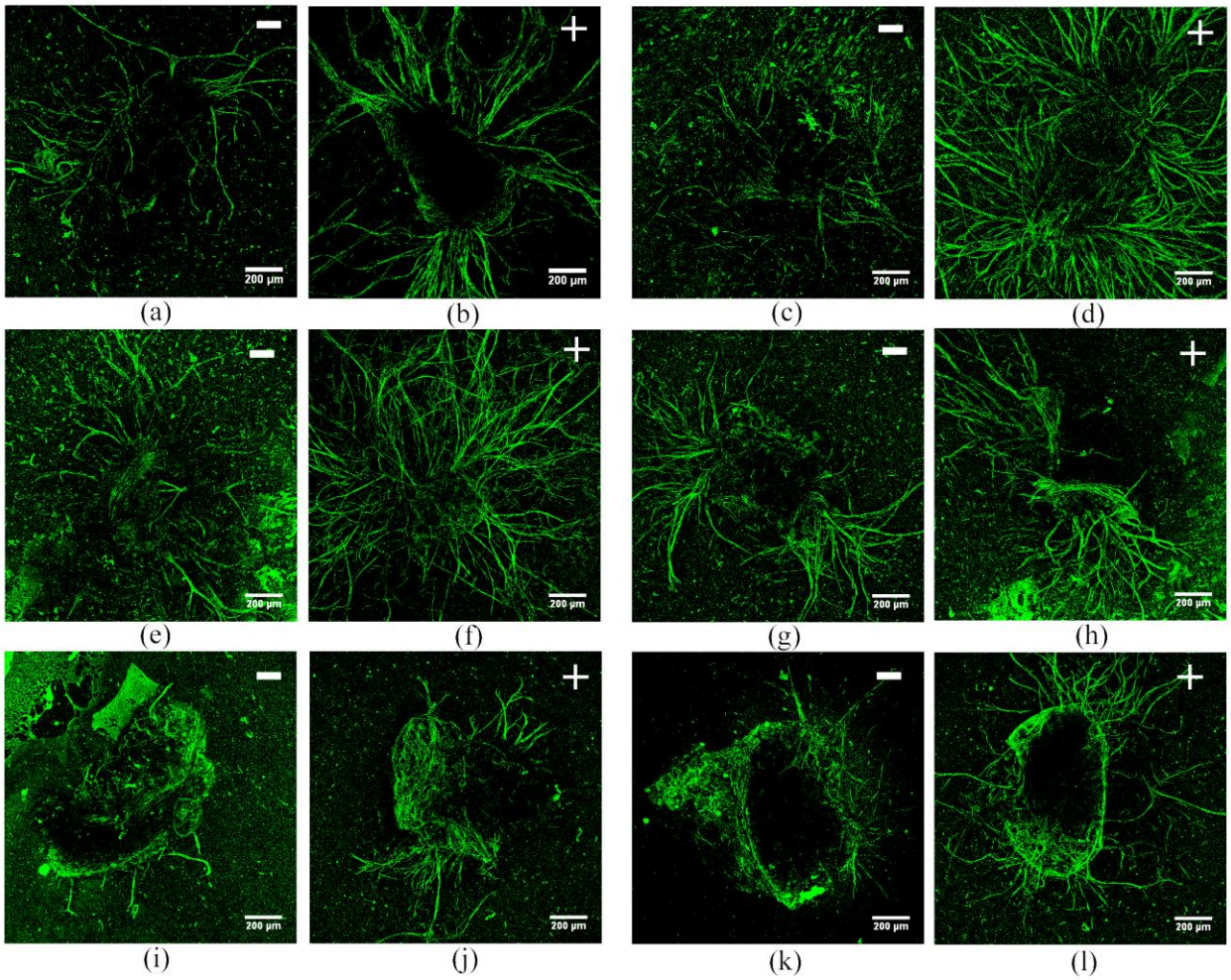

Figure 3.17 Confocal microscopy of DRG explants encapsulated and cultured within the collagen and collagen-genipin gels for 10 days. - indicates DRG explants only and + represents DRG explants and supplementary PRSCs. From top to bottom: (a-b) Explants cultured on laminin-coated coverslips; (c-d) Explants encapsulated in 1.5 mg/mL collagen hydrogels; (e-f) Explants encapsulated in 2 mg/mL collagen hydrogels; (g-h) Explants encapsulated in 2.5 mg/mL collagen hydrogels; (i-j) Explants encapsulated in 2 mg/mL collagen hydrogels crosslinked by 0.25 mM genipin; (k-l) Explants encapsulated in 2 mg/mL collagen hydrogels crosslinked by 0.5 mM genipin. Scale bar=200 μm.

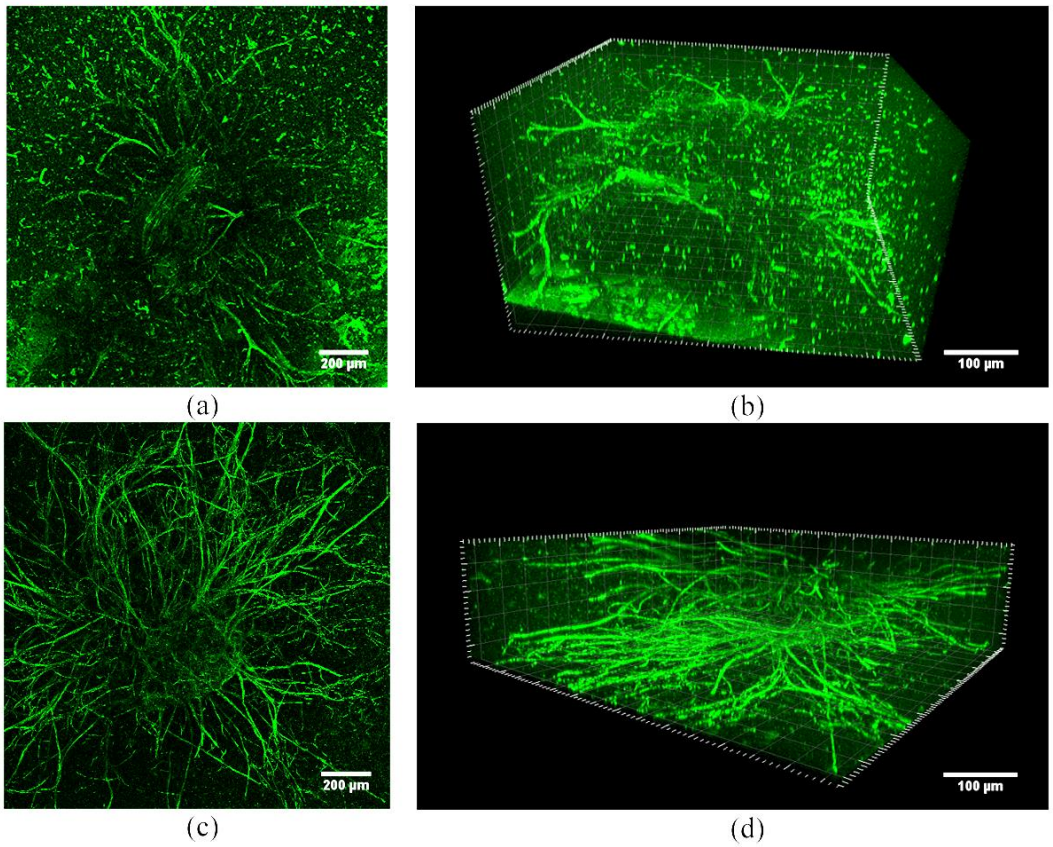

Figure 3.18 Representative confocal microscopic images of DRG explants encapsulated in the 2 mg/mL collagen gels and cultured for 10 days: (a-b) Explants encapsulated within the gel; (c-d) Explants encapsulated in the gel with supplementary PRSCs. 3D reconstruction images (b) (d) of confocal microscopy illustrate the morphology of DRG explants within the gels.

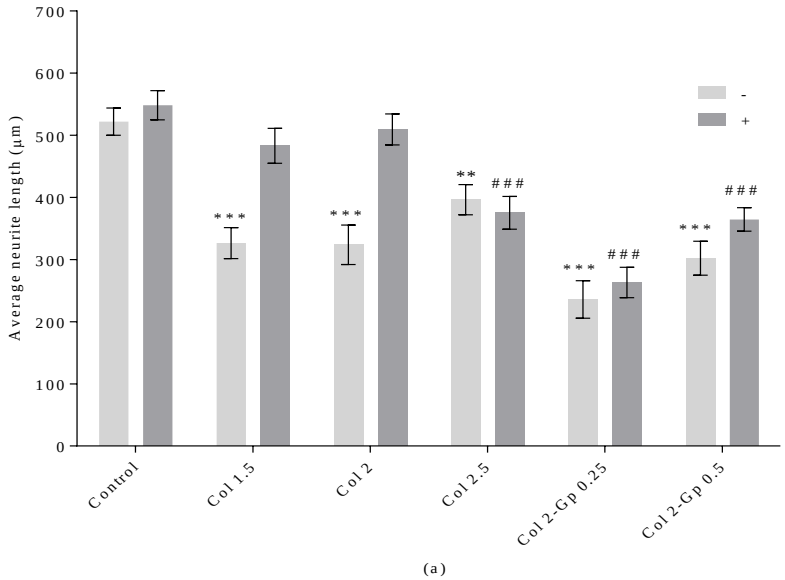

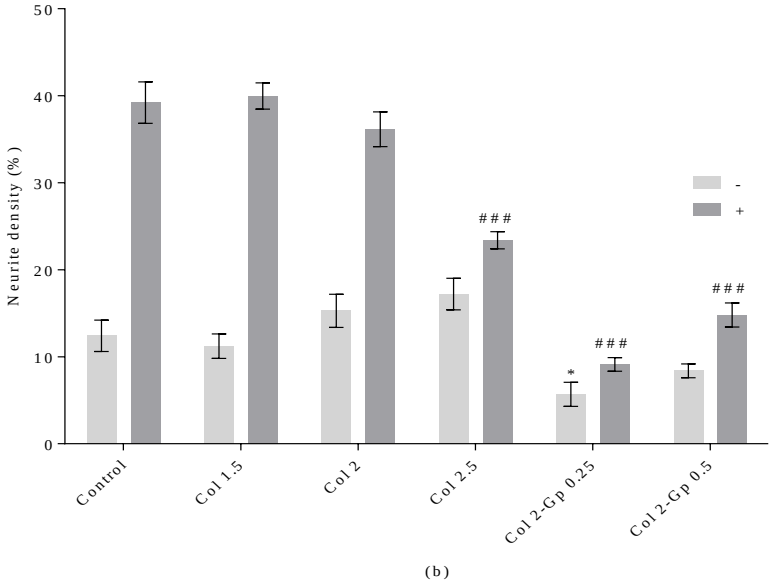

Figure 3.19 Quantitative analysis of neurite outgrowth of DRG explants encapsulated and cultured in collagen and collagen-genipin gels with (+) or without (-) supplementary PRSCs for 10 days: (a) Average neurite length per explant (μm, n=3); (b) Neurite density (%, n=3), is defined as the number of pixels covered by neurites divided the total number of pixels covered by neurites and explant. *p<0.05, **p<0.01, ***p<0.0001 when compared to the DRG explants cultured on laminin-coated coverslips. #p<0.05, ##p<0.01, ###p<0.0001 when compared to the DRG explants and supplementary PRSCs co-cultured on laminin-coated coverslips. Error bars stand for standard error.

3.6.2 Neurite Outgrowth of DRG Neurons Encapsulated in the Hydrogels

To evaluate the effect of incorporation of PRSCs in the injectable hydrogels on neurite outgrowth and axonal regeneration, DRG neurons were encapsulated in the gels and then cultured in DMEM/10 % HS medium for 10 days. The morphology of DRG sensory neurons was evaluated by immunohistochemistry staining and observed by confocal microscopy. DRG neurons were also cultured on laminin-coated coverslips with or without PRSCs and served as the control groups (+/-).

Figure 3.20 shows that all neurons with or without PRSCs (+/-) cultured on laminin-coated coverslips are multipolar, and display the longest neurite outgrowth and most branching processes when compared to the experimental groups. The co-culture of DRG neurons and PRSCs enhanced the number of branching point and the neurite length significantly, which indicated superior neurite outgrowth as shown in Figure 3.20 (a-b).

For neurons cultured in gels without PRSCs (-), incorporation of DRG neurons in physically crosslinked collagen gels displayed shorter and less neurite outgrowth when compared to the control group (-). Most neurons exhibited unipolar and bipolar morphology. Among all the collagen gels, neurons encapsulated by 2 mg/mL collagen gel showed the longest neurite regeneration (Figure 3.20 (e)). For collagen-genipin gels, there were no noticeable neurites growing within the gels as shown in Figure 3.20 (i) and (k). These results indicate that genipin had an inhibitory effect on neurite outgrowth of dissociated sensory neurons.

For neurons and PRSCs co-cultured in gels, neurons incorporated by collagen gels displayed bipolar and multipolar forms. Among all the experimental groups (+), 2 mg/mL collagen gel exhibited the longest neurite regeneration (Figure 3.20 (f)). Comparing with no neurite outgrowth in collagen-genipin gels (-), very few neurite-bearing neurons were observed in 2 mg/mL collagen crosslinked by 0.25 mM genipin (+) (Figure 3.20 (j)).

Figure 3.21 (b) and (d) display representative 3D reconstruction images of confocal images of neurite outgrowth in 2 mg/mL collagen gel without (-) or with (+) PRSCs. It was shown that DRG neurites could penetrate and grow within the gels. Incorporation of PRSCs in collagen gels resulted in longer neurite elongation and more neurites emerging from the soma. Comparing with neurons seeded onto the surface of gels (Figure 3.15), 3D gels provided less favorable environment for axonal regeneration and neurite outgrowth of neurons.

To further explore how the gels enriched with PRSCs affected neurite outgrowth, the results

of quantification analysis are shown in Figure 3.22. The average neurite length of neurons for the control groups (-/+) was 407 ± 23 and 501 ± 43 μm, and the percentage of neurite-bearing neurons was 36 ± 1.4 and 52 ± 1.1 %, respectively.

For neurons encapsulated in the gels without PRSCs (-), the average neurite length and the percentage of neurite-bearing neurons of 2 mg/mL collagen was 200 ± 48 μm and 40 ± 1.5 %, with a decrease of 51 % and an increase of 4 % when compared to the control group (-). Neurons cultured within the 2 mg/mL collagen gel (-) exhibited better neurite outgrowth than other experimental groups. One-way ANOVA determined no significant effect of collagen concentration on the neurite length but a significant effect on the percentage of neurite-bearing neurons. No neurite-bearing neurons were observed in collagen-genipin gels (-) indicating the inhibitory effect of genipin.

For neurons co-cultured with PRSCs in the gels (+), the average neurite length for 2 mg/mL collagen was significantly higher than other experimental groups. Compared to the control group (+), the average neurite length and the percentage of neurite-bearing neurons of 2 mg/mL collagen gel (+) were 382 ± 34 μm and 37.5 ± 1.6 % with a decrease of 24 and 14 %, respectively. One-way ANOVA determined that there was a significant effect of collagen concentration on the average neurite length, and the multi-comparison tests showed significant differences between groups, except Col 1.5 vs. Col 2.5. Statistically, the percentage of neurite-bearing neurons increased significantly with increasing collagen concentration. It was determined that genipin had a significant inhibitory effect on neurite outgrowth. Comparing with no neurite-bearing neurons in collagen-genipin gels (-), 7 % of the neurons encapsulated in Col 2-Gp 0.25 gel enriched with PRSCs exhibited neurite regeneration

Two-way ANOVA determined PRSCs and collagen concentration had significant effects on the average neurite length, while PRSCs had no significant effect on the percentage of neurite-bearing neurons.

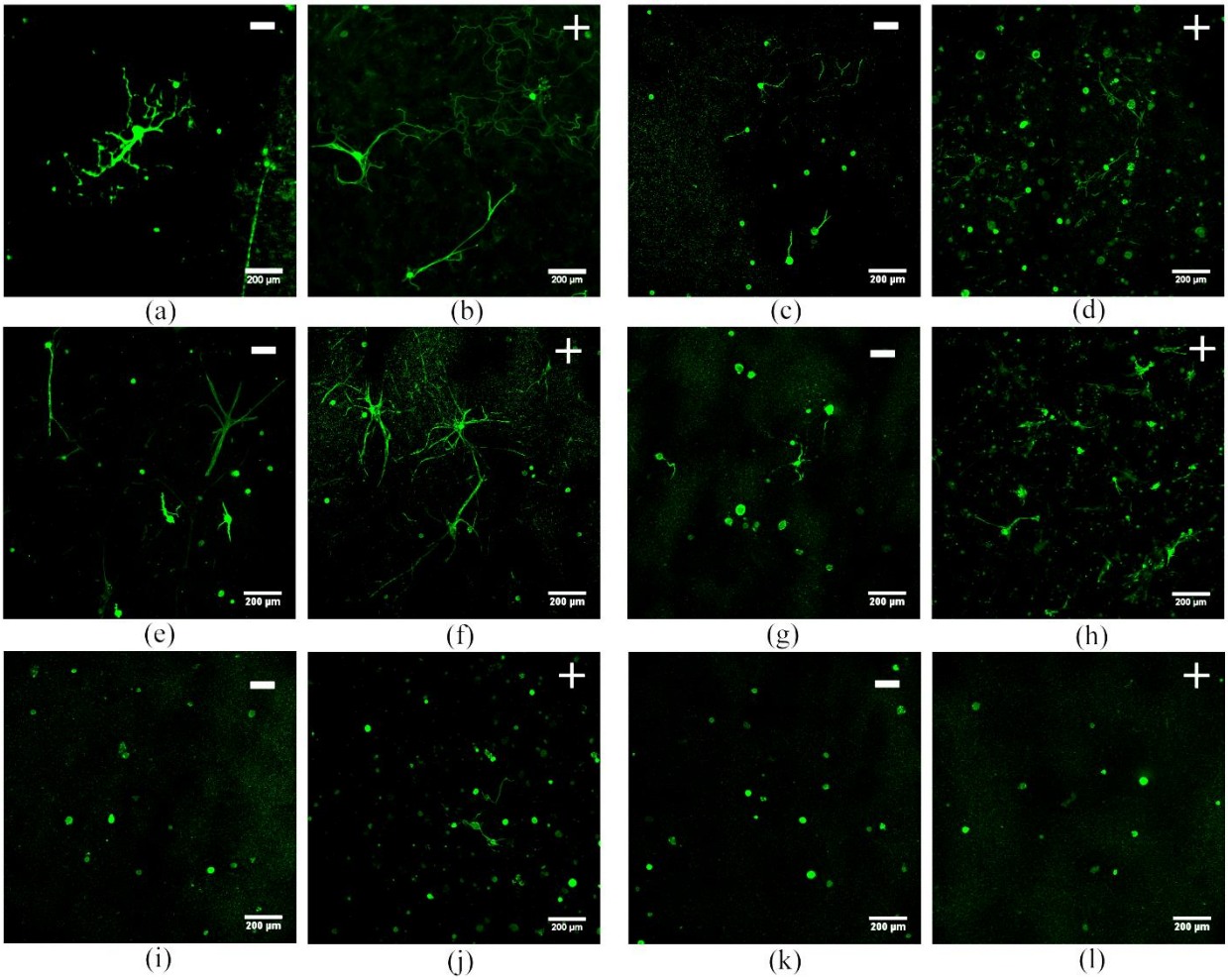

Figure 3.20 Confocal microscopy of dissociated DRG neurons encapsulated and cultured within collagen and collagen-genipin hydrogels for 10 days. - indicates DRG neurons only and + represents DRG neurons and supplementary PRSCs. From top to bottom: (a-b) Neurons cultured on laminin-coated coverslips; (c-d) Neurons encapsulated in 1.5 mg/mL collagen hydrogels; (e-f) Neurons encapsulated in 2 mg/mL collagen hydrogels; (g-h) Neurons encapsulated in 2.5 mg/mL collagen hydrogels; (i-j) Neurons encapsulated in 2 mg/mL collagen hydrogels crosslinked by 0.25 mM genipin; (k-l) Neurons encapsulated in 2 mg/mL collagen hydrogels crosslinked by 0.5 mM genipin. Scale bar=200 μm.

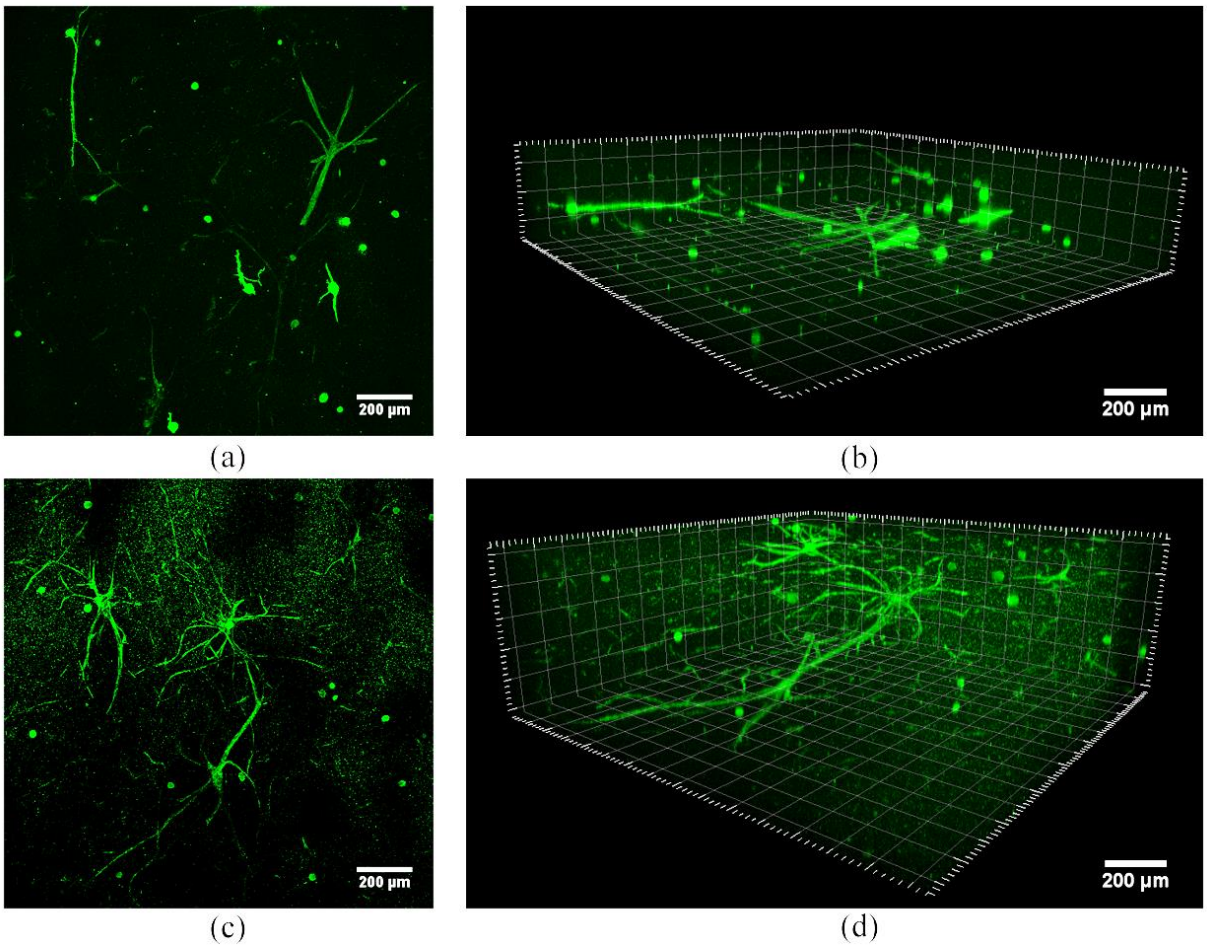

Figure 3.21 Representative confocal microscopic images of dissociated DRG neurons encapsulated in the 2 mg/mL collagen gel cultured for 10 days: (a-b) Neurons encapsulated in the gel; (c-d) Neurons co-cultured with supplementary PRSCs. 3D reconstruction images (b) (d) of confocal microscopy illustrate the morphology of DRG neurons cultured within the gel. Scale bar=200 μm.

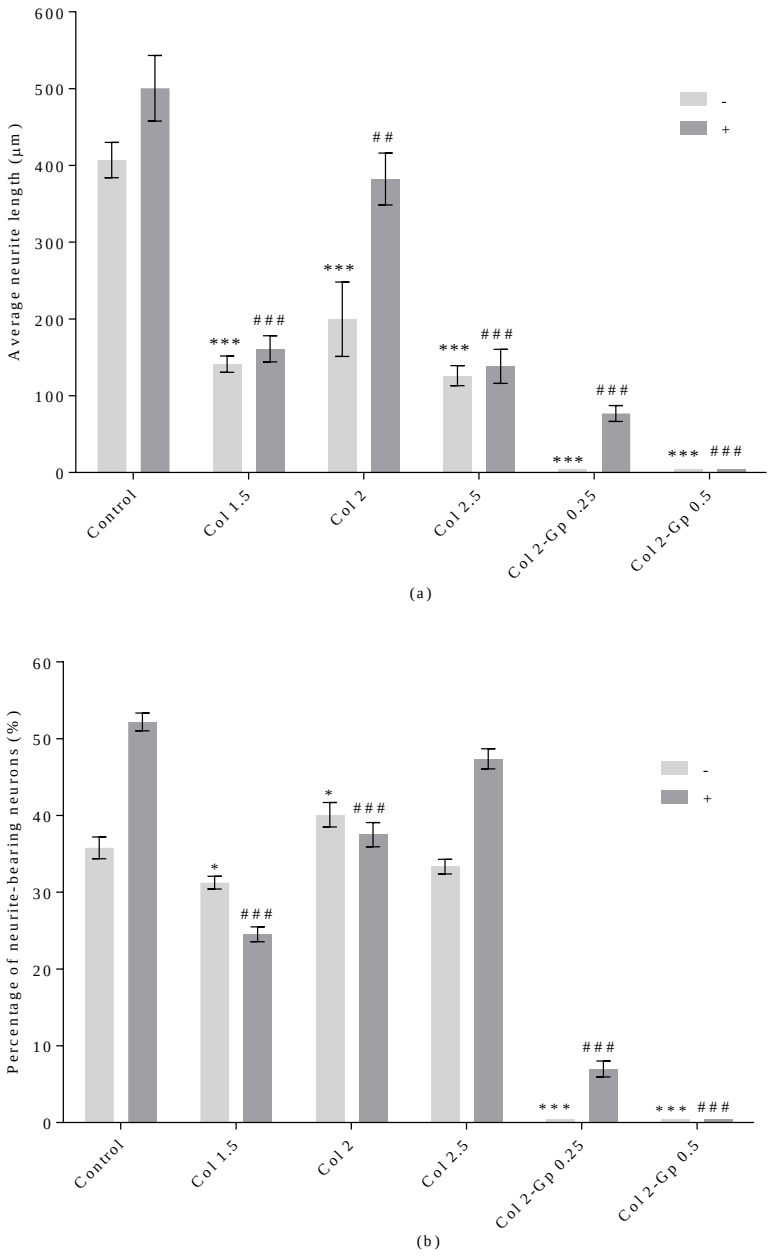

Figure 3.22 Quantitative analysis of neurite outgrowth of dissociated DRG neurons encapsulated in collagen and collagen-genipin gels with (+) or without (-) supplementary PRSCs cultured for 10 days: (a) Average neurite length per neuron (μm, n=10); (b) Percentage of neurite bearing neurons (%, n=3). *p<0.05, **p<0.01, ***p<0.0001 when compared to the DRG neurons cultured on laminin-coated coverslips. #p<0.05, ##p<0.01, ###p<0.0001 when compared to the DRG neurons and supplementary PRSCs co-cultured on laminin-coated coverslips. Error bars stand for standard error.

CHAPTER 4
DISCUSSION

Injectable hydrogel possesses great potential for nerve injury repair due to the minimally invasive procedure, shape-conforming feature, mild gelation conditions and simulation of the ECM environment. Biomolecules and supportive cells could be encapsulated within the injectable system and released in a controllable manner. In our study, the injectable collagen and collagen-genipin gels were fabricated and characterized to determine the role of chemical crosslinking in the gelation property, porosity, degradability and mechanical property. The neurite outgrowth of DRG explant and dissociated neuron as the *in vitro* cell models were investigated to assess the therapeutic potency of injectable hydrogels carrying supplementary PRSCs. It has been widely recognized that collagen is a very promising material due to the superior biocompatibility for some neural cells [136, 139, 142, 147, 148]. However, the rapid degradation and relatively weak structure may impede *in vivo* application. Genipin, a chemical crosslinker with low cytotoxicity, has been used to crosslink the amino groups of collagen to enhance structural stabilization and resistance to degradation [130, 133]. In most studies, genipin residues will be washed away prior to the cell seeding to reduce potential cytotoxicity [130]. However, as an injectable delivery system, the resident crosslinker cannot be displaced before implantation. This research gains new sights into the use of injectable collagen and collagen-genipin gels as the cell delivery substrates for nerve injury repair.

4.1 Preparation and Characterization of Collagen-based Gels

Type I collagen can be used as the injectable hydrogel through either physical or chemical crosslinking. Physically crosslinked collagen gels at concentrations of 1.5, 2 and 2.5 mg/mL were prepared and gelation occurred at 37 °C within one minute. Collagen under 1.5 mg/mL cannot form an intact gel, resulting in the unrealistic handling. With the increase of collagen concentration, the gels appeared firmer. Collagen gels (2 mg/mL) chemically crosslinked by addition of 0.25, 0.5, 1 and 5 mM genepin were prepared. The collagen-genipin gels appeared blue and became darker with the increase of time and genipin concentration. The collagen-genipin gels were visually firmer

than the collagen-only gels. To quantitatively compare and evaluate the effect of collagen and genipin concentration, characterization studies were performed in the aspects of gelation property, degradability, swelling behaviour and gel morphology.

The gelation properties were assessed in the rheological test. It was determined that both the physical collagen and chemical collagen-genipin solution can form gels around 31 °C. And the gelation time of collagen gels at 37 °C ranged from 27.3 to 35.8 s. The rapid gelation time at body temperature makes the use of collagen-based hydrogels for placement *in situ* highly feasible. The gelation time and gelation temperature decreased with increasing collagen concentration, whereas there was no significant effect of genipin concentration on these results. It is presumed that the gelation of the collagen-genipin mixture may initially result from the thermal crosslinking, and later be reinforced by chemical crosslinking. The gel strength of collagen gels at 300 s increased from 39.7 Pa at 1.5 mg/mL to 54.3 Pa at 2.5 mg/mL. The addition of genipin (0-5 mM) led to the increase of the stiffness from 43.9 to 58.9 Pa, which is presumably induced by the covalent crosslinking. The increasing tendency of gel stiffness with increasing collagen and genipin concentration has also been reported by other researchers [142, 149].

Hydrogels can absorb water from the surrounding environment. The swelling behaviour is dependent on the crosslinking level and the inner structure of the gel, which is a very important parameter correlated with the gel stiffness, porosity and fiber diameter. In our research, the swelling ratios of collagen and collagen-genipin gels were evaluated after incubation in PBS for 24 hours. Swelling ratios decreased with the increase of collagen and genipin concentration. Chemically crosslinked collagen-genipin gels displayed reduced swelling behaviour. SEM images showed that collagen crosslinked by higher concentration of genipin have a denser fibril network and smaller pore size, which might be responsible for the reduced swelling ratios.

It is reported that the size of the DRG neural cell bodies is 20-30 μm and that their neurite diameter ranges from 0.05 to 1.25 μm [150, 151]. An injectable substrate should provide favorable mesh size and mechanical properties to support neurite outgrowth. In our research, physical collagen gels showed fibrous and porous structures (Figure 3.6) with the average pore size of 3.3 μm, approximately. The average pore size decreased to 1.5 μm at 0.25 mM genipin with dense fibrillar network. With the increase of genipin concentration, the pore structure diminished significantly and finally formed very dense fibrillary clusters which might impede neurite extension within the gel.

To enhance the resistance to degradation, genipin is used as the chemical crosslinker to react with the amino groups on collagen [129]. Collagen and collagen-genipin gels were incubated in PBS for 1, 7, 15 and 30 days to evaluate the degradability *in vitro*. After 30 days, the weight remaining ratios of physical collagen gels were 55.3, 61.5, and 72.5 %, whereas the weight remaining ratio of 2 mg/mL collagen crosslinked by 5 mM genipin increased to 77 %. It was determined that the resistance to degradation was significantly improved by the addition of genipin effective from Day 15 to Day 30.

Overall, characterization studies have demonstrated the potency of collagen and collagen crosslinked by lower concentration of genipin as the injectable hydrogel. As well, the covalent crosslinking induced by genipin can be used to optimize and tune the gel stiffness, porosity, swelling behaviour and resistance to degradation.

4.2 Cytotoxicity Study of Collagen and Collagen-genipin Gels

Since the residual crosslinkers cannot be effectively washed away prior to the injection and gelation *in situ*, the crosslinkers should ideally be non-cytotoxic. Compared to other crosslinking agents for collagen, genipin has been determined about 10,000 times less cytotoxic than glutaraldehyde [113]. PRSCs were seeded onto or encapsulated within the injectable hydrogels for 3 days to evaluate cytotoxicity in 2D and 3D cultures.

For 2D cell culture, PRSCs exhibited distinct spindle-like phenotype and superior cell viability on 1.5, 2 and 2.5 mg/mL collagen gels slightly less than that of the tissue culture plate. Cell viability decreased slightly with increasing collagen concentration. The presence of genipin led most of the surviving PRSCs to adopt spherical shape, and high concentration of genipin over 1 mM inhibited cell survival significantly.

PRSCs were cultured within the 3D hydrogels and evaluated by Live/Dead assay. It was determined that the majority of PRSCs encapsulated into 1.5 and 2 mg/mL collagen gels displayed typical spindle-shape morphology, whereas PRSCs in 2.5 mg/mL mostly exhibited a round phenotype, which indicated a less favorable environment. Cell viability decreased with increasing collagen concentration. The majority of PRSCs showed spherical in 2 mg/mL collagen gel crosslinked by 0.25 mM genipin with a cell viability of 71 %. Very few PRSCs survived within 2 mg/mL collagen gels crosslinked by genipin over 0.5 mM, which revealed that higher genipin concentration was toxic to PRSCs.

It is concluded that physically crosslinked collagen gels are very promising as the cellular

delivery substrates for nerve injury repair. Collagen gels crosslinked by higher concentration of genipin over 1 mM are not permissive for PRSCs survival. As shown in Figure 4.1, PRSCs were more sensitive to the genipin concentration in 3D environment potentially resulting from the entrapment of genipin residues in the gels. Due to the cytotoxicity of higher concentration of genipin confirmed by the 2D and 3D cytotoxic studies, 0.25 and 0.5 mM genipin were used in subsequent tests.

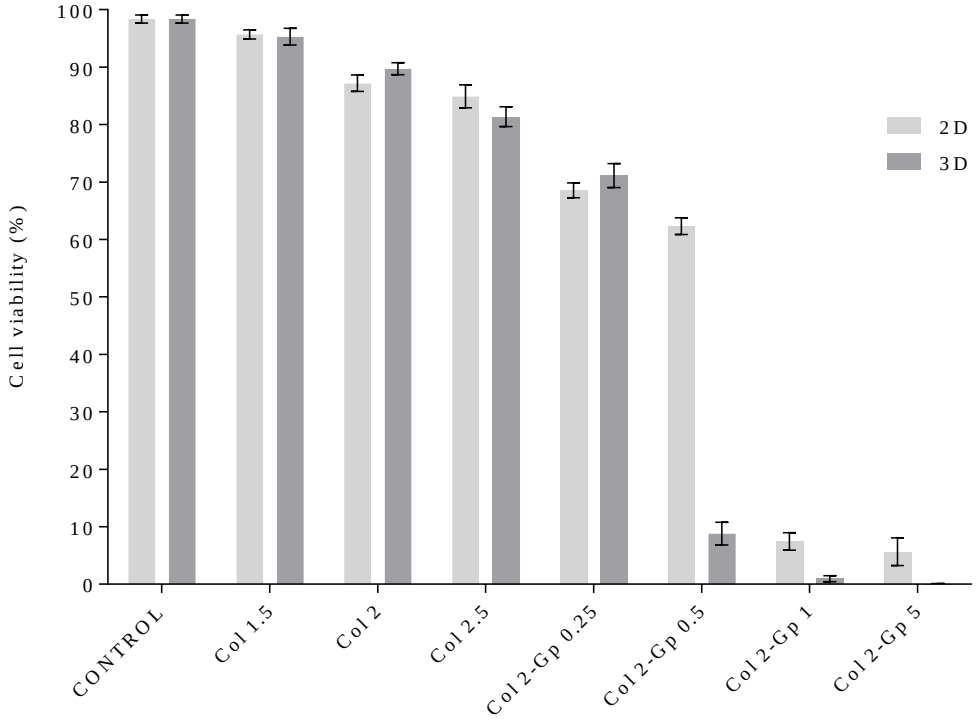

Figure 4.1 Comparison of cell viability of PRSCs in 2D and 3D hydrogel system.

4.3 *In Vitro* Assessment of DRG Neurite Outgrowth

DRG tissue is composed of abundant sensory neurons with axons projecting both to the spinal cord and distally in the PNS [39]. However, only the peripheral ends can regenerate *in vivo* [2-4]. Since DRG axons can be involved both in the CNS and PNS injury, the neurite outgrowth and axonal connections of DRG can be used as a general model to evaluate neural regeneration *in vitro*. In our research, DRG explant and dissociated neuron were exploited as the *in vitro* cell models to study the potency of injectable hydrogels carrying the PRSCs. DRG explants are directly dissected from the DRG which include both sensory neurons and glial cells. The unique advantages of the DRG explants model are to preserve the original cell interactions in DRG, which are lost in the DRG dissociated neurons model. However, comparing with the DRG explants model, dissociated

DRG neurons offer a clearer opportunity to unveil how therapies affect axonal regeneration of sensory neurons while reducing or controlling other influences. Both *in vitro* cell models provide important insights into combinational therapy of injectable hydrogels containing supplemental PRSCs. Based on the results of the cytotoxicity test, collagen (1.5, 2 and 2.5 mg/mL) and genipin (0.25 and 0.5 mM) were formulated to prepare the injectable hydrogels.

4.3.1 Effect of Gel Stiffness on DRG Neurite Outgrowth

Other researchers have shown that neurite outgrowth from neurons cultured in 3D matrix reduces with decreasing the pore size from 1.6 to 0.7 μm [152]. The mechanical strength of a matrix plays an important role in neural survival and neurite extension. It has been demonstrated that neurons exhibit more branches on softer 2D substrates (50-300 Pa) rather than stiffer substrates (300-550 Pa) [153]. Researchers have reported a wide stiffness range for type I collagen gels (*e.g.* 2 mg/mL collagen) from 15 to 57 Pa [131, 142, 149, 154]. Our research has determined that the gel stiffness of 2 mg/mL collagen was 43.9 Pa and the stiffness was enhanced with increasing the collagen and genipin concentration. Figure 4.2 shows the effect of collagen gel stiffness on the neurite length of DRG explants and dissociated neurons seeded onto the gels (a) and encapsulated within the gels (b). For 2D cultures, explants exhibited the longest neurite elongation on 2.5 mg/mL collagen gel (54.3 Pa) and dissociated neurons showed higher neurite length on 2 and 2.5 mg/mL collagen gels (43.9 and 54.3Pa). However, there was no significant difference in neurite length between DRG explants or dissociated neurons in the 3D culture systems. It has been determined that DRG explants and dissociated neurons were less sensitive to the gradient stiffness of 3D collagen gels.

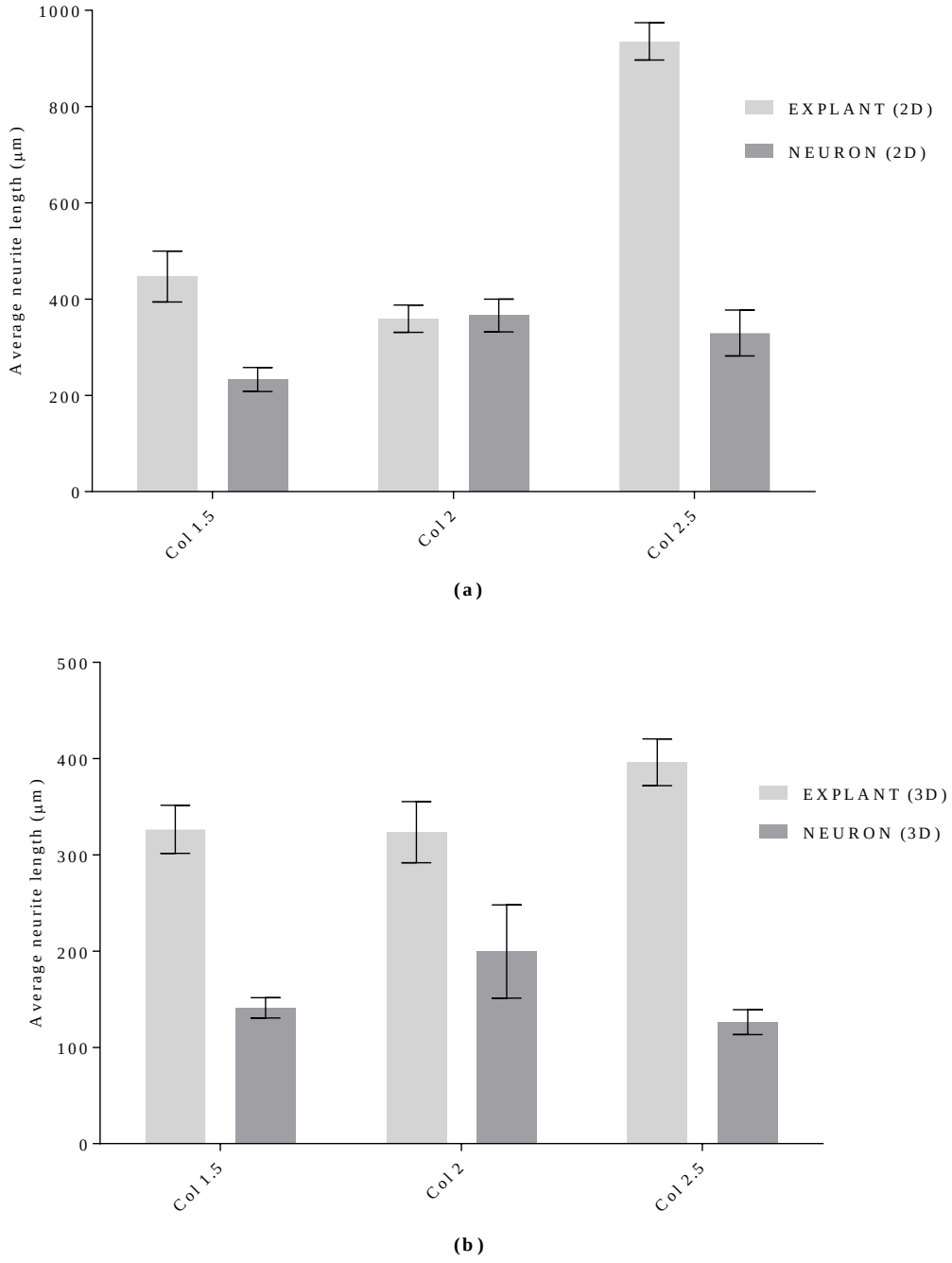

Figure 4.2 Effect of gel stiffness on the neurite length of DRG explants and dissociated neurons seeded on the gels (a) and encapsulated in the gels (b).

4.3.2 Neurite Outgrowth of DRG Seeded onto the Hydrogels

We evaluated the neurite outgrowth of DRG neurons seeded on top of (2D) collagen matrices as the preliminary study for subsequent 3D cultures. DRG explants and dissociated neurons were seeded onto the hydrogels and cultured for 10 days. NGF was added into the culture medium to explore its therapeutic potency for nerve injury repair.

DRG explants seeded onto the collagen and collagen-genipin gels of all concentrations exhibited neurite extension. Explants seeded onto the 2.5 mg/mL collagen gel showed the most neurite extension and branches. With the addition of genipin, there were fewer neurites growing from the explants comparing with the physical collagen gels. Immunofluorescent images (Figure 3.13) show that the presence of NGF in the medium results in significant boost of longer and denser neurites extension which demonstrates great promise in the use of molecular therapy for promoting axon regeneration [97]. Neurite outgrowth in culture was quantitatively evaluated as the average neurite length (μm) and neurite density (%). It was determined that the average neurite length and neurite density for 2.5 mg/mL collagen gels increased by 61 % and 63 % comparing with the control group (laminin-coated coverslip) indicating that these collagen preparations could provide a favorable and permissive substrate to support neurite outgrowth. Statistical analysis showed that genipin had a greater impact on neurite density rather than on neurite length. Quantitative results confirmed that NGF-conditioned medium enhanced both the average neurite length and neurite density significantly. In future work, NGF can be controllably delivered by the injectable hydrogels for nerve injury repair.

Comparing with the explant model, detailed branching structures and morphology were observed in dissociated DRG neuron culture. DRG neurons cultured on laminin-coated coverslips exhibited enormous neurite extension, often with multipolar morphology. When compared to the control group, physical collagen gels allowed for neurite growth but with less branching points. Also, most of neurons displayed bipolar structure. Neurons seeded onto 1.5 mg/mL collagen gel developed shorter neurite structure comparing with other experimental groups, suggesting a tendency to form abnormal dendrites, rather than axons. Quantitative results demonstrated that neurons seeded onto the collagen gels at higher concentrations possessed longer neurite extension, more similar to the explant culture. It was also demonstrated that collagen concentration had no significant impact on the percentage of neurite-bearing neurons. Even though neurite outgrowth was observed on the collage-genipin gels, the average neurite length and percentage of neurite-

bearing neurons reduced significantly with increasing genipin concentration. With the addition of NGF in the culture medium, longer axons and more neurite-bearing neurons were observed among all groups. It was presumed that the addition of NGF played an important role in promoting initial neurite formation. Comparing with the explant culture, DRG dissociated neurons were less tolerant to the use of genipin in collagen gels and the distinction between dissociated neuron and explant culture possibly resulted from more interaction between neurons and glial cells that is preserved in explant culture.

4.3.3 Neurite Outgrowth of DRG Encapsulated in the Hydrogels

While 2D cultures have demonstrated that neurite outgrowth on physical collagen gels are preferable to chemically crosslinked collagen-genipin gels, DRG sensory neurite response to 3D collagen-genipin matrices has been rarely reported. A 3D matrix can closely mimic the *in vivo* environment which helps to re-establish normal cell-cell interaction, protect cells from extrinsic disturbances, and allow neurites to grow freely in every direction. Cells can be premixed with the injectable hydrogel solution and evenly distributed within the gel *in situ* due to the fast gelation property. We encapsulated PRSCs within the hydrogels at a density of 40,000 cells/mL [77-79]. In our research, DRG explant and dissociated neuron were used as the *in vitro* cell models to examine the therapeutic potency of injectable hydrogels containing PRSCs for nerve injury repair.

Immunofluorescence studies showed that both collagen and collagen-genipin gels provided favorable and supportive 3D environment for neurite extension of DRG explants but not as well as the commonly used laminin-coated surface. Confocal images displayed neurites freely penetrating and growing within the 3D gels. Longer neurites extension was observed in physically crosslinked collagen gels compared to chemically crosslinked collagen-genipin gels. Neurite length and neurite density were measured to quantify the neurite outgrowth. It was determined that collagen concentration had no significant effect on neurite outgrowth in these cultures. The addition of genipin reduced the numbers of neurites per unit volume significantly. In contrast to the 2D study, DRG explants encapsulated into the 2 mg/mL collagen crosslinked by 0.25 mM genipin exhibited less neurite sprouting than 2 mg/mL collagen-0.5 mM genipin. While in the hydrogels enriched with supplementary PRSCs, the average neurite length and neurite density were dramatically enhanced for both collagen and collagen-genipin gels. These neurite outgrowth results demonstrated the efficacy of PRSCs for promoting outgrowth from DRG explants and confirmed that the idea of injectable hydrogels as the delivery substrates is feasible and promising

for nerve injury repair.

Sensory neurons from adult rats exist *in vivo* as mostly pseudo-unipolar morphology [39]. A pseudo-unipolar neuron has one long neurite with two branches and both branches have characteristics *in vivo* (action potential conduction, myelination, etc.) that identify them as an axon. However, neurons cultured on the laminin-coated coverslips as the control group exhibited multipolar morphology possibly due to the 2D environment. In this work, specific tests were not used to determine whether individual neurites had characteristics of axons or dendrites, but it is likely that shorter neurites may have had abnormal dendritic properties, as is sometimes observed in cultured adult DRG neurons.

It was determined that neurites in 3D matrices could penetrate and grow within the gels. Comparing with the multipolar morphology in 2D culture, pseudo-unipolar structures were observed in physical collagen gels indicating true axonal extension. The pseudo-unipolarization might result from the inner structure of the physical collagen gels which closely mimicked the *in vivo* state. Neurons cultured within the 2 mg/mL collagen gel exhibited the best outgrowth compared to other experimental groups. However, no neurite-bearing neurons were observed in collagen-genipin gels which indicated the inhibitory role of genipin in 3D environment. Embedment of PRSCs in collagen gels led to significant enhancement of neurite elongation and branching points. Neurons encapsulated in 2 mg/mL collagen gel containing PRSCs exhibited the longest neurite outgrowth. Comparing with no neurite outgrowth in collagen-genipin gels without PRSCs, very few neurite-bearing neurons were observed in 2 mg/mL collagen crosslinked by 0.25 mM genipin. Willits et al. have reported that the average neurite length of DRG neurons cultured in 2 mg/mL collagen gel for 4 days reached to 136 μm [142]. Our research showed the average neurite length for 2 mg/mL collagen gel was 200 μm. With the aid of PRSCs, the average neurite length reached to 382 μm. The dissociated DRG neuron model that we used was more sensitive to genipin addition to collagen gels than was the explant model, which was correlated to the results in 2D tests. The majority of neurites of both the explant and dissociated neuron models extended and aligned horizontally indicating the potential guidance of natural polymers.

CHAPTER 5
CONCLUSIONS AND FUTURE WORK

5.1 Conclusions

The overall goal of our study is to develop an injectable hydrogel system as the cell-delivery matrix and evaluate the therapeutic efficacy of 3D matrix *in vitro* for nerve injury repair. Physically and chemically crosslinked collagen and collagen-genipin hydrogels were prepared and characterized in terms of gelation properties, swelling behaviour, degradability and gel morphology. The rheometric results indicated that both collagen and collagen-genipin hydrogels could gel at pH 7.0, 37 °C within a time period of 40 s, approximately. The rapid gelation time and mild gelation condition enable the gel solution localized *in situ* and evenly encapsulation of supportive cells. Immediate gel stiffness of both physical and chemical gels was measured at 300 s and the results were consistent with the range reported by other researchers, in which neurite outgrowth could extend and proliferate. The covalent crosslinking between genipin and collagen led to significant enhancement of the gel stiffness. Genipin also has impacts on diminishing the swelling behaviour, forming dense microstructure, reducing the pore size, and more importantly, improving the resistance to degradation which is the weak spot of the applicability of physical collagen gels *in vivo*.

Even though genipin has been reported to be low cytotoxicity, most of the biocompatibility tests were performed using washed hydrogels, which is not realistic for injectable hydrogels. PRSCs were seeded onto or within the gels and cultured for 3 days. It was shown that physical collagen gels could easily support the survival of PRSCs, which displayed spindle-like phenotype during the culture. Cell viability was inversely proportional to the increase of collagen concentration. However, most of the surviving PRSCs cultured onto or within the collagen-genipin gels transformed into spherical shape and higher concentration of genipin over 1 mM had a significantly inhibitory effect on cell viability. PRSCs were more sensitive to the genipin in 3D environment possibly resulting from the entrapment of genipin residues in the gels.

DRG explants and dissociated neurons were used as the *in vitro* cell models to assess the potency of injectable hydrogels carrying the PRSCs. A preliminary 2D study was conducted on the collagen and collagen-genipin gels and NGF was added into the culture medium to explore the efficacy of cellular therapy on the neurite outgrowth. Neurite extensions were observed on the collagen and collagen-genipin gels of all concentrations, whereas there were less neurites with the presence of genipin when compared to the physical collagen gels. It was also shown DRG dissociated neurons were less tolerant to genipin. And this distinction between dissociated neuron and explant cultures possibly resulted from the aid of the glial cells preserved in explants culture. In contrast to the PRSCs, explants and dissociated neurons seeded onto the collagen gel at higher concentration (2.5 mg/mL) exhibited the most neurite extension and branches among all the experimental groups. The presence of NGF in the medium resulted in significantly longer and denser neurite extension. In future study, NGF could be encapsulated within the injectable hydrogels and released in a controllable manner to promote neurite outgrowth.

Research in DRG neurite response to 3D collagen-genipin matrices has been rarely reported. In our research, we encapsulated the DRG in 3D collagen and collagen-genipin hydrogels to mimic the *in vivo* environment and examined the effects of injectable material and supplementary PRSCs on neurite outgrowth. It was shown that collagen and collagen-genipin gels allowed the neurites of DRG explants to extending within the gels.

Comparing with the explant culture, DRG dissociated neurons were more sensitive to the presence of genipin. Even though neurites of DRG neurons could extend as pseudo-unipolar phenotype and presumably axonal extensions were observed within the physical collagen gels, no neurite-bearing neurons were observed in collagen-genipin gels. Enriched collagen hydrogels with PRSCs could enhance the neurite elongation and branches significantly. And the inhibitory role of genipin in neurite outgrowth of dissociated neurons was remedied with the aid of PRSCs. Our research lays the groundwork for future *in vivo* studies using the injectable hydrogels containing supportive cells and neurotrophic molecules for nerve injury repair.

5.2 Future Work

In order to achieve a better understanding of the chemical crosslinking mechanisms and the crosslinking level of collagen-genipin gels, Fourier transform infrared spectroscopy (FTIR) should be performed. It has been shown in our studies that genipin can significantly enhance the mechanical property and the resistance to degradation. The gel strength test was conducted at 300

s due to the equipment availability. However, the gel stiffness may be time dependant. Therefore, gel strength in long-term should be investigated. Moreover, as fibrillary network, porosity and microstructure are essential factors for axonal regeneration, quantitative analyses of the pore diameter and porous distribution should be determined by mercury porosimetry. Furthermore, encapsulation of PRSCs within the injectable hydrogel has shown great improvements in promoting DRG neurite outgrowth and neutralizing the inhibitory effects of genipin. Loading distribution, proliferation and migration studies should be evaluated in the future. Moreover, DRG dissociated neurons encapsulated in collagen gels exhibited pseudo-unipolar morphology indicating axonal elongation. The cell-material interaction, pseudo-unipolar structures and potential re-myelination should be investigated using more specific immunocytochemical techniques, and SEM.

REFRENCES

[1] Paxinos G, Mai JK. The human nervous system: Academic Press; 2004.

[2] CARLSTEDT T. Nerve fibre regeneration across the peripheral–central transitional zone. Journal of Anatomy. 1997;190:51-56.

[3] Golding J, Shewan D, Cohen J. Maturation of the mammalian dorsal root entry zone-from entry to no entry. Trends in Neurosciences. 1997;20:303-309.

[4] Perkins C, Carlstedt T, Mizuno K, Aguayo A. Failure of Regenerating Dorsal Root Axons to Regrow into the Spinal-Cord. 1980.7(4):323.

[5] Fawcett JW, Asher RA. The glial scar and central nervous system repair. Brain Research Bulletin. 1999;49:377-391.

[6] McKerracher Ld, David S, Jackson D, Kottis V, Dunn R, Braun P. Identification of myelin-associated glycoprotein as a major myelin-derived inhibitor of neurite growth. Neuron. 1994;13:805-811.

[7] GrandPré T, Nakamura F, Vartanian T, Strittmatter SM. Identification of the Nogo inhibitor of axon regeneration as a Reticulon protein. Nature. 2000;403:439-444.

[8] DeBellard M-E, Tang S, Mukhopadhyay G, Shen Y-J, Filbin MT. Myelin-associated glycoprotein inhibits axonal regeneration from a variety of neurons via interaction with a sialoglycoprotein. Molecular and Cellular Neuroscience. 1996;7:89-101.

[9] Prinjha R, Moore SE, Vinson M, Blake S, Morrow R, Christie G, et al. Neurobiology: Inhibitor of neurite outgrowth in humans. Nature. 2000;403:383-384.

[10] Chen MS, Huber AB, van der Haar ME, Frank M, Schnell L, Spillmann AA, et al. Nogo-A is a myelin-associated neurite outgrowth inhibitor and an antigen for monoclonal antibody IN-1. Nature. 2000;403:434-439.

[11] Mukhopadhyay G, Doherty P, Walsh FS, Crocker PR, Filbin MT. A novel role for myelin-associated glycoprotein as an inhibitor of axonal regeneration. Neuron. 1994;13:757-767.

[12] Kottis V, Thibault P, Mikol D, Xiao ZC, Zhang R, Dergham P, et al. Oligodendrocyte‐myelin glycoprotein (OMgp) is an inhibitor of neurite outgrowth. Journal of Neurochemistry. 2002;82:1566-1569.

[13] Wang KC, Koprivica V, Kim JA, Sivasankaran R, Guo Y, Neve RL, et al. Oligodendrocyte-myelin glycoprotein is a Nogo receptor ligand that inhibits neurite outgrowth. Nature. 2002;417:941-944.

[14] Miyai I, Yagura H, Oda I, Konishi I, Eda H, Suzuki T, et al. Premotor cortex is involved in restoration of gait in stroke. Annals of Neurology. 2002;52:188-194.
[15] Bartsch U, Bandtlow CE, Schnell L, Bartsch S, Spillmann AA, Rubin BP, et al. Lack of evidence that myelin-associated glycoprotein is a major inhibitor of axonal regeneration in the CNS. Neuron. 1995;15:1375-1381.
[16] Kim J-E, Li S, GrandPré T, Qiu D, Strittmatter SM. Axon regeneration in young adult mice lacking Nogo-A/B. Neuron. 2003;38:187-199.
[17] Li S, Liu BP, Budel S, Li M, Ji B, Walus L, et al. Blockade of Nogo-66, myelin-associated glycoprotein, and oligodendrocyte myelin glycoprotein by soluble Nogo-66 receptor promotes axonal sprouting and recovery after spinal injury. The Journal of Neuroscience: the official journal of the Society for Neuroscience. 2004;24:10511-10520.
[18] Simonen M, Pedersen V, Weinmann O, Schnell L, Buss A, Ledermann B, et al. Systemic deletion of the myelin-associated outgrowth inhibitor Nogo-A improves regenerative and plastic responses after spinal cord injury. Neuron. 2003;38:201-211.
[19] Bartsch U. Myelination and axonal regeneration in the central nervous system of mice deficient in the myelin-associated glycoprotein. Journal of Neurocytology. 1996;25:303-313.
[20] Ji B, Case LC, Liu K, Shao Z, Lee X, Yang Z, et al. Assessment of functional recovery and axonal sprouting in oligodendrocyte-myelin glycoprotein (OMgp) null mice after spinal cord injury. Molecular and Cellular Neuroscience. 2008;39:258-267.
[21] Faulkner JR, Herrmann JE, Woo MJ, Tansey KE, Doan NB, Sofroniew MV. Reactive astrocytes protect tissue and preserve function after spinal cord injury. The Journal of Neuroscience. 2004;24:2143-2155.
[22] Bush TG, Puvanachandra N, Horner CH, Polito A, Ostenfeld T, Svendsen CN, et al. Leukocyte infiltration, neuronal degeneration, and neurite outgrowth after ablation of scar-forming, reactive astrocytes in adult transgenic mice. Neuron. 1999;23:297-308.
[23] Fitch MT, Doller C, Combs CK, Landreth GE, Silver J. Cellular and molecular mechanisms of glial scarring and progressive cavitation: in vivo and in vitroanalysis of inflammation-induced secondary injury after CNS trauma. The Journal of Neuroscience. 1999;19:8182-8198.
[24] Fitch MT, Silver J. Activated macrophages and the blood–brain barrier: inflammation after CNS injury leads to increases in putative inhibitory molecules. Experimental Neurology. 1997;148:587-603.

[25] Jones LL, Margolis RU, Tuszynski MH. The chondroitin sulfate proteoglycans neurocan, brevican, phosphacan, and versican are differentially regulated following spinal cord injury. Experimental Neurology. 2003;182:399-411.
[26] McKeon RJ, Jurynec MJ, Buck CR. The chondroitin sulfate proteoglycans neurocan and phosphacan are expressed by reactive astrocytes in the chronic CNS glial scar. The Journal of Neuroscience. 1999;19:10778-10788.
[27] Davies SJ, Fitch MT, Memberg SP, Hall AK, Raisman G, Silver J. Regeneration of adult axons in white matter tracts of the central nervous system. Nature. 1997;390:680-683.
[28] Davies SJ, Goucher DR, Doller C, Silver J. Robust regeneration of adult sensory axons in degenerating white matter of the adult rat spinal cord. The Journal of Neuroscience. 1999;19:5810-5822.
[29] Grimpe B, Silver J. A novel DNA enzyme reduces glycosaminoglycan chains in the glial scar and allows microtransplanted dorsal root ganglia axons to regenerate beyond lesions in the spinal cord. The Journal of Neuroscience. 2004;24:1393-1397.
[30] Bradbury EJ, Moon LD, Popat RJ, King VR, Bennett GS, Patel PN, et al. Chondroitinase ABC promotes functional recovery after spinal cord injury. Nature. 2002;416:636-640.
[31] Mckeon RJ, Höke A, Silver J. Injury-induced proteoglycans inhibit the potential for laminin-mediated axon growth on astrocytic scars. Experimental Neurology. 1995;136:32-43.
[32] Cafferty WB, Yang S-H, Duffy PJ, Li S, Strittmatter SM. Functional axonal regeneration through astrocytic scar genetically modified to digest chondroitin sulfate proteoglycans. The Journal of Neuroscience. 2007;27:2176-2185.
[33] Coleman WP, Benzel E, Cahill DW, Ducker T, Geisler F, Green B, et al. A critical appraisal of the reporting of the National Acute Spinal Cord Injury Studies (II and III) of methylprednisolone in acute spinal cord injury. Journal of Spinal Disorders & Techniques. 2000;13:185-199.
[34] Jones LL, Oudega M, Bunge MB, Tuszynski MH. Neurotrophic factors, cellular bridges and gene therapy for spinal cord injury. The Journal of Physiology. 2001;533:83-89.
[35] Deumens R, Bozkurt A, Meek MF, Marcus MAE, Joosten EAJ, Weis J, et al. Repairing injured peripheral nerves: Bridging the gap. Progress in Neurobiology. 2010;92:245-276.
[36] Evans GR. Peripheral nerve injury: a review and approach to tissue engineered constructs. The Anatomical Record. 2001;263:396-404.
[37] Faroni A, Mobasseri SA, Kingham PJ, Reid AJ. Peripheral nerve regeneration: experimental

strategies and future perspectives. Advanced Drug Delivery Reviews. 2015;82-83:160-167.
[38] Fu SY, Gordon T. The cellular and molecular basis of peripheral nerve regeneration. Molecular Neurobiology. 1997;14:67-116.
[39] Marani E, Lakke EAJF. Peripheral Nervous System Topics. 2012:82-140.
[40] Schmidt CE, Leach JB. Neural tissue engineering: strategies for repair and regeneration. Annual Review of Biomedical Engineering. 2003;5:293-347.
[41] Matsuda S, Kobayashi N, Wakisaka H, Saito S, Saito K, Miyawaki K, et al. Morphological transformation of sensory ganglion neurons and satellite cells. Biomedical Reviews. 2000;11:39-52.
[42] Takahashi K, Ninomiya T. Morphological changes of dorsal root ganglion cells in the process-forming period. Progress in Neurobiology. 1987;29:393-410.
[43] Hart AM, Brannstrom T, Wiberg M, Terenghi G. Primary sensory neurons and satellite cells after peripheral axotomy in the adult rat. Experimental Brain Research. 2002;142:308-318.
[44] Schmalbruch H. Loss of sensory neurons after sciatic nerve section in the rat. The Anatomical Record. 1987;219:323-329.
[45] Chew DJ, Leinster VH, Sakthithasan M, Robson LG, Carlstedt T, Shortland PJ. Cell death after dorsal root injury. Neuroscience Letters. 2008;433:231-234.
[46] Ramer MS, Priestley JV, McMahon SB. Functional regeneration of sensory axons into the adult spinal cord. Nature. 2000;403:312-316.
[47] Ramer MS, Bishop T, Dockery P, Mobarak MS, O'Leary D, Fraher JP, et al. Neurotrophin-3-mediated regeneration and recovery of proprioception following dorsal rhizotomy. Molecular and Cellular Neuroscience. 2002;19:239-249.
[48] Malin SA, Davis BM, Molliver DC. Production of dissociated sensory neuron cultures and considerations for their use in studying neuronal function and plasticity. Nature Protocols. 2007;2:152-160.
[49] Melli G, Hoke A. Dorsal Root Ganglia Sensory Neuronal Cultures: a tool for drug discovery for peripheral neuropathies. Expert Opinion on Drug Discovery. 2009;4:1035-1045.
[50] Clark P, Britland S, Connolly P. Growth cone guidance and neuron morphology on micropatterned laminin surfaces. Journal of Cell Science. 1993;105:203-212.
[51] Vetter I, Pujic Z, Goodhill GJ. The response of dorsal root ganglion axons to nerve growth factor gradients depends on spinal level. Journal of Neurotrauma. 2010;27:1379-1386.

[52] Midha R, Munro CA, Dalton PD, Tator CH, Shoichet MS. Growth factor enhancement of peripheral nerve regeneration through a novel synthetic hydrogel tube. Journal of Neurosurgery. 2003;99:555-565.
[53] Mills CD, Allchorne AJ, Griffin RS, Woolf CJ, Costigan M. GDNF selectively promotes regeneration of injury-primed sensory neurons in the lesioned spinal cord. Molecular and Cellular Neuroscience. 2007;36:185-194.
[54] Hu J, Zhou J, Li X, Wang F, Lü H. Schwann cells promote neurite outgrowth of dorsal root ganglion neurons through secretion of nerve growth factor. Indian Journal of Experimental Biology. 2011;49:177.
[55] Wang M, Zhai P, Chen X, Schreyer DJ, Sun X, Cui F. Bioengineered scaffolds for spinal cord repair. Tissue Engineering Part B: Reviews. 2011;17:177-194.
[56] Doolabh VB, Hertl MC, Mackinnon SE. The role of conduits in nerve repair: a review. Reviews in the Neurosciences. 1996;7:47-84.
[57] Suri S, Schmidt CE. Cell-laden hydrogel constructs of hyaluronic acid, collagen, and laminin for neural tissue engineering. Tissue Engineering Part A. 2010;16:1703-16.
[58] Alluin O, Wittmann C, Marqueste T, Chabas J-F, Garcia S, Lavaut M-N, et al. Functional recovery after peripheral nerve injury and implantation of a collagen guide. Biomaterials. 2009;30:363-373.
[59] Rajaram A, Schreyer D, Chen D. Bioplotting Alginate/Hyaluronic Acid Hydrogel Scaffolds with Structural Integrity and Preserved Schwann Cell Viability. 3D Printing and Additive Manufacturing. 2014;1:194-203.
[60] Kalbermatten DF, Pettersson J, Kingham PJ, Pierer G, Wiberg M, Terenghi G. New fibrin conduit for peripheral nerve repair. Journal of Reconstructive Microsurgery. 2009;25:27-33.
[61] Lohmeyer J, Zimmermann S, Sommer B, Machens H, Lange T, Mailänder P. Bridging peripheral nerve defects by means of nerve conduits. Der Chirurg; Zeitschrift fur alle Gebiete der operativen Medizen. 2007;78:142-147.
[62] di Summa PG, Kingham PJ, Campisi CC, Raffoul W, Kalbermatten DF. Collagen (NeuraGen®) nerve conduits and stem cells for peripheral nerve gap repair. Neuroscience Letters. 2014;572:26-31.
[63] Sedaghati T, Yang SY, Mosahebi A, Alavijeh MS, Seifalian AM. Nerve regeneration with aid of nanotechnology and cellular engineering. Biotechnology and Applied Biochemistry.

2011;58:288-300.
[64] Kehoe S, Zhang X, Boyd D. FDA approved guidance conduits and wraps for peripheral nerve injury: a review of materials and efficacy. Injury. 2012;43:553-572.
[65] Grinsell D, Keating C. Peripheral nerve reconstruction after injury: a review of clinical and experimental therapies. BioMed Research International. 2014.
[66] Rodrigues MCO, Rodrigues AA, Glover LE, Voltarelli J, Borlongan CV. Peripheral nerve repair with cultured schwann cells: getting closer to the clinics. The Scientific World Journal. 2012.
[67] Agnew SP, Dumanian GA. Technical use of synthetic conduits for nerve repair. The Journal of Hand Surgery. 2010;35:838-841.
[68] Kim S-M, Lee S-K, Lee J-H. Peripheral nerve regeneration using a three dimensionally cultured Schwann cell conduit. Journal of Craniofacial Surgery. 2007;18:475-488.
[69] Arslantunali D, Dursun T, Yucel D, Hasirci N, Hasirci V. Peripheral nerve conduits: technology update. Medical Devices. 2014;7:405-424.
[70] Drury JL, Mooney DJ. Hydrogels for tissue engineering: scaffold design variables and applications. Biomaterials. 2003;24:4337-4351.
[71] Martin D, Schoenen J, Delrée P, Leprince P, Rogister B, Moonen G. Grafts of syngenic cultured, adult dorsal root ganglion-derived Schwann cells to the injured spinal cord of adult rats: preliminary morphological studies. Neuroscience Letters. 1991;124:44-48.
[72] Funakoshi H, Frisén J, Barbany G, Timmusk T, Zachrisson O, Verge V, et al. Differential expression of mRNAs for neurotrophins and their receptors after axotomy of the sciatic nerve. The Journal of Cell Biology. 1993;123:455-465.
[73] Acheson A, Barker PA, Alderson RF, Miller FD, Murphy RA. Detection of brain-derived neurotrophic factor-like activity in fibroblasts and Schwann cells: inhibition by antibodies to NGF. Neuron. 1991;7:265-275.
[74] Bunge RP, Bunge MB. Interrelationship between Schwann cell function and extracellular matrix production. Trends in Neurosciences. 1983;6:499-505.
[75] Chiu AY, Espinosa De Los Monteros A, Cole RA, Loera S, De Vellis J. Laminin and s-laminin are produced and released by astrocytes, schwann cells, and schwannomas in culture. Glia. 1991;4:11-24.
[76] Martin D, Robe P, Franzen R, Delree P, Schoenen J, Stevenaert A, et al. Effects of Schwann cell transplantation in a contusion model of rat spinal cord injury. Journal of Neuroscience

Research. 1996;45:588-597.
[77] Oudega M, Xu X-M. Schwann cell transplantation for repair of the adult spinal cord. Journal of Neurotrauma. 2006;23:453-467.
[78] Xu XM, Chen A, Guenard V, Kleitman N, Bunge MB. Bridging Schwann cell transplants promote axonal regeneration from both the rostral and caudal stumps of transected adult rat spinal cord. Journal of Neurocytology. 1997;26:1-16.
[79] Son Y-J, Thompson WJ. Schwann cell processes guide regeneration of peripheral axons. Neuron. 1995;14:125-132.
[80] Ansselin A, Fink T, Davey D. Peripheral nerve regeneration through nerve guides seeded with adult Schwann cells. Neuropathology and Applied Neurobiology. 1997;23:387-398.
[81] Hadlock TA, Sundback CA, Hunter DA, Vacanti JP, Cheney ML. A new artificial nerve graft containing rolled Schwann cell monolayers. Microsurgery. 2001;21:96-101.
[82] Evans GR, Brandt K, Katz S, Chauvin P, Otto L, Bogle M, et al. Bioactive poly (L-lactic acid) conduits seeded with Schwann cells for peripheral nerve regeneration. Biomaterials. 2002;23:841-848.
[83] Mosahebi A, Wiberg M, Terenghi G. Addition of fibronectin to alginate matrix improves peripheral nerve regeneration in tissue-engineered conduits. Tissue Engineering. 2003;9:209-218.
[84] Guenard V, Kleitman N, Morrissey T, Bunge R, Aebischer P. Syngeneic Schwann cells derived from adult nerves seeded in semipermeable guidance channels enhance peripheral nerve regeneration. The Journal of Neuroscience. 1992;12:3310-3320.
[85] Mosahebi A, Woodward B, Wiberg M, Martin R, Terenghi G. Retroviral labeling of Schwann cells: in vitro characterization and in vivo transplantation to improve peripheral nerve regeneration. Glia. 2001;34:8-17.
[86] Mosahebi A, Simon M, Wiberg M, Terenghi G. A novel use of alginate hydrogel as Schwann cell matrix. Tissue Engineering. 2001;7:525-534.
[87] Mosahebi A, Fuller P, Wiberg M, Terenghi G. Effect of allogeneic Schwann cell transplantation on peripheral nerve regeneration. Experimental Neurology. 2002;173:213-223.
[88] Strauch B, Rodriguez DM, Diaz J, Yu H-L, Kaplan G, Weinstein DE. Autologous Schwann cells drive regeneration through a 6-cm autogenous venous nerve conduit. Journal of Reconstructive Microsurgery. 2001;17:589-595.
[89] Fernandez-Valle C, Bunge RP, Bunge MB. Schwann cells degrade myelin and proliferate in

the absence of macrophages: evidence fromin vitro studies of Wallerian degeneration. Journal of Neurocytology. 1995;24:667-679.
[90] Someya Y, Koda M, Dezawa M, Kadota T, Hashimoto M, Kamada T, et al. Reduction of cystic cavity, promotion of axonal regeneration and sparing, and functional recovery with transplanted bone marrow stromal cell-derived Schwann cells after contusion injury to the adult rat spinal cord: laboratory investigation. Journal of Neurosurgery: Spine. 2008;9:600-610.
[91] Kamada T, Koda M, Dezawa M, Anahara R, Toyama Y, Yoshinaga K, et al. Transplantation of human bone marrow stromal cell-derived Schwann cells reduces cystic cavity and promotes functional recovery after contusion injury of adult rat spinal cord. Neuropathology. 2011;31:48-58.
[92] Takami T, Oudega M, Bates ML, Wood PM, Kleitman N, Bunge MB. Schwann cell but not olfactory ensheathing glia transplants improve hindlimb locomotor performance in the moderately contused adult rat thoracic spinal cord. The Journal of Neuroscience. 2002;22:6670-6681.
[93] Kromer LF. Nerve growth factor treatment after brain injury prevents neuronal death. Science. 1987;235:214-216.
[94] Schnell L, Schneider R, Kolbeck R, Barde Y A, Schwab ME. Neurotrophin-3 enhances sprouting of corticospinal tract during development and after adult spinal cord lesion. Nature. 1994;367:170-173.
[95] Levi-Montalcini R, Calissano P. Nerve growth factor. The saga of the nerve growth factor: preliminary studies, discovery, further development. 1997.
[96] Barde Y-A. Trophic factors and neuronal survival. Neuron. 1989;2:1525-1534.
[97] Tuszynski MH, Gabriel K, Gage FH, Suhr S, Meyer S, Rosetti A. Nerve growth factor delivery by gene transfer induces differential outgrowth of sensory, motor, and noradrenergic neurites after adult spinal cord injury. Experimental Neurology. 1996;137:157-173.
[98] Romero MI, Rangappa N, Li L, Lightfoot E, Garry MG, Smith GM. Extensive sprouting of sensory afferents and hyperalgesia induced by conditional expression of nerve growth factor in the adult spinal cord. The Journal of Neuroscience. 2000;20:4435-4445.
[99] Aloe L, Calzà L. NGF and related molecules in health and disease: Elsevier; 2003.
[100] Xu X, Yee W-C, Hwang PY, Yu H, Wan AC, Gao S, et al. Peripheral nerve regeneration with sustained release of poly (phosphoester) microencapsulated nerve growth factor within nerve guide conduits. Biomaterials. 2003;24:2405-2412.
[101] Labrador RO, Butí M, Navarro X. Influence of collagen and laminin gels concentration on

nerve regeneration after resection and tube repair. Experimental Neurology. 1998;149:243-252.
[102] Rosoff W, McAllister R, Esrick M, Goodhill G, Urbach J. Generating controlled molecular gradients in 3D gels. Biotechnology and Bioengineering. 2005;91:754-759.
[103] Kemp SW, Walsh SK, Zochodne DW, Midha R. A novel method for establishing daily in vivo concentration gradients of soluble nerve growth factor (NGF). Journal of Neuroscience Methods. 2007;165:83-88.
[104] Pakulska MM, Ballios BG, Shoichet MS. Injectable hydrogels for central nervous system therapy. Biomedical Materials. 2012;7:024101.
[105] Macaya D, Spector M. Injectable hydrogel materials for spinal cord regeneration: a review. Biomedical Materials. 2012;7:012001.
[106] Tan H, Marra KG. Injectable, Biodegradable Hydrogels for Tissue Engineering Applications. Materials. 2010;3:1746-1767.
[107] Meek MF, Coert JH. US Food and Drug Administration/Conformit Europe-approved absorbable nerve conduits for clinical repair of peripheral and cranial nerves. Annals of Plastic Surgery. 2008;60:110-116.
[108] Narotam PK, José S, Nathoo N, Taylon C, Vora Y. Collagen matrix (DuraGen) in dural repair: analysis of a new modified technique. Spine. 2004;29:2861-2867.
[109] Yoshii S, Oka M, Shima M, Taniguchi A, Taki Y, Akagi M. Restoration of function after spinal cord transection using a collagen bridge. Journal of Biomedical Materials Research Part A. 2004;70:569-575.
[110] Klapka N, Müller HW. Collagen matrix in spinal cord injury. Journal of Neurotrauma. 2006;23:422-436.
[111] Bellamkonda RV. Peripheral nerve regeneration: an opinion on channels, scaffolds and anisotropy. Biomaterials. 2006;27:3515-3518.
[112] Chen Y S, Hsieh C L, Tsai C C, et al. Peripheral nerve regeneration using silicone rubber chambers filled with collagen, laminin and fibronectin. Biomaterials. 2000;21:1541-1547.
[113] Sung H-W, Huang R-N, Huang LL, Tsai C-C. In vitro evaluation of cytotoxicity of a naturally occurring cross-linking reagent for biological tissue fixation. Journal of Biomaterials Science, Polymer Edition. 1999;10:63-78.
[114] King VR, Alovskaya A, Wei DY, Brown RA, Priestley JV. The use of injectable forms of fibrin and fibronectin to support axonal ingrowth after spinal cord injury. Biomaterials.

2010;31:4447-4456.
[115] Taylor SJ, Rosenzweig ES, McDonald JW, Sakiyama-Elbert SE. Delivery of neurotrophin-3 from fibrin enhances neuronal fiber sprouting after spinal cord injury. Journal of Controlled Release. 2006;113:226-235.
[116] Taylor SJ, Sakiyama-Elbert SE. Effect of controlled delivery of neurotrophin-3 from fibrin on spinal cord injury in a long term model. Journal of Controlled Release. 2006;116:204-210.
[117] Johnson PJ, Parker SR, Sakiyama‐Elbert SE. Controlled release of neurotrophin‐3 from fibrin‐based tissue engineering scaffolds enhances neural fiber sprouting following subacute spinal cord injury. Biotechnology and Bioengineering. 2009;104:1207-1214.
[118] Schense JC, Bloch J, Aebischer P, Hubbell JA. Enzymatic incorporation of bioactive peptides into fibrin matrices enhances neurite extension. Nature Biotechnology. 2000;18:415-419.
[119] Hall H. Modified fibrin hydrogel matrices: both, 3D-scaffolds and local and controlled release systems to stimulate angiogenesis. Current Pharmaceutical Design. 2007;13:3597-3607.
[120] Ahmed TA, Dare EV, Hincke M. Fibrin: a versatile scaffold for tissue engineering applications. Tissue Engineering Part B: Reviews. 2008;14:199-215.
[121] Novikova LN, Mosahebi A, Wiberg M, Terenghi G, Kellerth JO, Novikov LN. Alginate hydrogel and matrigel as potential cell carriers for neurotransplantation. Journal of Biomedical Materials Research Part A. 2006;77:242-252.
[122] Yu H, Chen X, Lu T, Sun J, Tian H, Hu J, et al. Poly (L-lysine)-graft-chitosan copolymers: synthesis, characterization, and gene transfection effect. Biomacromolecules. 2007;8:1425-1435.
[123] Chenite A, Chaput C, Wang D, Combes C, Buschmann M, Hoemann C, et al. Novel injectable neutral solutions of chitosan form biodegradable gels in situ. Biomaterials. 2000;21:2155-2161.
[124] Rowley JA, Madlambayan G, Mooney DJ. Alginate hydrogels as synthetic extracellular matrix materials. Biomaterials. 1999;20:45-53.
[125] Shin H, Jo S, Mikos AG. Biomimetic materials for tissue engineering. Biomaterials. 2003;24:4353-4364.
[126] Van Tomme SR, Storm G, Hennink WE. In situ gelling hydrogels for pharmaceutical and biomedical applications. International Journal of Pharmaceutics. 2008;355:1-18.
[127] Shoulders MD, Raines RT. Collagen structure and stability. Annual Review of Biochemistry. 2009;78:929.

[128] Nimni ME, Cheung D, Strates B, Kodama M, Sheikh K. Chemically modified collagen: a natural biomaterial for tissue replacement. Journal of Biomedical Materials Research. 1987;21:741-771.
[129] Butler MF, Ng YF, Pudney PD. Mechanism and kinetics of the crosslinking reaction between biopolymers containing primary amine groups and genipin. Journal of Polymer Science Part A: Polymer Chemistry. 2003;41:3941-3953.
[130] Sundararaghavan HG, Monteiro GA, Lapin NA, Chabal YJ, Miksan JR, Shreiber DI. Genipin-induced changes in collagen gels: Correlation of mechanical properties to fluorescence. Journal of Biomedical Materials Research Part A. 2008;87:308-320.
[131] Sundararaghavan HG, Monteiro GA, Firestein BL, Shreiber DI. Neurite growth in 3D collagen gels with gradients of mechanical properties. Biotechnology and Bioengineering. 2009;102:632-643.
[132] Bigi A, Cojazzi G, Panzavolta S, Roveri N, Rubini K. Stabilization of gelatin films by crosslinking with genipin. Biomaterials. 2002;23:4827-4832.
[133] Hwang Y-J, Larsen J, Krasieva TB, Lyubovitsky JG. Effect of genipin crosslinking on the optical spectral properties and structures of collagen hydrogels. ACS Applied Materials & Interfaces. 2011;3:2579-2584.
[134] Yan LP, Wang YJ, Ren L, Wu G, Caridade SG, Fan JB, et al. Genipin cross-linked collagen/chitosan biomimetic scaffolds for articular cartilage tissue engineering applications. Journal of Biomedical Materials Research Part A. 2010;95:465-475.
[135] Ma W, Chen S, Fitzgerald W, Maric D, Lin HJ, O'Shaughnessy TJ, et al. Three-dimensional collagen gel networks for neural stem cell-based neural tissue engineering. Macromolecular Symposia. 2005.227(1): 327-334.
[136] Huang F, Shen Q, Zhao J. Growth and differentiation of neural stem cells in a three-dimensional collagen gel scaffold. Neural Regeneration Research. 2013;8:313.
[137] Mio T, Adachi Y, Romberger DJ, Ertl RF, Rennard SI. Regulation of fibroblast proliferation in three-dimensional collagen gel matrix. In Vitro Cellular & Developmental Biology Animal. 1996;32:427-433.
[138] Rosner B, Hang T, Tranquillo R. Schwann cell behavior in three-dimensional collagen gels: evidence for differential mechano-transduction and the influence of TGF-beta 1 in morphological polarization and differentiation. Experimental Neurology. 2005;195:81-91.

[139] Wang B, Zhao Y, Lin H, Chen B, Zhang J, Zhang J, et al. Phenotypical analysis of adult rat olfactory ensheathing cells on 3-D collagen scaffolds. Neuroscience Letters. 2006;401:65-70.
[140] Bozkurt A, Brook GA, Moellers S, Lassner F, Sellhaus B, Weis J, et al. In vitro assessment of axonal growth using dorsal root ganglia explants in a novel three-dimensional collagen matrix. Tissue Engineering. 2007;13:2971-2979.
[141] Kofron CM, Fong VJ, Hoffman-Kim D. Neurite outgrowth at the interface of 2D and 3D growth environments. Journal of Neural Engineering. 2008;6:016002.
[142] Willits RK, Skornia SL. Effect of collagen gel stiffness on neurite extension. Journal of Biomaterials Science, Polymer Edition. 2004;15:1521-1531.
[143] Swindle-Reilly KE, Papke JB, Kutosky HP, Throm A, Hammer JA, Harkins AB, et al. The impact of laminin on 3D neurite extension in collagen gels. Journal of Neural Engineering. 2012;9:046007.
[144] Bhang SH, Lee T-J, Lim JM, Lim JS, Han AM, Choi CY, et al. The effect of the controlled release of nerve growth factor from collagen gel on the efficiency of neural cell culture. Biomaterials. 2009;30:126-132.
[145] Gingras M, Bergeron J, Déry J, Durham HD, Berthod F. In vitro development of a tissue-engineered model of peripheral nerve regeneration to study neurite growth. The FASEB Journal. 2003;17:2124-2126.
[146] Macaya DJ, Hayakawa K, Arai K, Spector M. Astrocyte infiltration into injectable collagen-based hydrogels containing FGF-2 to treat spinal cord injury. Biomaterials. 2013;34:3591-602.
[147] Kofron CM, Fong VJ, Hoffman-Kim D. Neurite outgrowth at the interface of 2D and 3D growth environments. Journal of Neural Engineering. 2009;6:016002.
[148] Bozkurt A, Brook GA, Moellers S, Lassner F, Sellhaus B, Weis J, et al. In vitro assessment of axonal growth using dorsal root ganglia explants in a novel three-dimensional collagen matrix. Tissue Engineering. 2007;13:2971-2979.
[149] Macaya D, Ng KK, Spector M. Injectable Collagen-Genipin Gel for the Treatment of Spinal Cord Injury: In Vitro Studies. Advanced Functional Materials. 2011;21:4788-4797.
[150] Windebank AJ, Wood P, Bunge RP, Dyck PJ. Myelination determines the caliber of dorsal root ganglion neurons in culture. The Journal of Neuroscience. 1985;5:1563-1569.
[151] O'Connor SM, Stenger DA, Shaffer KM, Ma W. Survival and neurite outgrowth of rat cortical neurons in three-dimensional agarose and collagen gel matrices. Neuroscience Letters.

2001;304:189-193.
[152] Krewson CE, Chung SW, Dai W, Mark Saltzman W. Cell aggregation and neurite growth in gels of extracellular matrix molecules. Biotechnology and Bioengineering. 1994;43:555-562.
[153] Flanagan LA, Ju Y-E, Marg B, Osterfield M, Janmey PA. Neurite branching on deformable substrates. Neuroreport. 2002;13:2411.
[154] Barocas VH, Moon AG, Tranquillo RT. The fibroblast-populated collagen microsphere assay of cell traction force. Journal of Biomechanical Engineering. 1995;117:161-170.